



Department of
Primary Industries



Final report

The gateway to selecting nutrient efficient livestock-‘Better doers’

Project code: B.GBP.0024

Prepared by: Drs Jude Bond and Nicholas J. Hudson
New South Wales Department of Primary Industries and
The University of Queensland

Date published: 30 May 2021

PUBLISHED BY
Meat and Livestock Australia Limited
PO Box 1961
NORTH SYDNEY NSW 2059

Meat & Livestock Australia acknowledges the matching funds provided by the Australian Government to support the research and development detailed in this publication.

This publication is published by Meat & Livestock Australia Limited ABN 39 081 678 364 (MLA). Care is taken to ensure the accuracy of the information contained in this publication. However MLA cannot accept responsibility for the accuracy or completeness of the information or opinions contained in the publication. You should make your own enquiries before making decisions concerning your interests. Reproduction in whole or in part of this publication is prohibited without prior written consent of MLA.

Abstract

In this project, we aimed to quantify the potential gains in productivity by sampling a population of sheep with different residual feed intake, methane emission and quantify differences in key rumen wall proteins involved in nutrient uptake and energy capture from these animals.

Through a series of investigations, we have exposed the main processes and metabolic pathways involved in nutrient absorption in sheep rumen with phenotypic variation in residual feed intake (RFI) and methane emission. These processes impact on the net energy absorbed in this part of the digestive tract which in turn effects how efficiently the animal can use the metabolizable energy from the diet and retain it in the body.

The phenotypic variation in animal performance in response to both environmental and commercial drivers is the basis of traits selected by geneticists in commercial breeding objectives. Innovations in the field of molecular biology like those used to generate the results in this project are bringing these procedures closer to their application for selection of important commercial traits. It is expected in the future the red meat industry will benefit significantly from these technologies.

Animal use was approved (AEC approval # 19-065) by the animal ethics committee of the University of New England.

Executive summary

Our research extended current knowledge of well-defined phenotypes such as residual feed intake (RFI) and methane (CH₄) emission in sheep to the processes regulating nutrient uptake and metabolism in the rumen wall. There are 3 datasets of protein markers through project 1. MLA B.GBP.0024, 2. MLA and commonwealth funding DAFF grant no.1193857-31 and 3. P.PSH.1036 Novel Dual Purpose Perennial Cereals for Grazing. The knowledge gained on the proteins in the rumen wall was integrated with information on mitochondrial content in cells controlling energy expenditure and metabolic efficiency in metabolically important tissues of the animals’ body (Table 2 outlines the data sets related to the results generated).

The Merino sheep experiment

We aimed to design an experiment that accounts in detail for the simple definition of efficiency as; Feed intake = energy retained – energy lost. Around 14 variable (traits) factors were simultaneously measured (feed intake_{60 days}, LWT_{60days}, average daily gain, body composition and gas emission). Metabolically important tissues were harvested at the end of the experiment providing an invaluable biobank resource for research into ruminant feed efficiency going forward.

1. The ‘Better Doer’ Merino wether experiment run out of Armidale has reinforced the concept that feed efficiency (FE) is a trait with a **complex physiological architecture that includes a significant mitochondrial component**.
2. Here, we defined FE as feed intake expressed relative to body mass at day 60, such that more efficient animals would consume less feed at a common body mass and therefore possess a negative residual. This measure of efficiency is about 80% similar to Koch’s Residual Feed Intake metric.
3. In relation to the phenotype used to define the ‘better doers’ and link these differences to protein markers in the rumen epithelium the phenotype defined was residual feed intake (RFI).

Rumen epithelium protein biomarkers

1. A different pattern of protein biomarkers (abundance of enzymes) in metabolic pathways in the rumen epithelium was found in sheep fed 1.5 x energy required for maintenance in with L or H CH₄ emission compared to that fed ad libitum the same diet with L or H RFI.
2. In the L and H CH₄ emitting rumen epithelium we found a greater abundance of proteins involved in the use of glucose as a nutrient for cellular energy in this phenotype. We also demonstrated the rumen epithelium possesses a methylglyoxal shunt pathway (side path of glycolysis) which is an indicator of metabolic efficiency in the L CH₄ sheep rumen epithelium.
3. In contrast, in the L and H RFI phenotype and those fed contrasting diets with different mineral balance (perennial wheat diets) the proteins with greater abundance were involved fatty acid oxidation (L or H RFI). The results provide evidence about the efficient use of simple sugars compared to fats to provide metabolites to form energy in the mitochondria of the rumen wall.
4. Despite the identification of numerous membrane bound nutrient transporters, surprisingly, few protein transporters had a difference in abundance linked to differences in phenotype or diet. Of note those that did vary with diet were calcium transporters found associated with mineral imbalance (high K⁺: Na⁺ ratio) in the perennial wheat fed sheep rumen epithelium. The implication for industry is that we need to fine tune the formulation of diets

in cereal forage crops commonly fed to sheep and cattle. It also sheds light on how to provide the best supplement strategies to correct mineral imbalance and any accompanying metabolic disturbance in sheep and dairy cattle. These provide valuable linkage between the agronomic and adoption outcomes for the LPP ‘Dual Purpose Perennial Cereals for Grazing Project.

5. The range of nutrient transporter identified shows the rumen epithelium has the capacity to absorb a wide range of nutrients. Providing flexibility to producers to use different feed sources for nutrition beyond the concept they often rely on that ‘supplementary feed is only what is available’. A new short chain fatty acid transporter was identified (SLCO2A1).
6. Linking known phenotypes to functional processes of protein cellular markers in the rumen wall (point 1-5) was a goal of this project and we have completed this task successfully.

Mitochondrial DNA copy number.

1. A few significant associations between FE and the other phenotypic measurements were detected, but none had particularly strong pairwise correlations when considered in isolation. In line with expectation, significant relationships between FE and CO₂ emissions ($P = 0.003$) and FE and CH₄ emissions ($P = 0.02$) implicate both host cellular mitochondrial metabolism and rumen microbial activity as key determinants of the ruminant efficiency phenotype.
2. Based on tissue samples collected from the Merino wether experiment, we quantitated mitochondrial content across six tissues (Longissimus dorsi (LD), Semitendinosus (ST), Soleus (SOL) muscles, and liver, rumen, skin) across ~40 wethers divergent in FE. Using Principal Components Regression analysis with FE as the response variable we discovered liver mitochondrial content is significantly associated with FE ($P = 0.0269$) with rumen approaching significance ($P = 0.065$). This is an exciting new finding indicating a) **sheep liver aerobic capacity is associated with whole animal FE** and b) that a circulating test reflecting liver aerobic capacity (or related liver function) might offer future hope for a diagnostic test for FE going forwards.
3. Low mitochondrial content tends to be associated with high efficiency – i.e. low intake relative to body mass - across tissues and **lends support to the reduction in physiological spare capacity argument (the quest for the ‘Corolla’ Cow) that has previously been proposed as a possible driver of production animal feed efficiency** (e.g. Hudson 2009; Reverter et al 2017; Cassar-Malek et al 2017). By analogy, more efficient production animals tend to have a smaller (‘Toyota corolla’) engine than their less efficient (fuel guzzling ‘Drag racer’) counterparts. Moreover, the correlation we detected between Merino rumen mitochondrial content and FE (0.18) is very similar to the 0.21 detected by Kong et al (2017) in the context of RFI phenotyped Hereford x Angus steers.
4. In comparing the six tissues screened for mitochondrial content (SOL, ST, LD, liver, rumen, skin) we detected **strong relationships between liver and rumen** on the one hand (0.49; $P = 0.003$), and to a lesser extent **the skeletal musculature** on the other. Given the absence of relationship between skin mitochondrial content and FE, it seems **unlikely the skin, at least when assessed in isolation, would yield a meaningful metabolic signal that could form a test for predicting FE.**
5. In terms of simple pairwise correlations, several tissues had significant correlations between their mitochondrial content and the various component phenotypes we measured. For example, **SOL mitochondrial content was significantly associated with whole animal oxygen consumption** ($P = 0.017$) and Brouwer’s heat estimation ($P = 0.017$). Semitendinosus mitochondrial content was significantly associated with both lean mass ($P = 0.046$) and bone mass ($P = 0.00034$). **Rumen mitochondrial content was significantly associated with**

average daily gain (ADG; $P = 0.028$), lean gain ($P = 0.021$) and nitrogen balance ($P = 0.014$). Finally, skin mitochondrial content was significantly associated with fat depth ($P = 0.05$).

6. An earlier examination of mitochondrial content in archived neck muscle samples from 134 Angus cattle individually phenotyped for RFI, Average Daily Gain and Daily Feed Intake found no significant relationships. The combination of data from this experiment and the ‘Better Doers’ Merino wether trial implies that variation in mitochondrial content of one or a small number of muscles is unlikely to reflect FE.

Benefits to industry/Implications

The research in this project has taken us a step closer to improving our understanding of the mechanisms underlying and diagnosing the efficient use of nutrients in ruminant livestock. The use of this information in the future by animal geneticists and nutritionists may be used to select ruminant livestock with more efficient phenotypes. Finally, it will enable producers to benefit from better feed composition formulation, feeding strategies and breeding programs to produce ruminant livestock more cost effectively, with body composition desirable to match the production system, environment, as well as reduce impact on the environment through reduced methane emission. In addition, the information gained through CT scans in our research gives us insights into the molecular mechanisms controlling fat distribution in the body, lean gain and bone health. Therefore, enabling producers to make informed decisions to produce sheep that meet market specifications and if implemented for buyers in the supply chain to buy carcasses according to body composition. Furthermore, the procedure has important implications for meat and eating quality for consumers.

More specifically we have exposed the processes and metabolic pathways involved in nutrient absorption in sheep with phenotypic variation in RFI and CH₄ emission. These processes impact on the net energy absorbed in this part of the digestive tract which in turn effects how efficiently the animal can use the metabolizable energy from the diet and retain it in the body. The phenotypic variation in animal performance in response to both environmental and commercial drivers is the basis of traits selected by geneticists in commercial breeding objectives. Innovations in the field of molecular biology are bringing these procedures closer to their application for selection of important traits. It is expected in the future the red meat industry will benefit significantly from these technologies.

Achievements- Methodology development

- Development of a procedure to quantify effects of phenotype and diet on cytosol and membrane rumen epithelium proteins. We also improved speed of interpretation of large proteome datasets using a bioinformatics approach called weighted gene network correlation analysis (WGNCA). (see outcome Rumen epithelium protein biomarkers 1- 5 above).
- In terms of the tissue mitochondrial content estimation that formed the basis of the University of Queensland sub-contract, highly sensitive molecular tests using duplex Taqman qRT-PCR chemistry were successfully developed and deployed for both sheep and cattle in a number of different biological contexts throughout the life of this project. These assay designs leveraged previous Australian investment in the cattle and sheep genome assemblies, and other Meat and Livestock Australia funded research. We found from a technical perspective that they work well across the various breeds and the taurine and indicine cattle sub-species. The assays represent a useful analytic tool with broad application for value adding to future ruminant metabolic studies.

Table of contents

Abstract	2
Executive summary	3
The Merino sheep experiment	3
Rumen epithelium protein biomarkers	3
Mitochondrial DNA copy number.	4
Benefits to industry/Implications	5
Achievements- Methodology development.....	5
1. Background	10
1.1 ‘Better doers’	10
1.2 Defining the ‘Better doers’ phenotype	10
1.3 Linking ‘Better doers’ phenotype to DNA and protein cellular markers of efficiency	11
1.4 Phenotypic variation in methane emission	11
1.5 The process of nutrient absorption.....	12
1.6 Significance to industry	13
2. Objectives.....	14
2.1 The ‘better doers’ phenotype	14
2.2 Project objectives.....	14
3. Methodology	15
3.1 Animal experiments	15
3.1.1 Phase 1 – Selecting growing merino wethers based on variation in the RHI phenotype.....	15
3.1.2 Phase 2 – Low or high RFI fed a high or low energy diet for 30 days.....	16
3.1.3 Low or high CH ₄ emission phenotype.	17
3.1.4 Perennial wheat and perennial wheat and Lucerne diets.....	17
3.2 Feed composition, diet formulation.	18

3.3	Measurement of Body composition	19
3.4	Measurement of CH₄, CO₂ and O₂ in respiration chambers	21
3.5	Isolation of epithelium and extraction of cytosol and membrane proteins	22
3.5.1	Sample preparation for LC-MS/MS analysis.....	22
3.6	Rumen fluid and blood metabolite quantitation.....	22
3.7	Statistical analysis	22
3.7.1	Low or High RFI phenotype	22
3.7.2	Low or high CH ₄ phenotype	23
3.8	Mitochondrial content assay	23
3.8.1	Rationale for the development of sheep and cattle mitochondrial content assays.....	23
3.8.2	Mitochondrial content assay design.....	24
4.	Results.....	25
4.1.3	Cumulative R ² and stepwise regression of significant traits to explain variation in FI _{60 days}	28
4.1.4	Selection of sheep into L or H RFI phenotype.	29
4.1.5	Phase 2 experiment; two phenotypes (L and H RFI) and two diets.	30
4.1.6	Protein identifications and quantification between H or L RFI and H or L diets	31
4.1.7	Functionally significant rumen epithelium proteins and enriched pathways in L or H RFI fed H or L diet found using WGCNA.....	31
4.1.8	Mitochondria and the ‘Better doer’ Merino animal trial	35
4.1.9	Neck muscle mitochondrial content and Angus cattle RFI.....	40
4.2	Phenotypic variation in CH₄ emission in ewes fed a maintenance energy diet; Rumen epithelium protein makers and mitochondrial content associated	40
4.2.1	Methane emission and digestive parameters in sheep selected for L or H CH ₄ group.....	40
4.2.2	Protein identification and quantitation of rumen epithelium proteins.....	41
4.2.3	Assignment of proteins to sub cellular compartment.....	42
4.2.4	Quantitative differences in epithelium protein abundance in H or L CH ₄ rumen epithelium.....	42

4.2.5	Metabolic pathways associated with significant fold changes in epithelium proteins in H or L CH ₄ emitting sheep.....	44
4.2.6	Differential abundance of proteins involved in cell defence against microbes in the epithelium of L or H CH ₄ sheep	45
4.2.7	Rumen fluid metabolites H or L CH ₄ phenotype	46
4.2.8	Metabolites in the blood	47
4.2.9	Rumen mitochondrial content and sheep divergent for heat production and methane emissions	47
4.3	Perennial wheat vs Perennial wheat plus Lucerne-fed sheep; Quantification of rumen epithelium proteome by TMT-MS.	48
4.3.1	Diet composition.....	48
4.3.2	Feed intake, Growth, Blood and Urine mineral content	48
4.3.3	Protein identifications and quantification between diets.....	52
4.3.4	Functionally significant proteins and enriched pathways in PW > PWL fed sheep found using WGCNA	52
4.4	Nutrient transport in rumen epithelium	58
4.4.1	Identification of proteins that transport nutrients and ions in the rumen epithelium.....	58
4.4.2	Proteins and the process of nutrient transport.....	59
5.	Discussion.....	60
5.1	Phenotypes	60
5.1.1	Phenotypic correlates of more efficient nutrient use in growing sheep: how to pick ‘better doers’.....	60
5.2	Quantification of cytosol and membrane proteins by SWATH-MS in rumen epithelium of sheep with low or high CH₄ emission phenotype	62
5.2.1	Mitochondrial content.....	64
6.	Conclusion and recommendations	65
6.1	Rumen epithelial proteins	65
6.2	Mitochondrial content	65
7.	References.....	66

7.1	Quantification of Low or high methane rumen epithelium proteins	66
7.2	Perennial wheat fed sheep; Rumen epithelium proteins	68
7.3	Mitochondrial DNA content assays.....	69
8.	Appendix	71
8.1	Feed composition.....	71
8.2	Workflow diagram for SWATH MS.....	72
8.3	Tandem mass spectrometry methodology.....	73
8.3.1	Quantification of rumen epithelium proteins by SWATH MS	73
8.3.2	Offline high pH (HpH) fractionation by HPLC	73
8.3.3	LC-MS/MS and data acquisition	73
8.3.4	Bioinformatic analysis to predict protein subcellular location and biological function.....	74
8.3.5	Data analysis	74
8.4	Quantification of rumen epithelium proteins by TMT-MS.....	74
8.4.1	Statistical analysis	75
8.5	Assignment of proteins to sub cellular compartment and function	75
8.6	Publications/communication	77
8.6.1	Journal articles	77
8.6.2	Full journal articles in draft.....	77
8.6.3	Conference attendance and proceedings	77
8.6.4	Meetings	77
8.6.5	Postgraduate students.....	78

1. Background

1.1 ‘Better doers’

In the commercial ruminant production situation when feed is limited, some animals are better able to maintain condition and productive capacity. These animals are often called ‘better doers’. In the sheep meat industry lower than expected growth rates of lambs sired by sires of high genetic merit for weaning weight are occurring, with the primary cause identified being nutritional constraints (Oddy and Wamsley 2013). In the extensive grazing systems across northern Australia, the issue of low efficiency manifests largely as poor resilience and loss of muscle mass in the dry season when forage quality and quantity is low. While some animals perform poorly during this time others appear to perform well, maintaining or gaining liveweight (growers) or producing calves (breeders).

Evidence for the physiological, metabolic and molecular basis of these differences in animal performance, relevant to several ruminant production systems, is beginning to emerge. Variation in efficiency of feed conversion occurs in cattle selected for residual feed intake (RFI; Herd and Arthur, 2009). Differences in the level of genes expressed at the cellular level in the liver have been reported (Chen *et al.* 2011). Recent work on rumen papillae of low RFI cattle (Kong *et al.* 2016) suggests a combination of low mitochondrial (mt) content and increased expression of genes involved with energy forming pathways are key indicators of the mechanism controlling this trait.

In sheep evidence of variation in nutrient use efficiency is associated with differences in whole tract digestive processes, rumen volume (Pinares-Patiño *et al.* 2003; Goopy *et al.* 2014; Bond *et al.* 2016), the genes expressed (Xiang *et al.* 2017) and proteins of the rumen epithelium (Bond *et al.* 2017). In ruminants, the proteins in the epithelium, lining the inner surface of the rumen regulate nutrient uptake and cellular energy transactions prior to their transfer to peripheral tissue, such as skeletal muscle (Dijkstra *et al.* 1993). In broilers, low breast muscle mt content is associated with more muscular birds with higher abdominal fat content (Reverter *et al.* 2017). Hence, we propose to investigate the processes regulating nutrient uptake and metabolism in the rumen wall in context with processes controlling energy expenditure and metabolic efficiency in peripheral tissue of the animals’ body (skeletal muscle). The knowledge gained on the genes and proteins in the rumen wall may be combined with information on mt content in cells to find relationships with phenotypes that outperform others.

1.2 Defining the ‘Better doers’ phenotype

The red meat industry is seeking ways to improve energy use ‘efficiency’ to optimise animal growth and the use of natural resources. The term ‘Efficiency’ is used in a number of ways to define different parameters or traits. These include feed intake efficiency (residual feed intake; RFI), whole body energy use efficiency or tissue and organ based measures of efficiency. Nutrient use efficiency is a broad term with underlying biological processes. The rumen epithelium is a major site of nutrient absorption and many proteins and cell compartments co-ordinate the processes of nutrient absorption as well as ion homeostasis. Part of our research took measures of important phenotypes such as RFI and focussed on defining ‘efficiency’ at the level of the rumen epithelium proteins. In addition, we have overlayed this information with a cross section of different diets which in a way simulate different environmental conditions in which sheep are fed to grow. The phenotype summaries link processes occurring in the rumen wall to whole body energy efficiency in relation to growth rate (liveweight, average daily gain), carcass composition (fat, lean and bone gain) or meat quality. In addition, we linked mitochondrial content (mtDNA) in relevant tissues such as the liver,

rumen, muscle and fat giving an indication of how efficiently these tissues produce or utilise energy in the form of Adenosine Tri Phosphate (ATP).

Feed cost represents a major cost to livestock producers. By selecting sheep that eat less, relative to average daily gain in liveweight producers can potentially reduce overall feed costs across a mob of animals and improve profit. This is particularly relevant during periods of feed gaps or drought when feed is supplemented and bought in on farm. Sheep that eat less also present an environmental benefit since methane (CH₄) emissions are highly correlated to dry matter intake (Blaxter and Clapperton 1965). Hence selection of these sheep will help reduce greenhouse gas emissions derived from animal production. In addition, sheep that eat less relative to their cohorts provide producers with more options to manage natural resources on farm.

1.3 Linking ‘Better doers’ phenotype to DNA and protein cellular markers of efficiency

Using our first of its kind method to identify proteins in isolated epithelium, the major protein functions found are related to short chain fatty acid (SCFA) metabolism and others to proteins that regulate the absorptive surface area of the rumen. Of those proteins identified around 25 % are associated with mt function. If quantitative differences in the level of these mt proteins exist, the information can be combined with measures of mt content in a tissue mass.

To quantify the functional groups of proteins and genes that regulate nutrient use and mitochondrial processes in the rumen wall will be combined with proteomic (proteins) studies. Since the proteins tell us what the final level of gene expression is with a given environmental/nutrient signal they are good biomarkers of nutrient and metabolic efficiency. Using this information, we will also determine the suitability of other tissues (epithelium e.g. skin or cheek) that could mirror digestive processes inside the animal and form the basis of a non-invasive test that can select animals that are ‘better doers’.

Fonseca et al. (2015) recently showed that there is lower Mitochondrial Transcription Factor A (a regulator of mt content) expression in more feed efficient Nellore cattle. Based on this range of information a qPCR assay will be developed and validated to screen cattle and sheep for mt content in a high throughput manner to assess their metabolic efficiency.

Hence, this project will develop and validate tools to identify ‘better doers’ for commercial and seedstock producers based on epithelial protein expression and muscle, gut and blood mt content. These tools will initially be established and validated on existing samples linked to available phenotypic data. The tests will then be used in a proof of concept animal experiment to predict ‘better doers’ and then validate that their relationship to better growth or production traits related to nutritional availability.

1.4 Phenotypic variation in methane emission

Ruminant livestock are a major contributor to Australian agricultural sector carbon emissions. In Australia enteric methane contributes to 8-10% of all greenhouse gas emissions. Enteric methane, emitted by ruminant livestock, contributes 75 -80 % of the agriculture sector emissions. Large abatement opportunities (2 -2.8 Mt CO₂ e) can potentially be delivered through reduced emissions from livestock using dietary strategies or selecting for livestock with lower intake and methane emission. To meet the demand of many of our key international markets, the Australian red meat

industry has an imperative to reduce GHG emissions and transition to lower carbon systems required to limit climate change.

Methane emitted by ruminants is produced by methanogenic rumen archaea that utilise by-products of fodder fermentation produced by other microbes in the rumen (Kittleman et al. 2014; Wallace et al. 2015). These metabolites include hydrogen, methyl donors and acetate. Methane emission from ruminants is positively correlated to feed intake (Blaxter and Clapperton 1965) and is measured as methane yield (CH_4 g/kg dry matter (DM) intake). Availability of higher quality feed (e.g. metabolisable energy 10-15 MJ/kg DM) allows feed to pass through the rumen faster but requires more feed to be eaten. Associated with lower emissions are short chain fatty acid profiles with a higher propionate to acetate ratio and a higher proportion of microbial populations such as *Sharpea* sp. and *Kandeliera* sp. (Kamke et al. 2016; Kumar et al. 2018) which produce metabolites such as lactate. The amount of substrate available for fermentation by microbes and absorption by the host is affected by the amount of feed eaten, the composition of digestible nutrients in the feed and mean retention time (MRT) of digesta in the rumen (Thornton and Minson, 1973). In turn, MRT of rumen digesta depends on dry matter intake (DMI), feed composition, size of the feed particles, rumen volume and a wide range of physiological affecters including innervation of the reticulo-rumen by branches of the vagus and splanchnic nerves (Leek, 1986).

Estimates of the heritability of MY range from 0 - 0.13 in sheep (Pinares-Patiño et al., 2013; Robinson et al., 2014) and 0.20 in beef cattle (Donoghue et al., 2013). This suggests that some aspects of CH_4 production are influenced by host genetics. Evidence to date indicates that some variation in MY of sheep lies in differences in rumen size (Bain et al., 2014) and rate of passage of digesta (Goopy et al. 2014; Pinares-Patiño et al. 2003; Bond et al. 2016).

1.5 The process of nutrient absorption

In ruminants, the main products of fermentation of dietary fibre are SCFAs, (acetate, propionate and butyrate) which account for more than 70 % of the animal's caloric intake Bergman *et al.* 1990. The rumen epithelium is well adapted to absorb short chain fatty acids. The best described model of SCFA absorption occurs transcellular movement along electrochemical gradients (SLC16A1) and occurs with the import of Na^+ . Sodium can be exported from the cell via active transport by Na^+ / K^+ ATPase. Hence the transport of nutrients is dependent upon the tonicity (concentration of metabolites) of the rumen fluid and availability of co- or counter ions for transport of nutrients by solute carrier protein (SLC) transporters. Generally, the tonicity of blood is much lower than rumen fluid creating a concentration gradient which facilitates diffusion of nutrients from the rumen fluid, across the epithelium, via cell membrane transporters, into the blood.

The rumen epithelium of sheep fed PW represent a diet with a high K^+ and low Na^+ ratio. Since nutrient transport of SCFAs is dependent on this process we wanted to examine how the rumen epithelium proteins reacted to these different mineral conditions. Perennial cereal crops for grain and grazing present many advantages for mixed farming (livestock/ cropping), including filling winter feed deficits for livestock, resting pasture, increasing animal carrying capacity, increasing animal growth rates and assisting with the management of weeds and crop residues. Despite the widespread use of cereal crops (wheat, triticale, barley) in conventional grazing systems, those diets have a high $\text{K}^+ : \text{Na}^+$ ratio which is known to substantially increase the risk of metabolic disorders in high-producing livestock.

1.6 Significance to industry

We detected a number of significant associations between RFI and the other phenotypic measurements. These include, LWT 60 days, average daily gain, fat gain EBW and methane emission. Consistent with other studies the RFI phenotype require less feed for the same weight and gain are leaner, emit less methane have a lower liver MT content. Therefore, representing animals that require lower feed costs and better environmental outcomes for the climate. Although the CH4 phenotype was linked to RFI phenotype this indicates the traits co-vary but are sufficiently different to select them separately. The deposition of fat is an important consideration for breeding traits since it affects the reproductive capacity and meat quality. Fat enables an animal to maintain some resilience to seasonal changes in pasture quality and quantity. Hence the significance to industry is that selection for RFI must be considered in relation to the production goals of the producer and production system or climate in a given operation.

Our results demonstrate how both host cellular mitochondrial metabolism and rumen epithelium proteins affect the efficiency of the RFI phenotype. The finding that known phenotypes are linked to differences in the protein cellular markers is significant and demonstrates that there are molecular mechanisms affecting efficiency of nutrient use at the cell level in the rumen wall. These may provide new ways to select nutrient efficient traits.

The knowledge gained and the overall goal will be the identification and selection of animals that will improve the overall feed efficiency of flocks and herds by 15 % by 2025 and will simultaneously reduce CH4 emissions.

The identification of nutrient transporters in the rumen epithelium has the capacity to absorb a wide range of nutrients including simple carbohydrates, amino acids, lipids, minerals and nitrogenous compounds. A comprehensive range of metabolic pathways to breakdown plant fodder is also available in the rumen microbiome. Therefore, the flexibility ruminants have in their digestive processes opens up a variety of feed sources that can be sourced or provided by producers feed ruminants. How well these are absorbed by the rumen impacts how efficient nutrient use is by the rumen epithelium. This in part contributes to phenotypic variation in traits such as RFI and methane emission.

The ruminal epithelial barrier is required for nutrient use efficiency in sheep. Surface of the epithelium is connected to the basal layer. Exposure of the barrier function to mechanical stress instructs s. basale epithelium cells to proliferate and thicken the s. corneum. Exposure of the barrier function to mechanical stress instructs s. basale epithelium cells to proliferate and changes in the level of tight junction proteins. It is likely chaff, or a roughage diet vs soft fresh forage has a different impact on the barrier function of the epithelium and hence immune responsiveness. For example, in the perennial wheat fed sheep rumen epithelium the barrier function was being reinforced or repaired and we did not see evidence to suggest an immune response was mounted. Instead we found the addition of lucerne to the diet of perennial wheat the proteins driving short chain fatty acid absorption instead of glucose were more abundant. Also, mineral transporters that regulate SCFA absorption in the diet had different abundance which indicates the lack of sodium in the diet probably has an impact on nutrient use efficiency. The implication for industry is how we fine tune the formulation of diets in cereal forage crops commonly fed to sheep and cattle to overcome fed gaps. It also sheds light on how to provide the best supplement strategies to correct mineral imbalance and any accompanying metabolic disturbance in sheep and dairy cattle.

Conditions such as feed restriction causing reduced SCFA absorption can be associated with metabolic disease states such as hypocalcaemia, ketosis, mastitis, diabetes. Inflammation leading to systemic inflammation can be caused when the barrier function is compromised or broken down. The role of cellular based inflammation in rumen epithelium leading to systemic inflammation in a range of disease states and their relationship to nutrient use efficiency warrants further research. As our protein markers found indicate this occurs in the low CH₄ rumen epithelium of ewes fed a 1.5 x energy diet it is likely these processes are the cause of energetic losses. The higher resistin protein levels probably cause lowered insulin sensitivity also contributing to reduced cellular energy from glucose in the low CH₄ rumen epithelium. In the perennial wheat fed sheep rumen epithelium the barrier function was being reinforced or repaired and we did not see evidence to suggest an immune response was mounted.

2. Objectives

2.1 The ‘better doers’ phenotype

- The primary objective of our animal experiment was to define what a ‘better doer’ is. **Completed in relation to feed intake efficiency and retention of energy in the body.**
- We then sought to link this phenotypic information with DNA and proteins markers to develop one or more tests to identify ‘better doers’. **Successful and completed.**
- Improve our understanding of the processes regulating nutrient transport efficiency in rumen epithelium. **Successful and completed**
- Knowledge of the impact of mineral imbalance on animal nutrition and nutrient use efficiency. **Successful and completed**
- Overcome metabolic disturbances which might reduce nutrient absorption and provide a sure bet way to overcome mineral imbalance using supplements. **Developing and completed**
- These would be used to improve management strategies for producers and improve selection and breeding programs. **Comprehensive definition of phenotypes will enable the successful outcome of this objective. Completed**
- Enable producers to make proactive strategic decisions to manage different groups of animals to utilise high quality forage more efficiently, reducing feed costs, combating constraints on feed availability while improving maintenance of weight, animal growth, reproductive performance and achieving genetic potential. **Completed**
- Provide valuable linkage between the agronomic and adoption outcomes of the LPP P.PSH.1036 Novel Dual Purpose Perennial Cereals for Grazing and ‘better doers’ project. **Completed.**

2.2 Project objectives

- a) The primary objective is to develop one or more tests to identify ‘better doers’ for use to improve management strategies for producers and in selection and breeding experiments.
 - Use our first of its kind procedure to isolate the epithelial cells of the rumen wall to quantify functional gene and protein groups that effect nutrient use efficiency in sheep and cattle (NSWDPI).

- Develop a validated assay to determine mt content in muscle (and other tissues) in cattle and sheep (UQ).
- b) Define the relationship between mitochondrial content and functional protein group abundance to find relationships that can define ‘better doers’ in different red meat production systems within northern and southern agro-climatic regions in Australia.
- c) Identify tissues, such as epithelium (skin or cheek) that could form the basis of a non-invasive animal diagnostic test that can select animals for advantageous digestive processes.

3. Methodology

3.1 Animal experiments

3.1.1 Phase 1 – Selecting growing merino wethers based on variation in the RHI phenotype

Animal use was approved (AEC approval # 19-065) by the animal ethics committee of the University of New England. One hundred and seventeen 6 mth old Merino wethers were used in this study. The wethers were F2 progeny of the Merino lifetime productivity project (AWI) at the Trangie research station (NSWDPI). All had the same history of rearing and access to feed, until the experiment described commenced. All wethers were shorn in November 2019 at UNE Kirby farm and treated with backline lice control (Extinosad™). Immediately after shearing the sheep were housed in groups of 10 in at UNE CART facility. The experiment commenced after 15 days acclimatisation in the animal house on a diet of chaffed lucerne (*Medicago sativa*) and oaten hay (*Avena sativa*) 50:50 w/w (Manuka feeds Quirindi, Australia). During the experiment 2 sheep died leaving 115 that were recorded.

The experimental activities and timeline to collect phenotype data on traits related to nutrient use efficiency including residual feed intake (RFI), liveweight ($Lwt_{60\text{ days}}$), body composition and heat expenditure (gas emissions) is outlined in Fig 1. In the experiment conducted we designed the feeding conditions and length of recording period to capture variation in feed intake like the method used to record residual feed intake trait (RFI) in cattle. Sheep were fed *ad libitum* the same diet (50 % cereal chaff: 50% Lucerne chaff) for 60 days. The day after feed was offered, residual feed was weighed, and new feed offered. Sheep were rotated in three blocks of the same 40 sheep from group pens to individual pens. Each rotation the sheep’s intake was recorded for 3 consecutive days. Each rotation took a 10 day period to complete measurements of all sheep. Each rotation was carried out 6 times for each sheep. The sheep’s liveweight ($Lwt_{60\text{ days}}$) was recorded every 7 days.

One week before the feeding period of 60 days commenced each sheep liveweight was recorded at the beginning and end of the week and all sheep were CT scanned (CT Lwt before). Feed intake and liveweight were measured for the next 60 days. Each day the sheep were fed at 0830 *ad libitum*. Liveweight was recorded each week on the same day. One week after the feeding period of 60 days the sheep’s liveweight was recorded at the beginning and end of the week and all sheep CT scanned (CT Lwt after). At the end of the 60 day feed trial, gas exchange of each sheep was measured in respiration chambers for 24 h over a 21 day period (Bond et al. 2017). Gas exchange (CH_4 , CO_2 , O_2) were recorded and faeces and urine for nitrogen and carbon retention were collected over a 22 h period.

Figure 1. Timeline and activities conducted in the 1st phase of the experiment to phenotype ‘Better doers’ sheep based on feed intake, liveweight, body composition and heat expenditure.

<u>Date</u>	<u>Activities 1st phase of experiment</u>
5.11.2019	<ul style="list-style-type: none"> • 120 6mth old Merino wethers transported to Kirby Farm UNE
6.11.2019	<ul style="list-style-type: none"> • All sheep shorn, treated for lice and put in group pens at Centre for animal research and training (CART) UNE. 3 sheep sold (1 ewe, 2 stags).
7-19.11.2019	<ul style="list-style-type: none"> • Sheep acclimatised to animal house, treated for shearing cuts that became infected and fed a diet ad libitum of 50:50 lucerne and cereal chaff once daily.
11-14.11.2019	<ul style="list-style-type: none"> • All sheep CT scanned D0 measurement
19.11.2019	<ul style="list-style-type: none"> • Start of the 60 days of sheep feed above diet. 40 sheep feed intake (FI) measured daily for 3 days in individual pens, then rotated to next group. All sheep measured for FI 5 repeats x 3 days through the 60 day trial. Liveweight measured once a week.
8.01.2020	<ul style="list-style-type: none"> • Acclimatise sheep to restricted space for respiration chamber measures using portable chambers in CART. • Formulate a high and low diet for second phase of experiment and order feed.
17.01.2020	<ul style="list-style-type: none"> • Develop CT scan procedure and check data is correct • End of the 60 day feeding period
28-31.01.2020	<ul style="list-style-type: none"> • All sheep (115 two died-unknown cause) CT scanned D70 measurement
01-25.02.2020	<ul style="list-style-type: none"> • All sheep put through respiration chambers- methane, oxygen and carbon dioxide measured for 24 hours once each sheep. Urine and fecal matter collected for Carbon and nitrogen balance measures. • Process all CT scan images from D0 and D70. Calculate fat, muscle and bone proportion, Carcass fat and muscle gain (g/d) in empty body using three parts of the carcass as estimates.
28.02.2020	<ul style="list-style-type: none"> • Compile all data into a summary and do statistical analysis to assign sheep to the ‘better doer’ and ‘lesser doer’ phenotype n=44. <p>End of 1st phase of the experiment – all sheep not selected as better doer or lesser doer assigned to an experiment run side by side for Australian feeding standards LPP project.</p>

3.1.2 Phase 2 – Low or high RFI fed a high or low energy diet for 30 days

Animal use was approved (AEC approval # 19-065) by the animal ethics committee of the University of New England. The second phase of the experiment was designed to select 40 sheep out of the 113 with divergence in phenotypic traits such as RFI, LWT, ADG, body composition or heat expenditure.

After assigning sheep to two groups ‘better doers’ (n=20) and ‘lesser doers’ (n=20) the sheep were fed two different diets (high or low diet) for 30 days. Each treatment group had 10 sheep.

The contrast in the diets was based on metabolizable energy (ME MJ/ kg DM) and crude protein % (CP). The high diet had a higher ME and CP % and 40 % rolled barley grain, 50 % Lucerne chaff and 10 % cereal chaff. The low diet consisted of 70 % cereal chaff and 30 % Lucerne chaff. Sheep were kept in individual pens and fed the diets once each morning, with residual feed recorded each day. A period of 8 days was used to adapt the sheep from 50% lucerne chaff: 50% cereal chaff to the high or low diet.

All sheep were housed in individual pens and residual feed intake recorded daily. Each week sheep was weighed to record liveweight (LWT). On day 0 (D0) and day 30 (D30) all sheep were CT scanned. After 25 days all sheep were put through respiration chambers overnight to collect gas emissions data (CH₄, CO₂, O₂), faeces and urine for nitrogen and carbon balance for calculation of energy retained.

3.1.3 Low or high CH₄ emission phenotype.

Animals, measurement of phenotypes and methods for sample collection, storage and preparation prior to analysis are described in Bond et al. 2017. The work was conducted under University of New England Animal Care and Ethics approval (AEC # 14-041). 10 high and 10 low CH₄ emitting sheep. 1.5 x maintenance energy requirement diet fed twice a day.

3.1.4 Perennial wheat and perennial wheat and Lucerne diets

Details of the pen feeding experiment are given by Newell et al. (2020). Briefly, a pen study comprising 48 crossbred ewes (Poll Dorset x Merino) housed individually were fed fresh cut forage for 4 weeks (15 May 2019 – 10 June 2019) prior to slaughter at a commercial abattoir. There were 12 sheep assigned to 4 diet treatment groups. Diet 1) perennial wheat (*T. aestivum* x *Thinopyrum ponticum*) line 11955, 2) perennial wheat and lucerne (*Medicago sativa* cv. Titan 9), 3) conventional wheat (*Triticum aestivum* cv. Wedgetail) and 4) wheat and Lucerne. The diets represented contrasting levels of potassium (K⁺): sodium (Na⁺) or calcium (Ca²⁺):magnesium (Mg²⁺) ratio. Feed was provided 3 times daily. Drinking water was always available.

A summary of the phenotypes and dietary plus other variables cross sectioned in this project is found in Table 1.

Table 1. Background information about the variables cross sectioned and the datasets analysed for the whole project.

Variable		Sheep experiment 1				2		3	
Genotype	Cattle	Merino				Predominantly Merino		Poll dorset X merino	
Physiological state		growing				Adult			
Sex		Wethers				Ewe		Ewe	
Phenotype	RFI	RFI				Low Methane emission	High methane emission		
Diet level fed	Ad Libitum	Ad libitum				1.5 x maintenance			
Diet composition	pasture	50:50				50:50 Cereal chaff:Lucerne chaff		PW	PW+L
Diet mineral		balanced				balanced		imbalance	
Phenotype x diet		Low RFI High energy diet	Low RFI Low energy diet	High RFI High energy diet	High RFI Low energy diet				
Rumen epithelium protein data		X	X	X	X	X	X	X	X
Mitochondria l content	x	X	X	X	X	X	X		

3.2 Feed composition, diet formulation.

Samples of the feed were collected throughout each experiment and submitted for analysis (Table 2). Samples were measured for dry matter (DM), neutral detergent fibre (NDF), crude protein (CP), ash, organic matter (OM), DM digestibility (DMD), metabolisable energy (ME), water soluble carbohydrates (WSC) and acid detergent fibre (ADF). The chemical composition of the feed on offer was analysed by the Feed Quality Service (<http://www.dpi.nsw.gov.au/content/about-us/services/das/feed-quality-service>, Department of Primary Industries, Wagga Wagga) using the methods described by the Australian Fodder Industry Association (AFIA 2014). In addition, for mineral composition of feed total nitrogen, crude protein, phosphorus, potassium, calcium, magnesium, sodium, chloride, manganese, copper, zinc, iron, nitrate, boron, sulphur, molybdenum, cobalt and selenium was analysed by the regional laboratory service (www.regionallabservices.com.au, Benalla, Victoria).

Table 2. Dry matter (DM) content and chemical composition (% DM basis, unless otherwise indicated) of the diets feed for each experiment.

A mineral supplement of 0.5 % AgLime (Calcium carbonate) and 0.5 % salt (sodium chloride) was added w/w of the total ration offered in High and low diet. Perennial wheat (PW) diets are taken from Table 2 in Newell *et al.* 2020. NA= information not available.

Feed component	High diet 40:50:10 Barley grain: Lucerne chaff: Cereal chaff	Medium diet 50:50 Lucerne chaff: Cereal chaff	Low diet 30:70 Lucerne chaff: Cereal chaff	PW	PW + Lucerne
Metabolisable energy (MJ /kg DM)	11.6	9.5	9.2	12.0	11.5
Crude protein	14.5	13.9	11.5	24.3	22.1
Dry matter	89.3	90.1	90.1	NA	NA
Neutral detergent fibre	35	49	56	45	40
Acid detergent fibre	20	31	33	NA	NA
Water soluble carbohydrates	5.7	8.1	10.2	NA	NA
DMD*	77	65	63	79	76
Phosphorus	0.20	0.22	0.25	0.25	0.21
Potassium	1.2	1.8	2.1	4.7	3.5
Calcium	0.95	0.83	0.62	0.34	0.82
Magnesium	0.29	0.30	0.23	0.12	0.14
Sodium	0.41	0.37	0.32	0.005	0.012
Chloride	0.12	0.11	0.89	0.74	0.59
Sulphur	0.20	0.22	0.20	0.35	0.31

*Estimated from *in vitro* analysis.

3.3 Measurement of Body composition

Wethers were CT scanned in the prone position using a GE HiSpeed QXi 4 Slice CT Scanner (GE medical systems, Beijing, PR China). Set-up and scanning of each sheep took approximately 5 mins for each sheep. Webbing straps were used to restrain the sheep in an upright position with their legs underneath their body (workflow summarised in Fig 2). The X-ray tube energy setting was 120 kV and 140 mA. 5 mm cross sectional slices were taken at 5 mm intervals between the 1st thoracic vertebrae through to the last vertebrae. Image analysis procedure was adapted from a method described by Kvame and Vangen (2006).

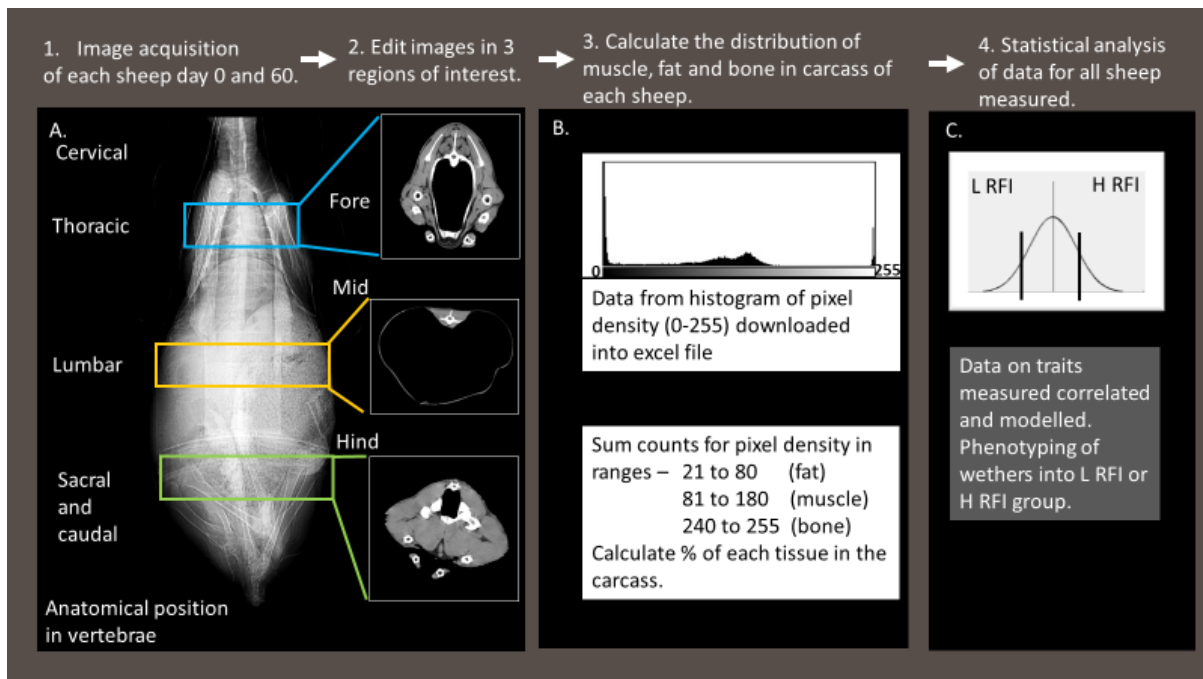
Figure 2. Illustration of body composition

Figure 2 illustrates the workflow. Each CT-DIACOM image was manually edited (OsiriX <http://www.osirix-viewer.com/>), to remove the lung, liver, heart, intestines and reticulo-rumen (RR). A series of at least 9 edited images in each of 3 regions (fore, mid and hind) in the carcass were saved in 16 bit resolution. The orientation of the anatomy varied depending on the position of the animal during the scan. Therefore, the fore region consisted of a series of at least 6 slices from 2nd thoracic vertebrae and a cross-section of the forelimbs. The mid region consisted of at least 6 images taken through the widest mid-section of the reticulo-rumen (RR) within the lumbar spine. The hind region consisted of at least 6 slices edited within the pelvis, through the sacral and caudal vertebrae containing the widest cross section of the hindlimbs. Edited images were then further processed to remove non-carcass tissues (cradle and restraining straps) using Image J (<http://imagej.nih.gov/ij/v1.47>).

A histogram of counts for each pixel in the grey scale range of 0-255 pixel densities was recorded for each image. There were triplicate images for each region (Fore, mid and hind n=9 total) for each animal, from which the proportion (%) of fat, muscle (lean) and bone were then determined. Greyscale pixel density used for boundaries were 21 to 80 fat, 81 to 180 for lean, and 240 to 255 bone. Firstly, background densities from 8-20 and 181-239 average counts were subtracted from each of two hundred and fifty five count values. The formulae for percentage of fat, lean and bone were according to the following example for fat;

Fat counts = sum of counts with a density (21-80)
 Fat % = Total Fat counts*100 / Total animal counts
 The sum of fat % in fore, mid and hind regions were averaged.
 Average Fat % = (fat % fore + fat % mid + fat % hind) / 3

To get the exact proportion of fat, lean and bone the sum of counts for each tissue was converted to a weight to estimate change in lean and fat weight over 60 days (gain g/d) for the whole body.

First the total counts for all nine images of each tissue were scaled for tissue density (fat = 0.95 g/cm³, lean = 1.05 g/cm³, bone = 1.45 g/cm³).

Fat Density (%) = Total Fat counts x 0.95

Then the scaled weight was normalised, for example;

Fat weight (%) = Fat density / Total density x 1

The normalised tissue density was converted to fat weight in empty body weight (EBW) for scans before and after the 60 day feed period. For example;

Fat weight (kg) = (live weight before 60 days kg) x 0.70) x (fat % before) / 100

Then tissue gain (g/d) was calculated, for example;

Fat gain (g/d) = (Fat weight Day 60 - Fat weight Day 0 (kg)/ 60 d) x 1000

The same calculations were used for Lean and Bone to measure the weight of Lean and Bone over 60 day's period.

3.4 Measurement of CH₄, CO₂ and O₂ in respiration chambers

The sheep were measured for gas emissions using eight open circuit RCs (Bird *et al.*, 2008). Measurement commenced at 10.00 am when the sheep were given their morning ration. The measurements were made over three weeks and liveweight data was recorded each week (Lwt RC). The method described by Bond *et al.* (2017) was used to run the chambers and calculate the CH₄ and CO₂ expelled by each sheep over a 22 h period. Gas exchange was sampled 2 ml / min and stored in a tedlar bag for measurement of O₂ using a Foxbox gas analysis system (Sable Instruments, Las Vegas, NV).

A daily feed intake (DMI_{RC}) was calculated to take account of variation in daily methane emission on the dry matter intake day before RC (FI day before) and DMI day of RC (FIRC) reported in previous studies (Bond *et al.* 2017). Linear regression of DMIRC versus DMI day before RC was significant (P < 0.001) with a correlation of 64 % DMIRC and 33 % DMday before RC.

The total amount of faeces were collected using a foot pad and thin mesh screen. The total weight of faeces collected on the foot pad was recorded at the end of the RC chamber period for each sheep. Ten % of the total weight of the faeces measured at each collection from each sheep, and stored at -20 °C until analysis for DM, C % and N %. Urine was collected in the tray underneath the respiration chamber separated from faeces by mesh screen. Urine was acidified with 100 mL of sulfuric acid (2.88 M H₂SO₄) to maintain a final pH < 2 and stored at -20 °C until further analysis for total C % and N %. The main digestibility measures were organic matter intake (OMI), organic matter digestibility (OMD), digestibility of organic matter intake (DOMI), faecal organic matter (FOM), estimated maintenance and total metabolizable energy (MEI).

Heat production in energy balance was calculated using Brouwer equation:

Heat (kJ/d) = 16.2 x O₂ + 5.0 x CO₂ – 6.0 x N - 2.2 x CH₄

Another method to compare the Heat (Brouwer equation) was Heat CO₂ method. First Heat CO₂ flux was calculated and then Heat was measured using the following formula.

Host CO₂ flux (g/d) = CO₂ (g/d) – 4 * CH₄ (g/d)

Heat CO₂ (Kj/d) = Host CO₂ flux (g/d) * 10.75

Heat CO₂ (Mj/d) = Heat CO₂ (Kj/d) / 1000

Heat CO₂ (MJ/kg) = Heat CO₂ (Mj/d) / Lwt ^ 0.75

3.5 Isolation of epithelium and extraction of cytosol and membrane proteins

Frozen tissue pieces of ventral rumen wall were collected post-mortem from sheep in experiments detailed in section 3.1.1. The epithelium proteins were isolated enzymatically from the underlying lamina propria and fractionated according to the method described by Bond *et al.* 2019. The two fractions extracted were for cytosol and membrane proteins. The only exception to Bond *et al.* 2019 was the cytosolic proteins were dialysed against 3 changes of 1% sodium dodecyl cholate (SDC) in 100 mM triethylammonium bicarbonate (TEAB; pH 8.5) over 18 h. The membrane fraction supernatant was dialysed with 3 changes of 1% SDS in 100 mM Tris (pH 8.5), over an 18 h period. Protein concentration of cytosol and membrane proteins were quantified using the Pierce™ BCA protein assay (Thermo scientific, Rockford, IL, USA) and 2D Quant Kit (GE Healthcare, NJ, USA) respectively.

3.5.1 Sample preparation for LC-MS/MS analysis

An equal amount of protein (approximately 1 µg) from each sample was used for further testing. SDS in the membrane samples was removed using a detergent removal column (S-Trap™; Profiti, Farmingdale, NY, USA) as per the manufacturer’s instructions and finally eluted using 100 mM Tris-HCl (pH 8.8). Post SDS removal, samples were reduced with 10 mM DTT followed by alkylation with 20 mM iodoacetamide (IAA) in the dark. The reaction was quenched with excess DTT for 15 min. Samples were digested at 37 °C, overnight with trypsin at a 1:50 ratio. The digests were quenched with formic acid, and samples were desalted using self-packed SDB-RP StageTips Kamath *et al.* 2017. For more detail on the methods used to quantify proteins by tandem mass spectrometry please see appendix x.

3.6 Rumen fluid and blood metabolite quantitation

¹H NMR spectra were acquired at 298K in 3 mm tubes on a Bruker Avance 900 NMR spectrometer with CryoProbe using a SampleJet (96 tube racks) for sample introduction. Samples were maintained at 4oC in the SampleJet prior to introduction into the probe and an equilibration time of 6 min was allowed before commencement of acquisition. Standard Bruker pulse sequences were used. NMR spectra were processed with Topspin 3.2 software, using multiplication by a sine bell, shifted by 90°, prior to Fourier transformation and manual phase correction. Spectra were referenced to internal 4,4-dimethyl-4-silapentane-1-sulfonic acid (DSS) (d0.0). Metabolite concentrations were determined by integration relative to the integral of the internal standard, difluorotrimethylsilylmethylphosphonic acid (DFTMP) (386mM).

3.7 Statistical analysis

3.7.1 Low or High RFI phenotype

Traits measured in 113 wethers over 60 days were carried out using minitab (www.minitab.com; v18). Descriptive statistics (mean, SD) of all the traits measured were tabulated. Pearson correlation coefficients and level of significance of a summary of traits related to growth, body composition measured by CT scan images and gas emission were analysed to show the strength of the correlation as well as significance between traits. Those with a correlation above $r = 0.3$ in bold text had a $P <$

0.001 and those below $r = 0.3$ had a significance of $P < 0.05$. Following this the summary of traits ($n=14$) were analysed using a cumulative R^2 stepwise regression. The rank of the most significant traits that explain the response $FI_{60\text{days}}$ and the cumulative increase in R^2 , coefficient and standard error of the coefficient are reported.

The phenotype for FE was equation 1.

$$FI_{60\text{days}} = \text{intercept} + LWT_{60\text{days}} + \text{error}.$$

That found that best described the variation in $FI_{60\text{days}}$ was the classic Koch et al. (1963) model describing RFI by the equation 2.

$$FI_{60\text{days}} = \text{intercept} + LWT_{60\text{days}} + ADG + \text{error}.$$

Were ‘error’ term in the equation represents the residuals from the RFI model equation 1. Sheep with negative residuals (-ve) were grouped as the low RFI animals ($n= 52$) and sheep with positive residuals were termed high RFI animals ($n=61$). The means and standard deviation of the H or L RFI phenotype were reported.

3.7.2 Low or high CH₄ phenotype

The analyses (www.Rproject.org) were based on measurements from 62 ewes. Robinson *et al.* (2014) showed that methane emissions in the RC were related to feed intake on the day of testing and the two previous days. Consequently, the relationship between CH₄, CO₂ emissions and dry matter intake on the day before (DMIDB) and on the day of RC (DMIRC) testing were examined by fitting a linear regression model. The possibility of a curvilinear response to feed intake was tested by fitting a quadratic term for DMIDB, which was not significant ($P = 0.28$).

The fitted linear model, which explained 76 % of the variation in CH₄ emissions, was:

$$CH_4 \text{ (g/d)} = 2.29 (\pm 2.30) + 11.56 (\pm 1.5) * DMIRC + 5.54 (\pm 2.3) * DMIDB$$

This equation implies that CH₄ emissions depend on DMI in the RC and the previous day, so a DMII was calculated as;

$$DMII = 0.676 \times DMIRC + 0.324 \times DMIDB$$

Methane yield was calculated using the intake index as $MY_i = CH_4 \text{ g} / \text{kg DMII}$.

The fitted regression coefficients were used to adjust methane emissions (g/d) of each animal to the average level of feed intake;

$$CH_{4\text{adjDMI}} = CH_4 - 11.56 \times (DMIRC - \text{mean}(DMIRC)) - 5.54 \times (DMIDB - \text{mean}(DMIDB))$$

$CH_{4\text{adjDMI}}$ equals the predicted level of CH₄ emissions at the average levels of DMI in the RC and on the previous day before measurement in RC. From these figures we selected 10 H CH₄ and 10 low CH₄ ewes with a balance of sires, block effects. Tissues from these sheep were used for analysis by proteomics and mitochondrial content.

3.8 Mitochondrial content assay

3.8.1 Rationale for the development of sheep and cattle mitochondrial content assays

Highly sensitive molecular tests for estimating sheep and cattle tissue mitochondrial content have been successfully designed and implemented. Measuring mitochondrial content gives a cell and tissue level indication of aerobic capacity, or the upper ability of the cell to make ATP (the universal

currency of energy in all life forms) in the presence of oxygen. Because mitochondria must be synthesised and maintained - and consume physical space in the cell - their presence does not come for free, and the energetic cost must be paid for by feed. This indicates that it would be wasteful for farm animals to possess a higher mitochondrial content than is required to meet production, product quality and animal welfare considerations.

The assay design process was facilitated by previous investment in the cattle and sheep genome assemblies. From a technical perspective, the assays have been shown to work well across species, breeds and taurine / indicine sub species allowing us for the first time to estimate variation in ruminant mitochondrial content (and also assess to what extent that variation connects to whole animal phenotypes of commercial importance) across a range of biological circumstances.

A primary motivation for this aspect of the study was to test the ‘Corolla Cow’ hypothesis, that more efficient ruminant farm animals would possess a small economical ‘engine’ as represented by low tissue mitochondrial content. The logic is that reducing spare physiological capacity saves on the collective cost of developing, running and repairing that extra capacity. This is an important consideration in production efficiency if that physiological capacity is over and above what is required for growth / production. The overall pattern of mitochondrial content data from the ‘Better Doer’ Merino trial is consistent with this hypothesis, i.e. that more efficient animals have a tendency towards lower tissue mitochondrial content.

3.8.2 Mitochondrial content assay design

Treating cattle and sheep separately, we compared a set of primer pairs that would independently amplify a portion of nuclear (n) DNA (as a measure of the number of cells or tissue volume in the assay) and mitochondrial (mt) DNA (as a measure of the mitochondrial content of the cells or tissue volume in the assay). A set of technical criteria were applied to ensure highly specific, efficient PCR amplification which was experimentally compared in the first instance using Sybr Green chemistry. The best performing cattle and sheep assays were ultimately modified into duplex Taqman assays that simultaneously amplify the mt and n DNA within a single reaction well. This modification in design and chemistry increases binding specificity and reduces technical error which should lead overall to more accurate and precise estimates.

Some proportion of the observed sample to sample variation will be technical error with the remainder being true biological variation. Previous estimates in monoclonal DF-1 chicken cells presumed to have stable mitochondrial contents indicated technical errors of about 1.5-fold using a similar method of DNA purification followed by qPCR using TaqMan duplex chemistry. This implies, for example, if we observe a total variation of 4-fold across a set of biological samples, that 2.5-fold will be real biological variation once the 1.5-fold of technical variation has been accounted for.

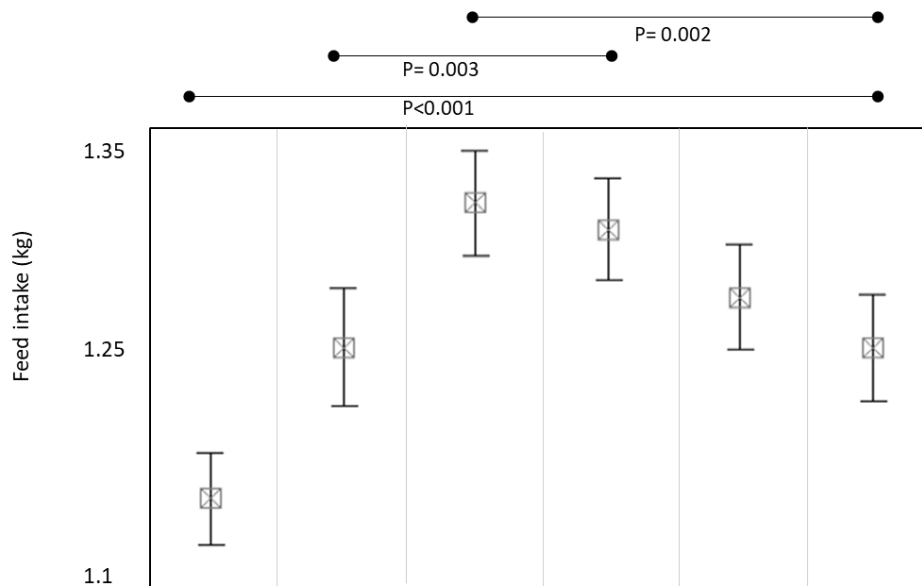
4. Results

4.1 Phenotypic correlates of residual feed intake in growing Merino wethers: how to pick ‘better doers’; Rumen epithelium protein markers and mitochondrial content associated.

4.1.1 Summary of feed composition, feed intake, growth, body composition and gas emission.

The chemical composition of the diet is shown in Table 1. The mean DM of the feed was 91.7 %, with 12.6 % CP, 53.0 % NDF and 9.3 MJ ME /kg DM. Dry matter digestibility (DMD) estimated from in vitro analysis ($63.8 \% + 1.92 \%$) was typical of a fibrous roughage diet. Figure 3a shows the pattern of $FI_{60 \text{ days}}$ increased to a peak at day 30 ($1.31 \pm 0.163 \text{ kg}$), plateaued from day 30-40 ($1.30 \pm 0.152 \text{ kg}$) then dropped between day 40- to 60 on average 70 g / d to a final average of $1.23 \pm 0.172 \text{ kg}$ on day 60. There was a significant ($P < 0.001$) increase in feed intake between day 0-10, and all other points. Feed intake at day 20-40 was significantly higher ($P = 0.003$) than day 10-20. Day 20-40 FI was higher than day 50-60 ($P = 0.002$). Despite this liveweight increase was positive and linear ($r^2 = 0.99$) from $30.12 \pm 4.091 \text{ kg}$ to $35.44 \pm 4.136 \text{ kg}$ over 60 days (figure 3b).

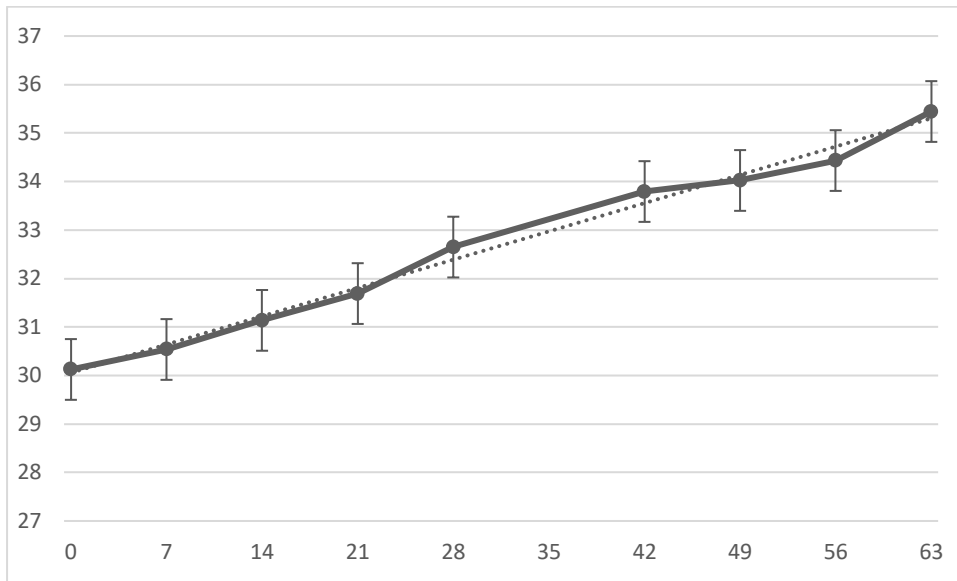
Figure 3a. Interval plot with table of means and s.d. of 113 merino wethers fed a diet of 50 % Lucerne chaff : 50 % cereal chaff ad libitum for 60 days to show the trends in feed intake.



FI days	0-10	10-20	20-30	30-40	40-50	50-60
n	113	113	112	113	112	113
Mean \pm s.d.	1.15 ± 0.141	1.23 ± 0.179	1.31 ± 0.158	1.30 ± 0.152	1.26 ± 0.157	1.23 ± 0.163

The bar above the plot shows significant differences between points. Feed intake was measured in three groups of $n = 38$ in individual pens for at least three days. The rotation was repeated six times for all sheep throughout the 60 day period. When not in individual pens they were kept in groups of 8-10 in larger group pens and fed the same diet *ad libitum* in troughs.

Figure 3b. A line plot of the liveweight 60 days of the same 113 Merino wethers recorded for 60 days.



All sheep were measured for liveweight every seven days for 60 days except at Christmas time. Dotted line $y = 0.0833x + 30.056$ ($r^2 = 0.99$) is the regression equation of LWT over time.

A summary of the means and s.d. of all traits measured is shown in Table 3. $FI_{60 \text{ days}}$ was $1.25 \text{ (kg)} \pm 0.145$, $LWT_{60 \text{ days}}$ (kg) 32.33 ± 3.909 and ADG was 0.083 ± 0.023 (kg/d).

Liveweight corresponding to the CT scan week was initially 28.03 ± 3.788 kg and increased to 35.66 ± 4.074 kg. The proportion of fat at the beginning of the experiment was $5.06 \% \pm 2.112$ and increased to $9.82 \% \pm 2.169$ at the end of the 60 day feeding period (Table 3). Whereas, the proportion of lean and bone at the beginning of the experiment was $76.02 \% \pm 2.363$ and $18.92 \% \pm 2.485$ and decreased to $73.98 \% \pm 2.488$ and $16.19 \% \pm 1.758$ respectively. The relative proportion (%) of fat increased in relation to lean gain throughout the test period. The rate of gain in fat was 24.20 ± 7.490 g/d, lean 59.20 ± 20.070 g/d and bone 0.56 ± 0.82 g/d. Back fat gain 0.093 ± 1.049 (mm) and eye muscle depth gain 0.12 ± 0.380 (mm) and eye muscle area increased (0.908 ± 1.069 cm²). Average staple length was 38.7 ± 10.86 mm and fibre diameter 16.3 ± 1.25 µm.

On average the wethers daily CH₄ emission was 22.6 ± 3.11 g / d and methane yield was 19.64 ± 2.199 CH₄ g/kg DMI_{RC}.

Table 3. The mean, standard deviation (SD) for feed intake, liveweight and average daily gain (ADG), for body composition, fat, lean and bone % on day 0 and day 60 of CT measurement as well as fat, lean and bone gain (g/d), gas emissions dry matter intake index (DMI_{RC} kg) for period sheep were measured for methane in respiration chambers, daily methane (g/d), and methane yield (CH₄ g/kg DMI_{RC}) for all sheep (n=113). Also shown is mean and standard deviation for back fat depth gain (mm; n=101), eye muscle area gain (cm²; n=107), eye muscle depth (cm; n=94), staple length (mm) and fibre diameter (µm) measured in n=93 wethers.

Variable	Mean	SD
FI _{60 days} (kg)	1.25	0.145
LWT _{60 days} (kg)	32.33	3.909
ADG (kg/d)	0.083	0.0230
CT Lwt _{Day-0}	28.03	3.788
% Fat Day-0	5.06	2.112
% Lean Day-0	76.02	2.363
% Bone Day-0	18.92	2.485
CT Lwt _{Day-60}	35.66	4.074
% Fat Day-60	9.82	2.168
% Lean Day-60	73.99	2.488
% Bone Day-60	16.19	1.758
Fat gain _{EBW} (g/d)	24.20	7.490
Lean gain _{EBW} (g/d)	59.20	20.07
Bone gain _{EBW} (g/d)	0.56	0.823
Back fat depth Day-0 (mm)	2.05	0.473
Eye muscle area Day-0 (cm ²)	7.28	1.210
Eye muscle depth Day-0 (cm)	2.08	0.344
Back fat depth Day-60 (mm)	2.97	1.060
Eye muscle area Day-60 (cm ²)	8.19	1.320
Eye muscle depth Day-60 (cm)	2.19	0.340
Back fat depth gain (mm)	0.93	1.049
Eye muscle area gain (cm ²)	0.908	1.069
Eye muscle depth gain (cm)	0.12	0.380
Staple length (mm)	38.7	10.86
Fibre diameter (µm)	16.3	1.25
DMI _{RC} (kg)	1.15	0.102
CH ₄ (g/d)	22.6	3.11
MY (CH ₄ g/kg DMI _{RC})	19.64	2.199

4.1.2 Inter-relationships between FI, growth, body composition and CH₄ emission traits.

Pearson correlation between FI, growth, body composition and gas emission traits that were significant ($P < 0.001$, $P < 0.05$) are shown in Table 4. There was a strong positive correlation between FI_{60 days}, LWT_{60 days} ($r = 0.799$) and DMI_{RC} ($r = 0.768$). The correlation between FI_{60 days} and ADG ($r = 0.359$), fat gain ($r = 0.478$), lean gain ($r = 0.287$), staple length ($r = 0.394$) and fibre diameter ($r = 0.320$) and daily CH₄ ($r = 0.489$) was lower.

LWT_{60days} had the highest correlation to DM_{li} ($r = 0.633$) while daily CH₄ emission was lower ($r = 0.365$). There was no significant correlation between LWT_{60days} and ADG. LWT_{60days} and fat gain ($r=0.288$) and staple length ($r=0.289$) were slightly correlated. Significant correlations between ADG and with lean gain ($r=0.729$), DM_{RC} ($r=0.354$), daily CH₄ ($r=0.448$), and MY ($r=0.256$) existed.

Other correlations are shown in the table.

Table 4. Pearson correlation between traits with $r > 0.300$ have a $P < 0.001$ and those below $r = 0.300$ have a $P < 0.05$ represented in bold text.

	FI _{60 days} (kg)	LWT _{60 days} (kg)	ADG (kg/d)	Fat gain (g/d)	Lean gain (g/d)	Back fat depth (mm)	Eye muscle area (cm ²)	Eye muscle depth (cm)	Staple length (mm)	fibre diameter (µm)	DM _{RC} (kg)	CH ₄ (g/d)
LWT _{60 days} (kg)	0.799											
ADG (kg/d)	0.359	0.085										
Fat gain (g/d)	0.478	0.288	0.315									
Lean gain (g/d)	0.287	0.083	0.729	0.109								
Back fat depth (mm)	0.178	0.245	-0.003	0.137	-0.039							
Eye muscle area (cm ²)	0.202	0.062	0.216	0.126	0.212	0.085						
Eye muscle depth (cm)	0.066	0.009	0.065	0.014	0.062	0.162	0.591					
Staple Length (mm)	0.394	0.289	0.125	0.096	0.124	0.036	0.252	0.065				
Fibre diameter (µm)	0.32	0.26	0.128	0.031	0.045	0.038	0.139	-0.039	0.315			
DM _{RC} (kg)	0.768	0.633	0.354	0.384	0.385	0.124	0.153	0.110	0.385	0.393		
CH ₄ (g/d)	0.487	0.365	0.448	0.153	0.414	0.152	0.224	0.177	0.227	0.093	0.570	
MY CH ₄ (g/Kg DM _{RC})	-0.019	-	0.256	-0.111	0.185	0.071	0.13	0.112	-	-0.165	-0.1	0.759

4.1.3 Cumulative R² and stepwise regression of significant traits to explain variation in FI_{60 days}.

A stepwise regression was used to rank traits that were significant variables and fit a model that best explained FI_{60 days} (Table 5). Lwt_{60 days} ($R^2 = 61.2\%$; $P < 0.001$) and ADG ($R^2 = 68.3\%$; $P < 0.01$) explained the majority of variation in FI_{60 days}. The addition of fat gain to the model made a small improvement in the fit ($R^2 = 71.8\%$; $P = 0.002$). Interestingly, staple length increased the fit ($R^2 = 74.0\%$; $P = 0.06$) such that 1 g of feed eaten equalled a 1mm increase in staple length. Daily CH₄ gave a small ($R^2 = 74.0\%$) but significant ($P=0.024$) increase in the fit to explain FI_{60 days}. Whereby for each 6 g eaten there was an increase in daily methane emission (g/d). Therefore, the model that is classically used to explain the residual feed intake phenotype (Koch et al. 1963) best described the better and lesser doer phenotype.

Table 5. Regression equations to rank of significant traits to account for variation in FI 60 days and other traits.

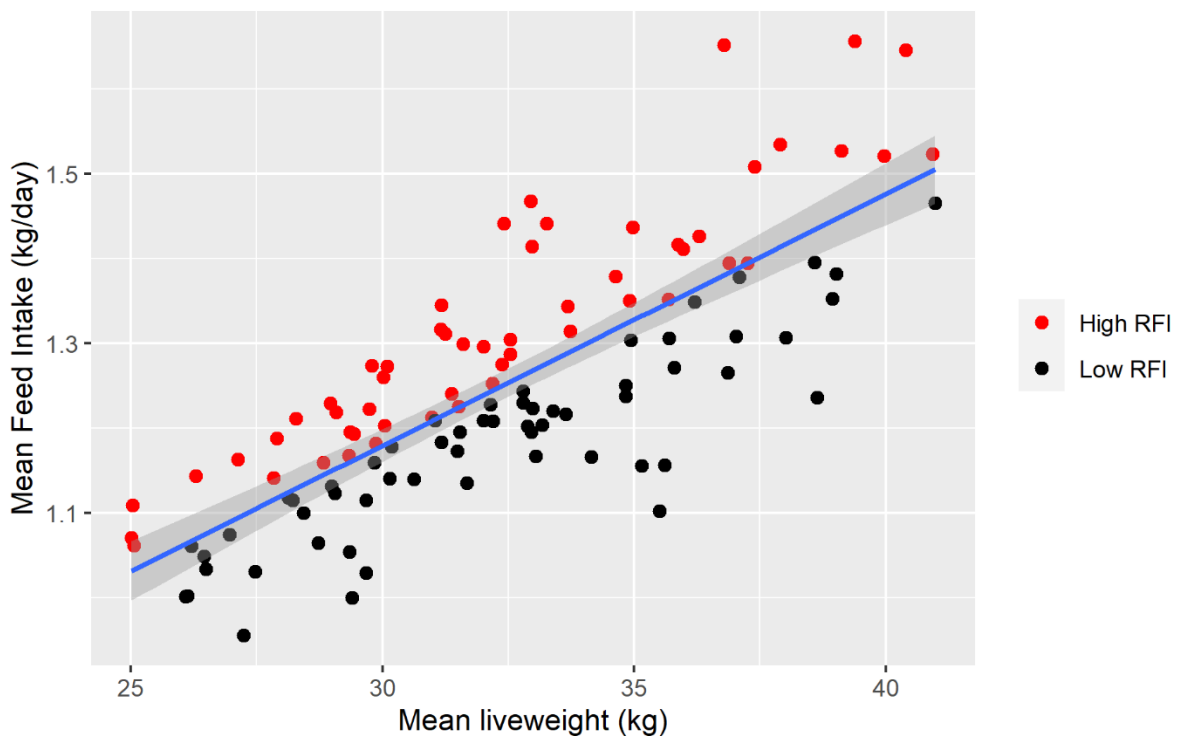
Trait	Cumulative R ²	Coefficient \pm s.e.	P value
Response = FI _{60days} (kg)			
Intercept		-0.0018 \pm 0.10954	
1. LWT _{60days} (kg)	61.2	0.023 \pm 0.0022	0.001
2. ADG (kg/d)	68.3	0.090 \pm 0.0358	0.01
3. Fat gain (kg/d)	71.8	0.004 \pm 0.0011	0.002
4. Staple length (mm)	74.0	0.001 \pm 0.0007	0.059
5. CH ₄ (g/d)	74.7	0.006 \pm 0.0027	0.024

4.1.4 Selection of sheep into L or H RFI phenotype.

Using equation 1 in table 5, those with negative residuals (-ve) were grouped as the low feed efficient animals (n= 5) and sheep with positive residuals were termed high feed efficient animals (n=58) according to residuals that were negative or positive. Figure 4 illustrates this relationship between FI_{60 days} and LWT_{60 days}. The phenotype model here was used to make correlation with other metabolically active tissues using the mitochondrial content DNA assay (UQ sub contract).

Figure 4. Linear regression of mean FI_{60 days} (y axis; kg) against mean LWT_{60 days} (x axis; kg) for 60 days.

The residuals deviating from the line of best fit (blue solid line) represent the sheep with low feed efficiency (block dots n=55) and high feed efficiency (red dots n=58) phenotype.



Following the description of a ‘better doer’ shown above based on the residuals from the equation 2 in table 5 (FI_{60 days} = intercept + LWT_{60 days} + ADG + error) we grouped sheep into L and H RFI

phenotype. A summary of the data is shown in Table 6. At *ad libitum* feeding level H RFI growing Merino wethers ate ($1.31 + 0.150$ kg) more than L RFI ($1.19 + 0.118$ kg) for the same liveweight (32.3 ± 4.01 kg) and average daily gain (0.08 ± 0.024 kg/d). The fat gain was higher in the H RFI sheep (26.2 ± 7.850 g/d) and lower in the L RFI sheep (22.5 ± 6.796 g/d). H RFI ate more and emitted more methane ($22.10 + 2.871$ g/d) compared to L RFI (23.18 ± 3.381 g/d) sheep.

Table 6. mean and s.d. for traits related to L or H RFI.

Variable	RFI	N	Mean	s.d.	P value
FI _{60 days} (kg)	L	61	1.19	0.118	0.001
	H	52	1.31	0.150	
LWT _{60 days} (kg)	L	61	32.39	3.854	ns
	H	52	32.26	4.008	
ADG (kg/d)	L	61	0.082	0.0233	ns
	H	52	0.084	0.0246	
Fat gain (g/d)	L	61	22.53	6.796	0.01
	H	52	26.15	7.850	
Lean gain (g/d)	L	61	58.15	16.920	ns
	H	52	60.44	23.340	
Bone gain (g/d)	L	61	0.65	0.855	ns
	H	52	0.46	0.779	
Gain EMA (cm ²)	L	53	0.69	1.109	0.01
	H	48	1.15	0.978	
Gain EMD (cm)	L	58	0.08	0.410	ns
	H	49	0.16	0.338	
Gain fat depth (mm)	L	52	0.93	1.190	ns
	H	42	0.92	0.859	
Staple length (mm)	L	53	36.92	10.640	0.05
	H	41	41.01	10.700	
Fibre diameter (µm)	L	52	16.11	1.192	ns
	H	41	16.50	1.307	
DMI _{RC} (kg)	L	61	1.22	0.080	0.001
	H	52	1.19	0.115	
CH ₄ (g/d)	L	61	22.10	2.871	0.01
	H	52	23.18	3.301	
MY CH ₄ (g/kg DMI _{RC})	L	61	19.71	2.203	ns
	H	52	19.54	2.212	

4.1.5 Phase 2 experiment; two phenotypes (L and H RFI) and two diets.

Wethers phenotyped for L or H RFI (as described above) were allocated to two diets with n=10-11 per diet X RFI group. The high diet was composed of Lucerne, Oaten Chaff and barley grain in a ratio of 40:50:10 respectively and the low diet was composed of Lucerne, Oaten Chaff in a ratio of 30:70. The chemical composition of the diet is shown in Table 1. The mean DM of the feed in the high diet was 89.3 %, with 14.5 % CP, 35.0 % NDF and 11.6 MJ ME /kg DM. The mean DM of the feed in the low diet was 90.1 %, with 11.5 % CP, 56.0 % NDF and 9.2 MJ ME /kg DM. Dry matter digestibility (DMD) estimated from *in vitro* analysis was 77 % for the high diet and 63 % for the low diet.

There was no significant difference between RFI phenotype for FI_{30days}, LWT_{30 days}, ADG, DMIrc or daily CH₄ emission (Table 7). FI_{30days} was significantly ($P < 0.001$) higher fed the high diet, as was DMIrc ($p = 0.003$). There was no significant diet effect on LWT_{30 day} or ADG. Daily CH₄ emission was higher on the high diet ($P < 0.003$).

From these a number of tissues were collected including sheep rumen wall tissue from which rumen epithelium was enzymatically isolated and membrane proteins extracted quantification by TMT tandem mass spectrometry (MS/MS).

Table 7. Mean and s.d. of growth and gas emission of sheep fed high diet (Lucerne, Oaten Chaff, barley grain 40:50:10) or low diet (Lucerne, Oaten Chaff 30:70) in two phenotypes (L or H RFI).

			L RFI		H RFI		
Variable	diet	N	Mean	StDev	Mean	StDev	P value Diet
FI _{30days} (kg)	H	11	1.61	0.164	1.75	0.204	0.001
	L	10	1.35	0.163	1.39	0.173	
LWT _{30 days} (kg)	H	11	43.1	4.22	44.22	4.220	ns
	L	10	43.6	3.85	42.87	5.080	
ADG (kg/d)	H	11	0.04	0.004	0.05	0.005	ns
	L	10	0.04	0.004	0.04	0.005	
DMIrc (kg)	H	11	1.13	0.198	1.24	0.115	0.001
	L	10	1.00	0.123	0.98	0.128	
CH ₄ (g/d)	H	11	22.43	4.130	25.78	3.860	0.003
	L	10	21.09	2.844	20.26	2.858	

4.1.6 Protein identifications and quantification between H or L RFI and H or L diets

4842 proteins were identified from the membrane fraction of these 1872 were quantified using the fold change cut off of $FC > 1.2$, and significance $P < 0.05$.

4.1.7 Functionally significant rumen epithelium proteins and enriched pathways in L or H RFI fed H or L diet found using WGCNA

Weighted gene correlation network analysis (WGCNA) was used to find clusters of protein identifications of interest, which are enriched for pathways or cellular processes of functional significance.

Using WGCNA 5 clusters were found with varying numbers of proteins in each.; blue $n = 249$, turquoise $n = 256$, brown = 127, green = 31, yellow $n = 67$ which showed associations with phenotype, diet or an interaction between phenotype and diet (Figure 4). All ensemble protein accession numbers in each cluster list were converted to uniprot KB accession numbers in www.uniprot.org using the retrieve mapping tool. To find function enrichment of uniprot ids for metabolic pathways each cluster list was submitted to Database for Annotation, Visualization and Integrated Discovery

(DAVID) v6.8 <https://david.ncifcrf.gov/>, selecting Ovine airies as species and list in the functional annotation tool.

The most interesting clusters in terms of differences in protein abundance related to different phenotype appeared to be the blue and turquoise cluster. In the blue cluster the better doer or L RFI phenotype had a cluster of proteins which were lower than the lesser doer or H RFI independent of diet. In contrast in the turquoise cluster. We did not see a clear difference between diets. There was an interaction between phenotype and diet in the brown cluster. Due to the short time we had to analyse the results (4 weeks) we concentrated on the turquoise cluster to find if there were proteins with functional significance related to a biological process (WGCNA) and with fold change greater than 1.3 and ANOVA $P < 0.05$ are represented in Table 8.

In the WGCNA turquoise cluster proteins with greater abundance in the L RFI vs H RFI were for metabolic pathway which had a significant (Benj $P < 0.001$; False Discovery Rate FDR $q < 3.0 \times 10^{-7}$) enrichment score of 7.6 (Benj $P < 0.001$; False Discovery Rate FDR $q < 4.8 \times 10^{-6}$; Table 8). Also relevant to energy transactions in the rumen epithelium we found 6.8 fold enrichment for biological process fatty acid metabolism (Benj $P < 0.001$; False Discovery Rate FDR $q < 1.1 \times 10^{-1}$).

In the WGCNA blue cluster with greater abundance in the H RFI than the L RFI for significant biological process or metabolic pathway are shown in Table 9.

Figure 4. Eigen plot of proteins clusters with quantitative differences between ‘better doer’ high diet (BDHD), ‘better doer’ low diet (BDLD), ‘lesser doer’ high diet (LDHD) and ‘lesser doer’ low diet (LDLD).

Better doers represent the L RFI phenotype and lesser doers the H RFI phenotype.

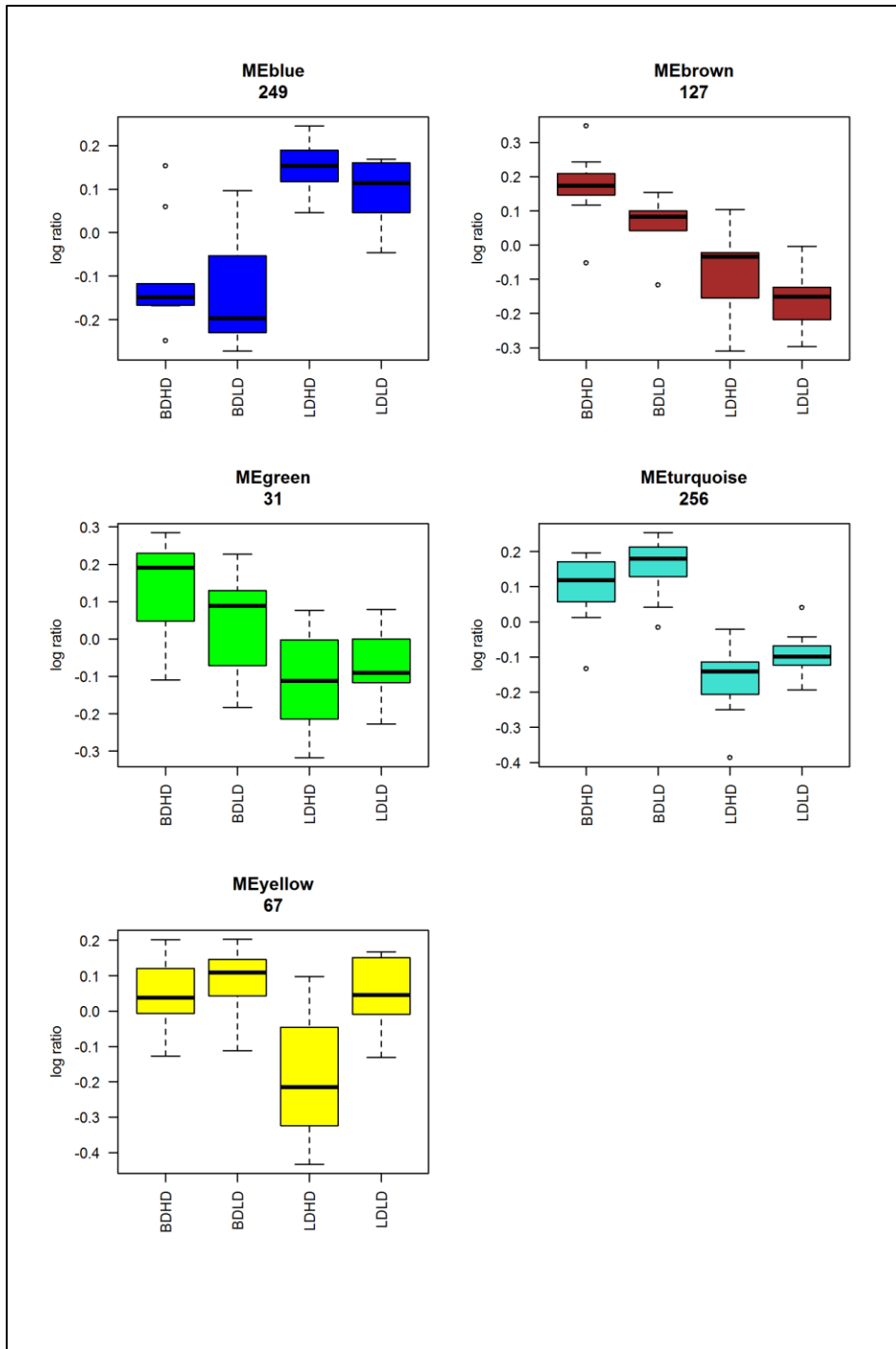


Table 8. Proteins found with greater abundance in the L RFI vs H RFI functionally enriched for metabolic pathway or functional process with significant fold change 1.3 and $P < 0.05$ in the turquoise cluster.

	Entry	Protein names	Gene names	FC	Pvalue
Metabolic pathways	W5PTI2	GPI-anchor transamidase (Phosphatidylinositol-glycan biosynthesis class K protein)	PIGK	1.32	3.42E-07
	O78747	NADH-ubiquinone oxidoreductase chain 1	NADH1 ND1	1.33	0.000
	O78757	NADH-ubiquinone oxidoreductase chain 6	NADH6 ND6	1.60	0.000
	W5Q696	DNA-directed RNA polymerase II subunit RPB7	POLR2G	1.37	0.042
	W5QG39	Complex I-MNLL (NADH dehydrogenase [ubiquinone] 1 beta subcomplex subunit 1)		1.29	0.013
Fatty acid metabolism	W5Q4U2	Carnitine O-palmitoyltransferase	CPT1A	1.28	4.48E-06
	W5QG36	Very-long-chain (3R)-3-hydroxyacyl-CoA dehydratase	HACD2	1.32	3.93E-08
	W5PUC2	Uncharacterized protein	ACADS	1.40	3.02E-07

Table 9. DAVID functional enrichment analysis of the blue cluster rumen epithelium proteins which had higher abundance in the H RFI vs the L RFI phenotype.

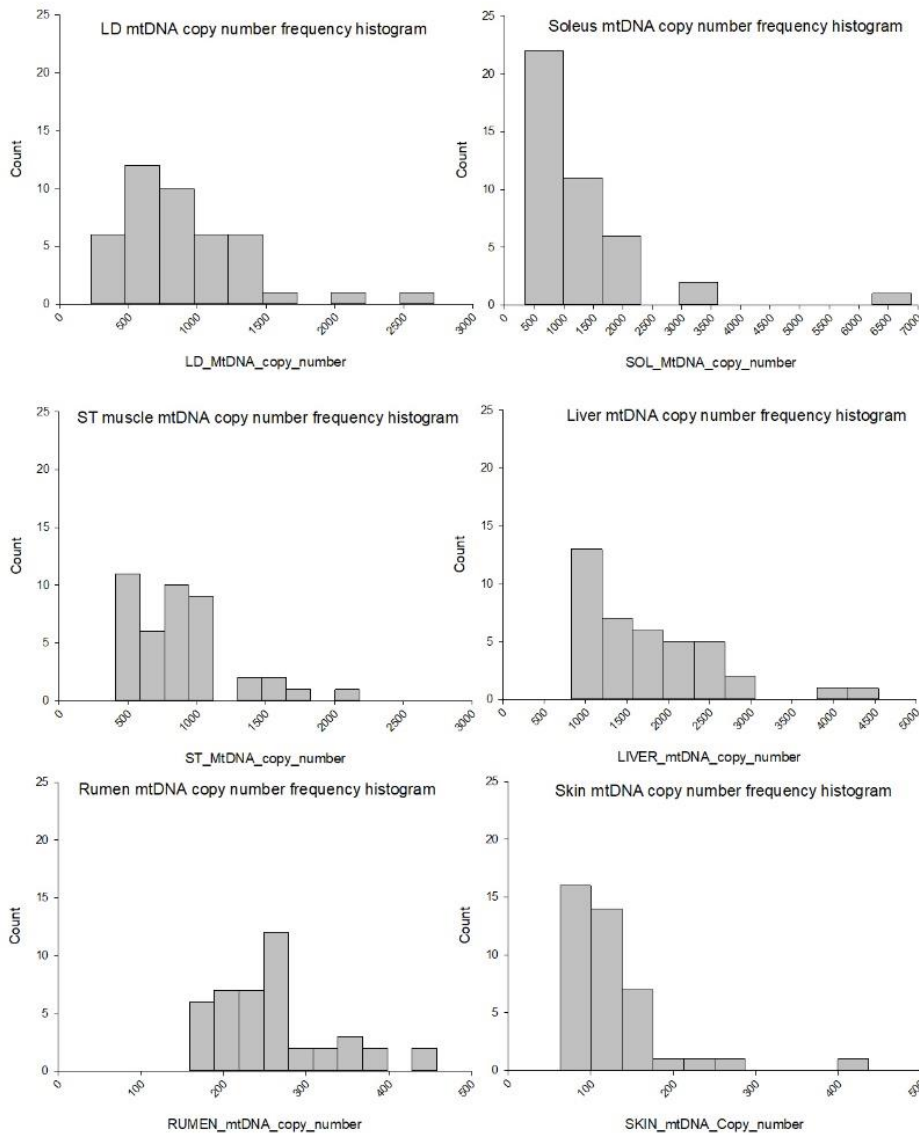
KEGG Pathway enriched	genes	%	P value	Fold enrichment	Benjamini P value	FDR (q)
Complement and coagulation cascades	10	4.4	1.3E-6	9.0	2.5E-4	2.4E-4
Carbon metabolism	10	4.4	3.2E-5	6.1	3.0E-3	2.9E-3
Biosynthesis of amino acids	8	3.5	6.0E-5	7.9	3.7E-3	3.7E-3
Biosynthesis of antibiotics	12	5.3	2.4E-4	3.9	1.1E-2	1.1E-2
Citrate cycle (TCA cycle)	5	2.2	1.2E-3	10.4	4.6E-2	4.5E-2
Lysosome	8	3.5	1.8E-3	4.5	5.8E-2	5.7E-2

4.1.8 Mitochondria and the ‘Better doer’ Merino animal trial

A detailed background and the full experimental methodology and outputs of this animal trial are discussed elsewhere in this report. In brief, this trial presented an ideal opportunity to deploy the sheep mitochondrial content assay with a view to a) determining how much variation exists across individual sheep (Figure 5) and b) estimating how much variation in whole animal FE is explained by tissue mitochondrial content.

The physiological association detected between FE and sheep CO₂ emissions ($P = 0.003$) immediately indicates a likely role for the mitochondria, given the CO₂ emissions measured are entirely produced by the TCA cycle in the mitochondrial matrix of the host animals’ cells. However, the oxygen consumed by the sheep was not associated with FE. This disparity is noteworthy. It perhaps implies the exact fate of the oxygen within the animal’s tissues is important - the tissue specific pattern and timing of combustion in the mitochondria.

Figure 5. Variation in sheep mitochondrial content across six metabolically important tissues



Processing within the mitochondria of the target tissues will ultimately produce carbon dioxide and consume the oxygen, with oxygen being the final acceptor molecule in the mitochondrial electron transport chain. On the other hand, some of the oxygen absorbed by the animal can be stored in haemoglobin (in red blood cells) and myoglobin (in the skeletal musculature) rather than actively respired in the cells. Animal to animal variation in this oxygen storage could uncouple oxygen consumption from carbon dioxide production.

In particular, red blood cell counts, and total blood volume likely differ across individuals. Red muscle fibres contain dramatically more myoglobin than white muscle fibres, so muscle fibre composition could also play a substantive role here. Moreover, cells and tissues with high maintenance costs in non-edible portions of the carcass will consume oxygen and liberate carbon dioxide without positively contributing to animal production (as measured by lean gain). This combination of issues complicates the pairwise relationships among the metabolic gases and FE. More knowledge of animal to animal variation in the oxygen storage capacity of blood and the skeletal musculature may have value for resolving matters in this space.

From the total pool of 113 sheep that were individually phenotyped for FE (and a set of relevant intake, growth, carcass phenotypes and metabolic characteristics) tissue samples taken from 43 extreme performers (i.e. low intake or high efficiency and high intake or low efficiency) were quantitated for mitochondrial content.

The six tissues we quantitated were: LD, SOL, ST, liver, rumen and skin. These tissues were selected to represent important components of the skeletal musculature (LD, SOL and ST), important components of digestion and central metabolism (rumen and liver), while the skin was chosen given its potential availability as a practical testing site ‘on farm.’

Substantial individual to individual variation was discovered across those 43 Merino sheep (Figure 5, Table 10).

Table 10. The log₂ transformed mitochondrial content data across a range of tissues collected from Merino wethers selected for high or low residual feed intake.

Variable	n	Mean	St dev
LD	43	9.60	0.75
SOL	42	9.99	0.87
ST	42	9.68	0.54
Liver	40	10.65	0.61
Rumen	43	7.97	0.38
Skin	41	6.90	0.54

LD, Longissimus dorsi; ST, semitendinosus; SOL, soleus.

Although this experiment was not designed to compare the tissues *per se* (each tissue was run on a different rotor, so we cannot statistically disentangle tissue from rotor), the overall picture broadly suggests the aerobic capacity of the sheep tissues in descending order is: liver and muscle > rumen >

skin (Figure 6). The rumen wall has the tightest (lowest standard deviation) data perhaps reflecting its high physical (structural) uniformity across individuals. On the other hand, the three skeletal muscles (particularly the SOL) have much higher individual variation. This may reflect tissue heterogeneity resulting from mixed myofibre composition and other sources of structural variation. Future work could explore this heterogeneity by quantitating more independent DNA samples per muscle in an effort to generate a more representative muscle-level value.

Figure 6. Cross-tissue comparisons in mitochondrial content in sheep

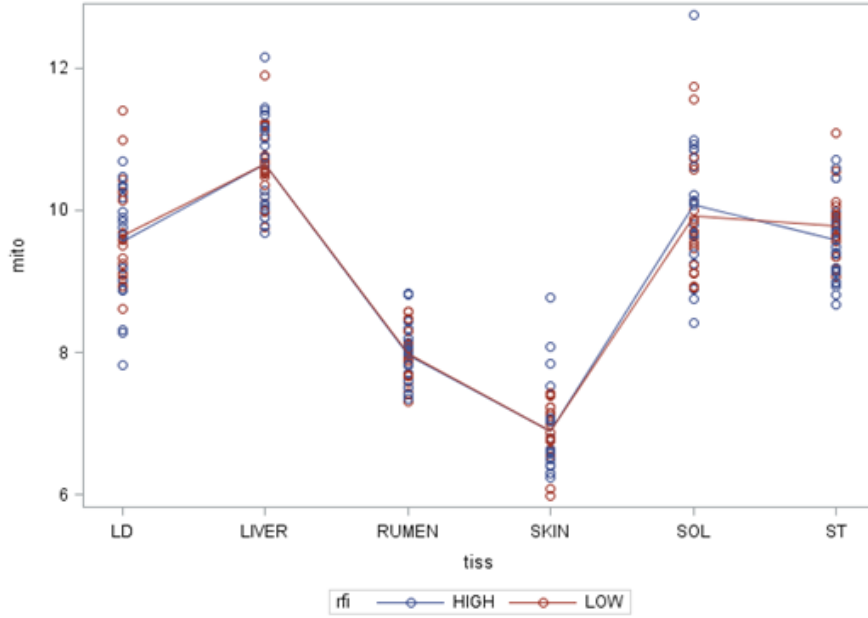


Figure 7. Hierarchical cluster analysis of tissue to tissue relationships in sheep based on individual patterns in mitochondrial content

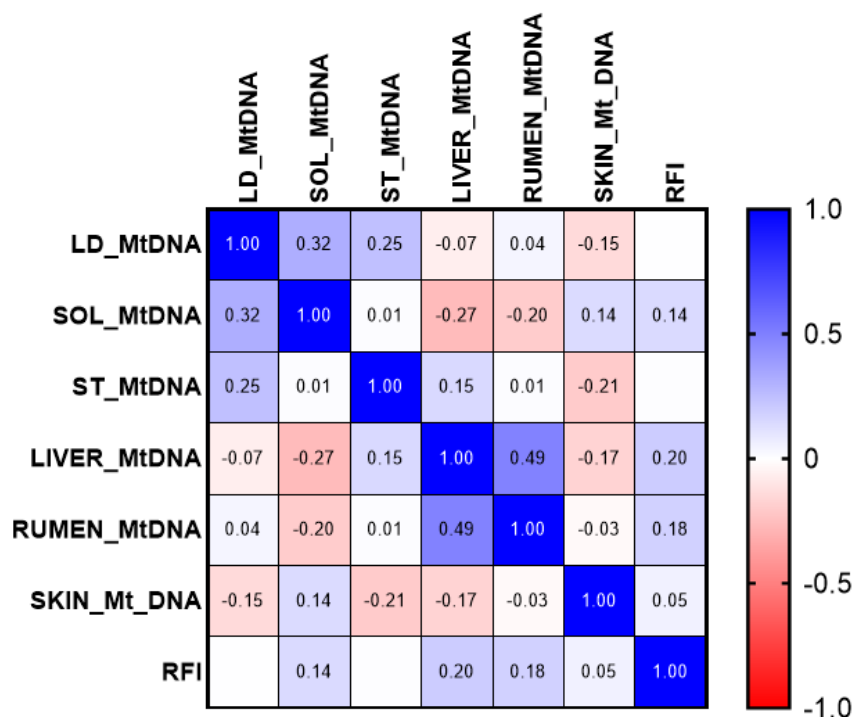


Hierarchical cluster analysis on the 36 sheep for whom all six tissues were successfully quantitated for mitochondrial content suggests the six tissues are metabolically related to each other as follows (Figure 7). The shortest branch lengths (most related tissue samples) connect liver and rumen ($r = 0.49, P = 0.003$), with a second independent cluster comprising the three skeletal muscles. Skin forms a branch on its own. This indicates that sheep tissue aerobic capacity is coordinated for the

liver and rumen consistent with a common pattern of regulation / cross talk between central metabolism and digestion. The aerobic capacity of the skeletal musculature is also coordinated given the observed clustering of the three muscles, with the more glycolytic ST forming a separate branch to the more oxidative LD and Sol. This is in line with observations made in broiler chickens by Reverter et al (2017). The skin is an outlier and receives its own branch in the tree.

A correlation matrix of the six mitochondrial content quantitated tissues and whole sheep FE shows that there are no negative correlations (Figure 8). Four of the six tissues have a positive correlation (liver at 0.20, rumen at 0.18, SOL at 0.14, and skin at 0.05) with two tissues (LD and ST) showing no correlation. Positive correlations indicate a low mitochondrial content is broadly associated with a low intake (i.e. high efficiency) and vice versa. None of these pairwise correlations reaches significance at the 0.05 threshold. Nevertheless, taken as a collection of observations this pattern is of interest as it lends support to the hypothesis of the ‘Corolla Cow’, namely that reduced aerobic capacity across a number of tissues is predicted to be associated with increased feed efficiency (Hudson 2009; Reverter et al 2017; Cassar-Malek 2017). Our Merino rumen finding here is also broadly in line with Kong et al (2017) who previously determined that low rumen mitochondrial content is associated with more efficient Hereford x Angus steers.

Figure 8. Pairwise correlations between tissue mitochondrial content and whole animal FE in sheep



Two statistical approaches indicate a significant relationship between liver mitochondrial content and whole animal FE. Firstly, a Principal Components Least Squares Regression analysis using FE as the dependent variable finds liver mitochondrial content is a significant explanatory variable of FE ($P = 0.029$) along with methane emissions, carbon dioxide emissions, nitrogen balance and heat calculated from carbon dioxide emissions. With this statistical approach rumen mitochondrial content approaches significance at the 0.05 threshold ($P = 0.065$). This can be taken as further indication of a co-ordinated metabolic axis existing between the rumen and the liver connecting the

demands of digestion on the one hand with the demands of central control of ruminant metabolism on the other.

Secondly, a stepwise linear regression approach picking the best five models based on one variable, based on two variables and based on three variables is well represented by tissue mitochondrial content estimations. For example, liver mitochondrial content is among the best five models for one variable. When examining two variables, liver mitochondrial content plus methane, and soleus mitochondrial content plus methane are among the best five models. Based on three variables, skin mitochondrial content, soleus mitochondrial content and rumen mitochondrial content are all among the top five when coupled with two different measures of methane (methane emissions expressed in g/d and methane yield expressed relative to dry matter feed intake) in each case.

All 14 variables assessed here by this modelling approach (i.e. all variables except those used to directly derive FE such as intake) collectively explain 37% of the FE variation. This is an intermediate amount of explanatory power. This reinforces the difficulty in modelling a complex physiological trait like FE, and explains why the 1 (4% explained), 2 (15% explained) and 3 (25% explained) factor models discussed above can only explain modest to intermediate amounts of FE variation.

Taken together, these various findings of explanatory variables for FE open up two possibilities. Firstly, that a blood test reflective of liver aerobic capacity / function could represent an attractive candidate for predicting ‘Better Doers’ in an applied situation. And secondly, that a combination of a skin test for mitochondrial content coupled with knowledge of methane emissions may also have potential as a useful research tool (but presumably not an ‘on farm’ test). More experimental work in independent populations of animals is required in both cases to validate these ideas.

Moving beyond FE to the other measured phenotypes, a number of significant pairwise relationships were identified. For example, SOL mitochondrial content was significantly associated with whole animal oxygen consumption ($P = 0.017$) and Brouwer’s heat estimation ($P = 0.017$). Semitendinosus mitochondrial content was significantly associated with both lean mass ($P = 0.046$) and bone mass ($P = 0.000034$). Rumen mitochondrial content was significantly associated with ADG ($P = 0.028$), lean gain ($P = 0.021$) and nitrogen balance ($P = 0.014$). Finally, skin mitochondrial content was significantly associated with fat depth ($P = 0.05$).

The various relationships between mitochondrial content and function and production animal efficiency have recently starting to emerge in earnest, across species and systems, in the scientific literature. Our experimental findings here using the ‘Better Doers’ Merino wether model as our phenotype can be added to independent associations detected in beef cattle (Kong et al 2017), dairy cattle (Dorji et al 2021) and pigs (Carmelo and Kadarmideen 2020; Fu et al 2017) using a combination of mitochondria DNA copy number, mRNA abundance and protein abundance.

Reverter et al (2016) previously found low mitochondrial content in breast muscle was associated with more muscular broilers; this is consistent with a similar relationship to feed efficiency although feed efficiency was not directly measured in this study. Cantalapiedra-Hijar et al (2018) have recently argued for a reappraisal of the feed efficiency situation in ruminant farm animals, expressing their belief that feed efficient animals likely have lower metabolic rate independent of intake reduction, perhaps due to higher efficiency of mitochondrial ATP synthesis. Nevertheless, overall this appears to be an area with some conflicting results. For example, not all studies find associations between mitochondrial content and / or function with feed efficiency, and those that do are not always in the same direction. Disentangling the possible combination of biological reasons, technical reasons, and definitional reasons lies beyond the scope of this report.

4.1.9 Neck muscle mitochondrial content and Angus cattle RFI

As previously reported, we detected substantial animal to animal variation (the highest individual value being 6.5-fold higher than the lowest value) in neck muscle mitochondrial content across 134 RFI phenotyped Angus animals. This variation is very much in line with a previous study across 80 commercial broilers (Reverter et al 2017) where a 5-fold bird to bird variation was observed. However, here we detected no significant relationship between the observed variation in mitochondrial content and the whole animal phenotypes (RFI, DFI and ADG) that were provided. Furthermore, no significant sire effect was apparent, and estimates of heritability of the mitochondrial content trait were correspondingly very low. It is not clear whether this absence of signal reflects the biological reality or is because the particular choice of individual muscle was not metabolically relevant or is a consequence of a technical issue of needing a number of replicate DNA samples per muscle because of the complexity of muscle fibre heterogeneity.

An earlier examination of hormone treatment (bovine somatotropin, bST), genetics and nutrition in *Bos indicus* cross and *Bos taurus* (Holstein Fresian) steers found no significant effect on tissue mitochondrial content, although some of the observed trends were in line with biological expectation. For example, the observed trend for high caloric intake (i.e. Lucerne *ad libitum*) to increase cattle mitochondrial content in muscle is in line with previous nutritional observations made in the muscle (e.g. Gomez-Perez et al 2012) and liver (Nadal-Casellas et al 2010) of inbred rodents. With regard to exogenous bST treatment we observe that both liver and muscle show a trend of increased mitochondrial content with the liver appearing the more responsive of the two tissues. The muscle observation is broadly consistent with Short et al (2008) who found human skeletal muscle had increased mitochondrial activity in response to growth hormone treatment.

4.2 Phenotypic variation in CH₄ emission in ewes fed a maintenance energy diet; Ruminal epithelium protein makers and mitochondrial content associated

4.2.1 Methane emission and digestive parameters in sheep selected for L or H CH₄ group

Since digestive function varies between H or L CH₄ phenotype a summary describing the relevant digestive parameters are shown in Table 11. Daily CH₄ (g/d; $P < 0.001$), CO₂ (g/d; $P = 0.01$) emission and methane yield (MY g CH₄/kg DMI; $P < 0.001$) were significantly lower in the L CH₄ sheep than H CH₄ sheep when adjusted for liveweight ($P = 0.487$) and DMI in the respiration chamber (RC; $P < 0.001$). Mean retention time (MRT) of rumen feed particles ($P = 0.03$) and of rumen liquids ($P = 0.004$) was also significantly less in the L CH₄ sheep than H CH₄ sheep. There was no statistical difference in N and C balance or dry matter digestibility between sheep in the two CH₄ phenotypes.

Table 11. Descriptive statistics for phenotypic traits related to CH₄ emission in high or low emitting sheep; dry matter intake index (DMI_{rc}) adjusted for intake on the day of respiration chambers (RC) and day before RC (Bond *et al.* 2016).

Statistical differences in the variables representing the high (H; n=10) and low (L; n=10) CH₄ groups. MRT = mean retention time of digesta over 24 h (d), particles = the solid component of digesta simulated by use of chromium mordanted feed, Liquid = the soluble or liquid component of digesta simulated by use of a dose of cobalt Bond *et al.* 2016, ns = not significant

Variable	Phenotype	Mean	SE	P value
Liveweight (kg)	High CH ₄	66.3	1.68	ns
	Low CH ₄	63.0		
DMI _{rc} (kg)	High CH ₄	1.46	0.039	ns
	Low CH ₄	1.34		
CH ₄ (g/d)	High CH ₄	28.8	0.88	0.001
	Low CH ₄	23.5		
CO ₂ (g/d)	High CH ₄	1023.9	0.01	0.01
	Low CH ₄	904.7		
MY (gCH ₄ /kg DMI)	High CH ₄	19.9	0.003	0.003
	Low CH ₄	17.8		
N balance (g/d)	High CH ₄	14.5	0.75	ns
	Low CH ₄	13.7		
C balance (g/d)	High CH ₄	367.6	9.99	ns
	Low CH ₄	358.0		
DMD (g/kg)	High CH ₄	642.4	5.62	ns
	Low CH ₄	661.1		
MRT rumen particles/d)	High CH ₄	1.04	0.032	0.029
	Low CH ₄	0.90		
MRT rumen (liquids/d)	High CH ₄	0.70	0.019	0.004
	Low CH ₄	0.59		

4.2.2 Protein identification and quantitation of rumen epithelium proteins

Comprehensive proteomic analysis of sheep rumen epithelial proteome identified 803 proteins in the cytosol fraction and 2546 proteins in the membrane fraction (peptides matched 1, protscore $P < 0.05$, peptide FDR < 1%). Selective enrichment of rumen tissues (Bond *et al.* 2019), initial solubilisation using detergent (SDS) and HpH fractionation of proteins enabled the in-depth characterization of proteins.

Following the identification of the proteins in both cytosolic and membrane fractions the identifications in each fraction were combined to obtain the total number of proteins identified. Notably, 220 proteins were unique to the cytosol fraction, 583 found in both fractions and 1963 identified unique to the membrane fraction (Total n=2766).

Through a collective cytosol and membrane ovine epithelial proteome, our study reported peptide level evidence for over 34 % of open reading frames (ORFs) reported in a cluster of genes specific for the epithelium described previously in the published transcriptome of the whole depth ovine rumen wall from the same sheep Xiang et al. 2016.

4.2.3 Assignment of proteins to sub cellular compartment

To expand the knowledge of the location and function of the proteins identified we used an array of bioinformatic tools. Subcellular location predictions by WoLF PSORT revealed a large proportion of identified proteins were localised in the cytosol ($n=1062$), nucleus ($n=440$), mitochondria ($n=420$), plasma membrane ($n=368$) or extracellular ($n=361$). Smaller proportions were assigned to the endoplasmic reticulum ($n=63$) peroxisome ($n=33$) or golgi ($n=6$) (Appendix 1.5).

Of all the proteins identified 23% were predicted membrane proteins with at least one transmembrane domain (TMHMM). The plasma membrane category had a majority of proteins with multiple transmembrane domains ($n=219 > 1$ TMHMM). Those assigned to the cytoplasm or extracellular compartment were largely single transmembrane domain proteins (1 TMHMM). A proportion of the proteins assigned extracellular contained a predicted secreted protein sorting sequence (Signal P $n=191$ and SecretomeP $n=136$). Of the 420 proteins categorised as mitochondrial up to 207 had a predicted mitochondrial target protein sequence.

Appendix 1.5. Mapping the location of these proteins puts into context the biological mechanisms and functional significance of quantitative differences in their abundance between CH₄ phenotypes.

4.2.4 Quantitative differences in epithelium protein abundance in H or L CH₄ rumen epithelium

In the cytosol fraction we found 11 proteins which had a fold change >1.5 in the H and L CH₄ emitting ewes and were significantly different using ANOVA ($P > 0.05$). Seven proteins (CARS, LDHD, LSS, ME1, NCOA2, PSMB5, MYOF) had significantly higher fold change in the L CH₄ group compared to 4 (HAGH, LGALS3BP, Actin-related protein 2/3 complex subunit, SCCPDH) in the H CH₄ group.

In the membrane fraction we found 44 proteins which had a fold change >1.5 and were significantly different using ANOVA ($P > 0.05$) in the H and L CH₄ emitting ewes. 21 proteins had significant increase in abundance in the L CH₄ group (RETN, AZU1, PNPT1, CARKD, CYCS, 5 uncharacterised proteins, PDIA4, IGHM, ADPGK, FGG, PCBD2, PITRM1, AP1B1, PRPF40A, FASTKD2, DCTN1, MPO) compared to the H CH₄ phenotype. 23 proteins had significant increase in abundance in the H CH₄ group (SLC40A1, HSD17B11, GOSR1, RIOX1, NOV, EEF1A1, MRPL48, SerpinB12, GSTM3, RHOA, PEX14, GCNT3, SEC23IP, NOS2, DEK, SYNE2, TAF4B, STAT1, DNASE1L1, IL1R2, RPL34, LEMD3 and 1 uncharacterised protein) compared to the L CH₄ phenotype. Table 12 shows a subset of these proteins which have significant fold change (FC) in protein abundance which can be related to metabolic pathways or cell defense to microbes explained in the following sections.

Table 12. A subset of the combined cytosol and membrane fraction rumen epithelium proteins with quantitative significant differences ($P < 0.05$; >1.5 fold change (FC) associated with low or high CH₄ emission phenotype.

Only the proteins with relevance to the overall interpretation of the research presented are shown in this table. Accession number for ensemble *Ovine arires* database is shown in column on left. The corresponding Uniprot accession code, protein and gene name from gene ontology data (using retrieve ID mapping in Uniprot), number of peptides matched to the sequence and fold change are also shown. If a protein was annotated as ‘uncharacterised’ a BLAST protein homology search was

used to name, the protein with highest homology to *Ovine airies* sequence. Subcellular location is allocated by sequence homology (see methods for procedure used).

Protein	Entry	Protein names	Gene names	location	No. Pep matched	FC
L > H CH4 FC						
ENSOARP00000006 849.1	W5P8U2	Lactate dehydrogenase D	LDHD	mito	1	2.20
ENSOARP00000008 043.1	W5PC82	Malic enzyme	ME1	mito	5	1.57
ENSOARP00000002 425.1	W5NW78	Resistin	RETN	extra	2	2.37
ENSOARP00000004 349.1	W5P1Q0	AP complex subunit beta	AP1B1	endosome	2	1.92
ENSOARP00000010 314.1	W5PIP4	Azurocidin 1	AZU1		1	2.48
ENSOARP00000009 967.1	W5PHQ0	Myeloperoxidase	MPO		1	3.50
ENSOARP00000020 820.1	W5QDM2	Proteasome subunit beta	PSMB5	cyto-nucleus	2	1.60
ENSOARP00000022 795.1	P62896	Cytochrome c	CYC	mito	4	1.57
ENSOARP00000003 016.1	W5NXW9	Immunoglobulin heavy constant mu	IGHM		4	1.63
H > L CH4 FC						
ENSOARP00000017 830.1	W5Q540	Hydroxyacylglutathione hydrolase	HAGH		1	2.56

ENSOARP00000017 599.1	W5Q4F9	Solute carrier family 40 protein	SLC40A1		1	3.72
ENSOARP00000020 752.1	W5QDF4	Glutathione S-transferase (EC 2.5.1.18)	GSTM3		2	1.77
ENSOARP00000017 986.1	W5Q5J6	Nitric oxide synthase (EC 1.14.13.39)	NOS2		3	1.67
ENSOARP00000014 105.1	W5PUH3	Interleukin 1 receptor type 2	IL1R2		2	1.52

4.2.5 Metabolic pathways associated with significant fold changes in epithelium proteins in H or L CH₄ emitting sheep

Enzymes that had significant fold change were associated with two major energy utilising pathways, glycolysis and the tricarboxylic acid cycle. This indicates there was a difference between the L and H CH₄ phenotype in the metabolism of nutrients in the epithelium. The 11 enzymes involved in the glycolysis pathway or the reverse process storing glucose as glycogen were identified in tissue from each CH₄ phenotype (Figure 4). A side pathway of glycolysis, the methylglyoxal (MGO) pathway was found in which 2 proteins had higher fold change between CH₄ group. There are several steps in the MGO pathway the first of which methylglyoxal synthase converts dihydroxyacetone phosphate (DHAP) via triosephosphate isomerase (TPI) to methylglyoxal by-passing glycolysis. The first two enzymes in the pathway methylglyoxal synthase (PARK7) and glyoxylase I (GLO1) or lactoylglutathione lyase were identified. In the next step lactoylglutathione is converted to D-lactate and glutathione by glyoxylase II also called hydroxyacylglutathione hydrolase (HAGH). In the H CH₄ epithelium HAGH was 2.56 fold higher than in the L CH₄ epithelium. MGO is a toxic compound which requires rapid detoxification by the MGO pathway. Associated with the higher abundance of HAGH was a higher FC (1.77 FC) in the H compared to the L CH₄ of enzyme S-transferase (GSTM3). The enzyme produces GSH and functions to detoxify compounds, such as products of oxidative stress, by conjugation with glutathione.

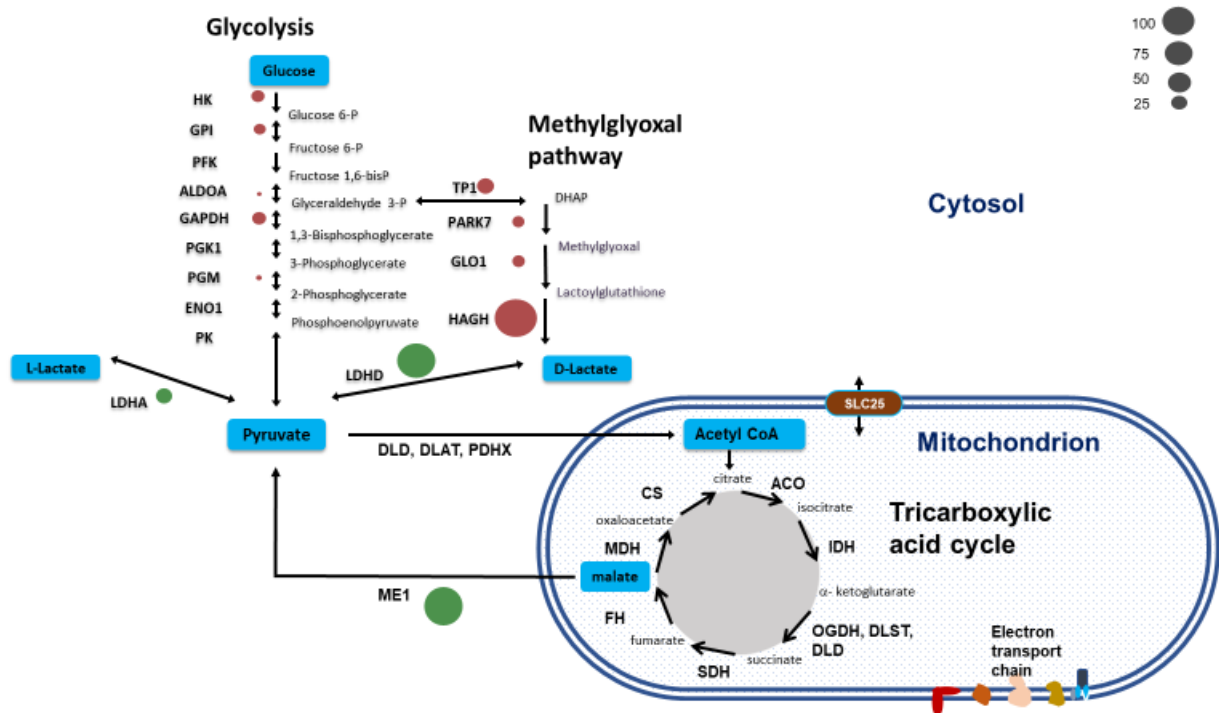
In the last step of the MGO pathway methylglyoxal is converted to D-lactate, which may be converted to pyruvate by D-lactate dehydrogenase. Lactate dehydrogenase D (LDHD) was 1.9 fold higher in the L CH₄ epithelium than the H CH₄ sheep. Malic enzyme (ME1) was 1.57 fold higher in the L CH₄ group and is known to play an important role in the conversion of malate then to pyruvate through the TCA cycle (Figure 9).

Also related to regulation of insulin sensitivity and glucose uptake by cells we found resistin (RETN) was 2.37 fold higher in the L CH₄ phenotype.

Figure 9. A diagram representing the enzymes involved in the 11 steps of the glycolytic and methylglyoxal pathway, TCA pathway and associated pyruvate or malate cycling found in the

rumen epithelium of sheep.

Significant fold change in proteins is highlighted in table 12 and an increase in the abundance of an enzyme in the low CH₄ group shown by green bubble, whereas increase in the abundance of an enzyme in the high CH₄ group shown by red bubble.



Abbreviations are HK; hexokinase, GPI; glucose-6-phosphate isomerase, PFK; phosphofructokinase-1, ALDOA; fructose-bisphosphate aldolase, GAPDH; glyceraldehyde-3-phosphate dehydrogenase, PGK1; phosphoglycerate kinase, PGM; phosphoglycerate mutase, ENO1; enolase 1, PK; pyruvate kinase, LDHA; L-lactate dehydrogenase LDHD; D-lactate dehydrogenase, TPI1; triosephosphate isomerase, PCK2; pyruvate carboxykinase -2, P; phosphate. DLAT; acetyltransferase, DLD; dihydrolipoyl dehydrogenase, PDHX; dihydrolipoamide acetyltransferase, CS; citrate synthase, ACO; aconitase, IDH; isocitrate dehydrogenase, OGDH; oxoglutarate dehydrogenase, DLST; Dihydrolipoamide S-succinyltransferase, FH; fumarate hydratase, MDH; malate dehydrogenase, ME1; malic acid enzyme, PCK2; pyruvate carboxykinase -2. ALAT; alanine aminotransferase; PAG; phosphate-activated glutaminase.

4.2.6 Differential abundance of proteins involved in cell defence against microbes in the epithelium of L or H CH₄ sheep

We found proteins related to various vesicles or subcellular locations of phagosome (n=46), lysosome (n=35), peroxisome (n=47) and endosome (n=35) which support the interpretation of changes in protein abundance in the L or H CH₄ sheep related to function of cell defence against microbes (Table 12). In the H CH₄ sheep, we found increased abundance of nitric oxide synthase (NOS₂) of the peroxisome. Of the proteins allocated to the phagosome Galectin 3 binding protein (LGALS3BP; FC 1.7) was significantly higher in the H than L CH₄ sheep. Also, interleukin 1 receptor (IL1 R2; 1.52 FC) and iron transporter (SLC40A1) were 1.52 and 3.7 fold higher, respectively, in the H than L CH₄ sheep.

In the L CH₄ sheep myeloperoxidase (MPO) was 3.5 fold higher than in H CH₄ sheep epithelium which is a phagosome protein. AP complex subunit beta (AP1B1) which makes up part of the endosome

had a greater fold change (1.9 FC) in the L than the H CH₄ sheep. Azurocidin 1 (AZU1) a known anti-microbial, had a 2.48 higher FC in the L than the H CH₄ sheep.

4.2.7 Rumen fluid metabolites H or L CH₄ phenotype

Since we expected different metabolic conditions in the rumen of each CH₄ phenotype to affect protein expression in the cytosol or membrane proteins of the rumen epithelium in contact with these conditions, a subset of the metabolites identified and quantified in the rumen fluid (3h after feeding) are shown in Table 2. These include 13 amino acids (AA), 3 short chain fatty acids (SCFA's) and 6 carbohydrates. The main metabolites were acetate, butyrate, propionate and glucose which all had a concentration above 5 µM in the rumen fluid of sheep feed a fibrous 1.5 x maintenance diet. No significant difference between any of the metabolites identified in the rumen fluid was found between L or H CH₄ phenotype at this sampling time point.

Table 13. Metabolites concentration (µMol) quantified using NMR in rumen fluid collected postmortem approximately 3 h after feeding in L or H CH₄ emitting sheep.

Metabolite	Mean L n=10	Mean H n=8	Stdev
Carbohydrates			
maltose	262.4	241.8	243.43
b-ribose	369.8	261.4	142.50
xylose	56.6	38.2	26.19
lactate	199.4	257.8	73.32
Dihydroxy acetone (DHA)	86.0	68.2	22.92
glucose	7597.7	5728.3	3448.68
Short chain fatty acids			
acetate	51773.6	54647.9	1505.33
propionate	14688.4	15743.1	2385.40
butyrate	9685.3	9855.4	1385.76
Amino acids			
tryptophan	53.1	54.2	16.61
Phenyl alanine	129.1	133.8	46.26
tyrosine	99.5	98.0	35.74
proline	664.3	700.6	287.08
glycine	545.0	550.4	212.50
lysine	1021.9	906.9	235.32

aspartate	841.6	909.0	218.13
glutamate	843.9	847.6	259.15
alanine	731.5	736.5	259.61
isoleucine	254.5	249.6	87.43
valine	389.7	388.7	116.13
leucine	347.7	353.3	106.03
threonine	177.4	225.3	129.91

4.2.8 Metabolites in the blood

Serum samples from 15 sheep out of the 20 profiled for proteins were analysed for β -hydroxy butyrate (BHB), glucose and D-lactate and L-lactate. (Table 14). Glucose ($P=0.02$) was significantly higher in the L CH₄ phenotype and L-lactate higher ($P=0.002$) in the H CH₄ phenotype.

Table 14. Blood metabolites (mM) of sheep related to quantitative differences in proteins of rumen epithelium in L or H CH₄ emitting sheep.

	Mean High CH ₄	Mean Low CH ₄	StdDev	<i>P</i> value
Glucose	4.06	5.61	1.410	0.02
L-lactate	6.35	2.08	4.940	0.002
D-lactate	0.03	0.06	0.051	ns
BHB	0.28	0.30	0.067	ns

4.2.9 Rumen mitochondrial content and sheep divergent for heat production and methane emissions

As previously reported, rumen samples from sheep divergent in methane emissions and heat production were quantitated for mitochondrial content. No significant differences in rumen mitochondrial content were detected between treatment groups. The absolute differences observed across treatments were modest, so these results are unlikely to change with larger samples sizes. Overall, these data imply that the differences in mRNA and proteins relating to the mitochondria previously reported in the rumen tissues (Bond et al., ‘Better Doers’ Milestone Report 2) of these same sheep are made against a very stable cellular mitochondrial content background. Put another way, individual components of the mitochondria appear to be specifically modified to help govern flux through particular metabolic pathways (such as the glyoxylate shunt) in low methane emitting sheep, but the overall aerobic demand of the component rumen cells in those different groups of animals is probably not markedly different.

4.3 Perennial wheat vs Perennial wheat plus Lucerne-fed sheep; Quantification of rumen epithelium proteome by TMT-MS.

4.3.1 Diet composition

The diet chemical and mineral composition of PW or PW+L diets are summarised in Newell *et al.* 2020 and Table 2 (appendix 1). Briefly, in the PW diet had 24.3 % CP, 45.0 % NDF and 12.0 MJ ME /kg DM, whereas the PW + diet had 22.1 % CP, 40.0 % NDF and 11.5 MJ ME /kg DM. Mineral content of PW fed diets had extremely low sodium (Na^+) levels whilst potassium (K) was above the threshold level (3 % DM). With the addition of Lucerne to the PW diet calcium (Ca^{2+}) higher, K^+ was significantly lower than with PW alone and Na^+ remained lower than the recommended amount required in the diet.

4.3.2 Feed intake, Growth, Blood and Urine mineral content

PW + L fed lambs ate more (1.33 kg/d) than the lambs fed the PW diet (1.27 kg/d, $P < 0.001$; Newell *et al.* 2020). There was no difference in changes in lamb liveweight over time. Growth rates were relatively low (<110 g/d) for both diets.

The following section is taken from Refshauge *et al.* (2021; figure 10). The addition of Lucerne increased the dietary supply of Ca, Mg and Na and decreased K and P. When compared to PW offered more Ca, Mg, K, less Na and P ($P < 0.001$; Refshauge *et al.* 2021 in revision). There were significant differences over time for all minerals and mineral ratios ($P < 0.001$). PW offered diets with higher DCAD, K: Na + Mg, K: Na, Ca: P and Tetany index ($P < 0.001$).

Plasma Mg declined significantly throughout the study ($P < 0.001$) and after one week on PW, there was a significant reduction in that group ($P < 0.01$) that did not remain different to the PW+L diet after that week (figure 11). Plasma Ca increased throughout the study ($P < 0.001$), while plasma Na decreased over the study, as did plasma K and plasma P ($P < 0.001$), with no diet effects.

The urinary excretion of Mg increased in PW + L diet ($P < 0.001$) after one week on the forages but was not different thereafter (figure 12). The excretion of Ca, Na and P was very low and decreased, while K excretion increased during the study ($P < 0.001$).

Figure 10. Forage mineral content, adjusted for intake in the biculture diets, for sodium, calcium, magnesium, potassium and phosphorus (% DM). Black dashed lines (- - -) indicate known minimum requirements.

Some thresholds are off the scale (sodium 0.09%, magnesium 0.09%, as well as the maximum tolerable level for potassium 3.0%) (Masters *et al.* 2017). Horizontal axis label is week (Week 1, Week 2 and Week 3). Lighter coloured lines is the data, solid lines are means.

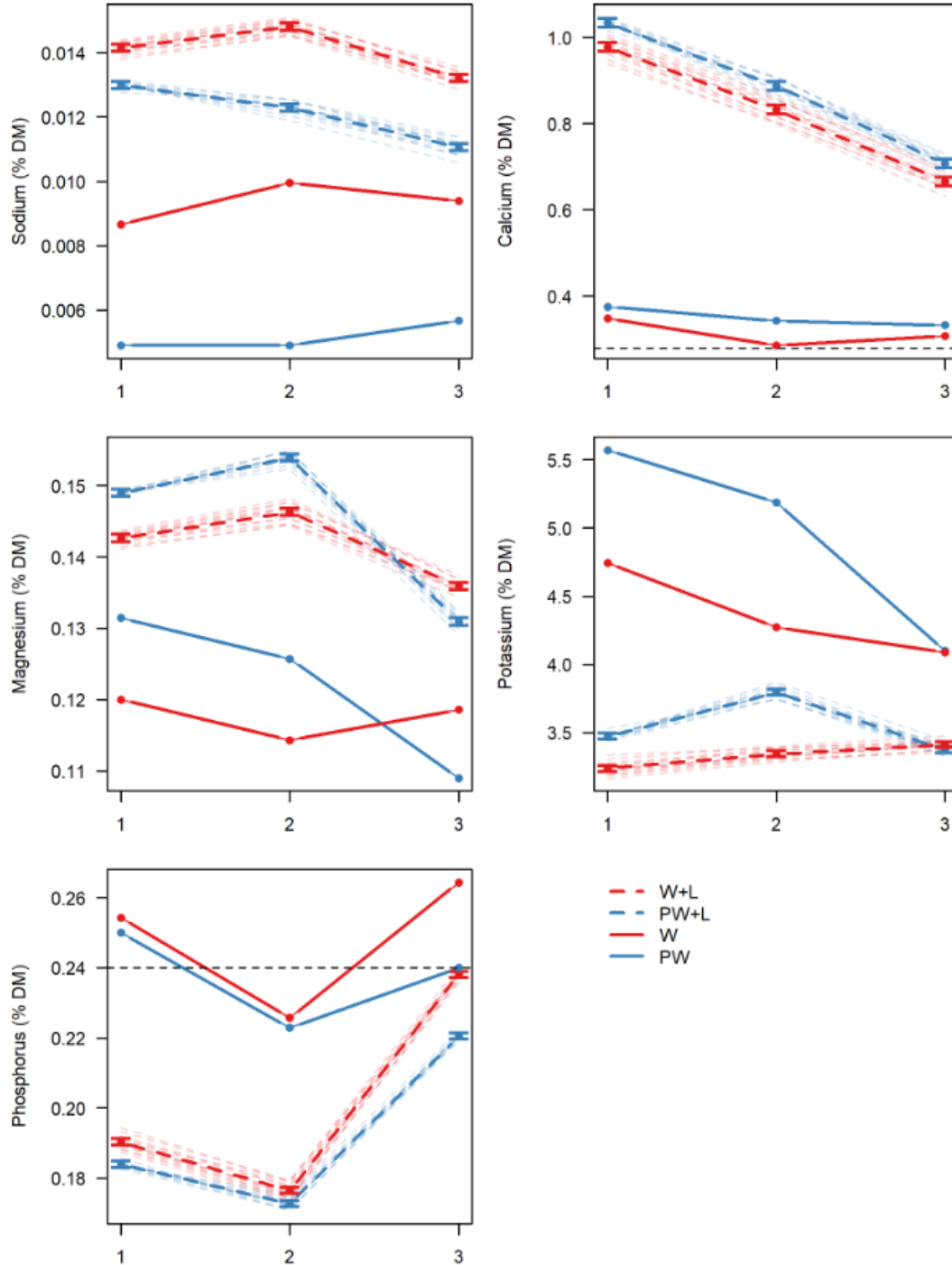


Figure 11. Plasma mineral concentrations. Black dashed lines (- - -) indicate known minimum levels.

The minimum level for magnesium (7 mg/L) is off the scale. Toxic concentrations of potassium are not indicated, minimum levels may be 93 mg/L (2.4 mmol/L, Suttle 2010). Horizontal axis label is week (Week 1, Week 2 and Week 3). Lighter coloured lines is the data, solid lines are means.

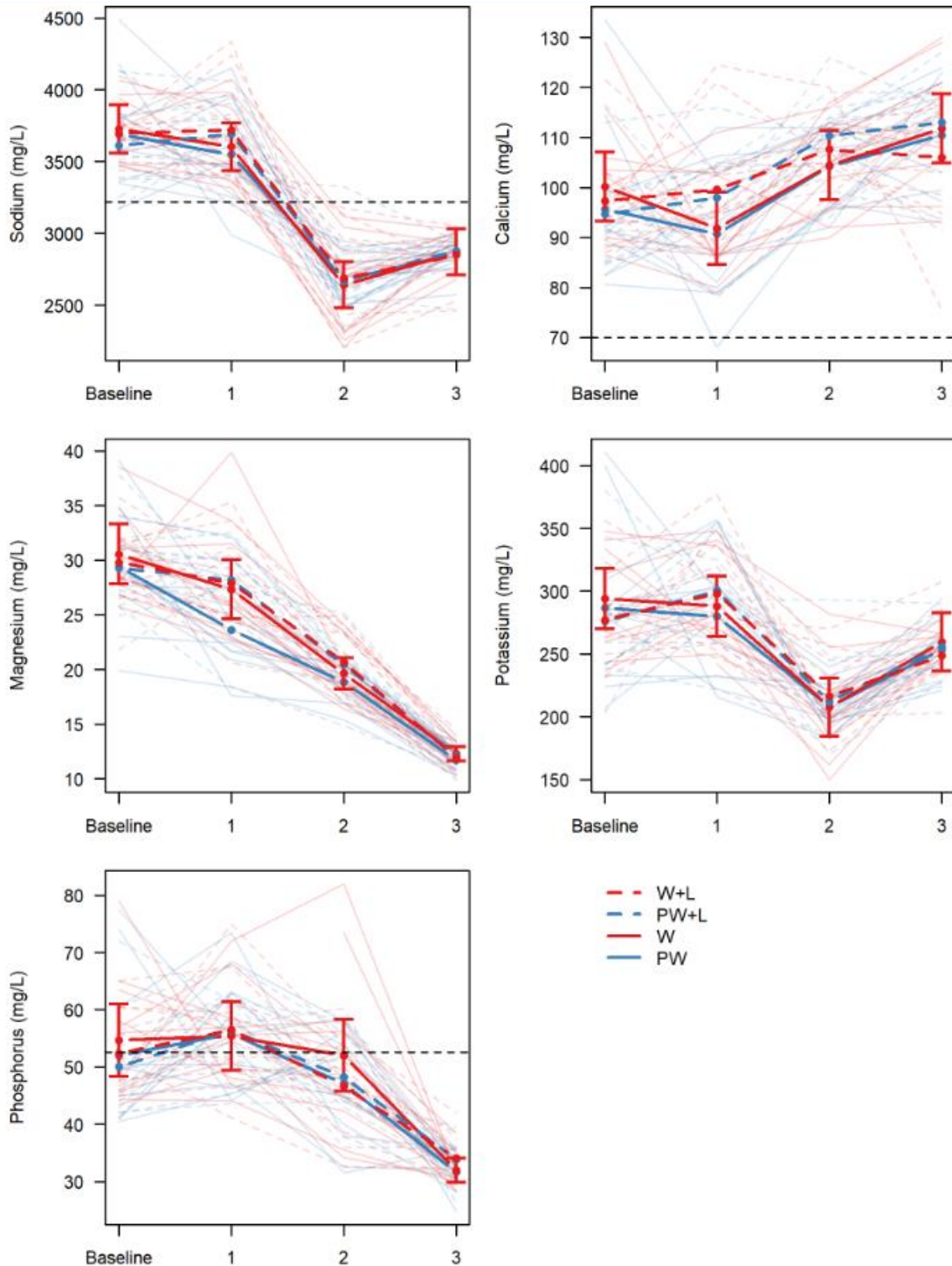
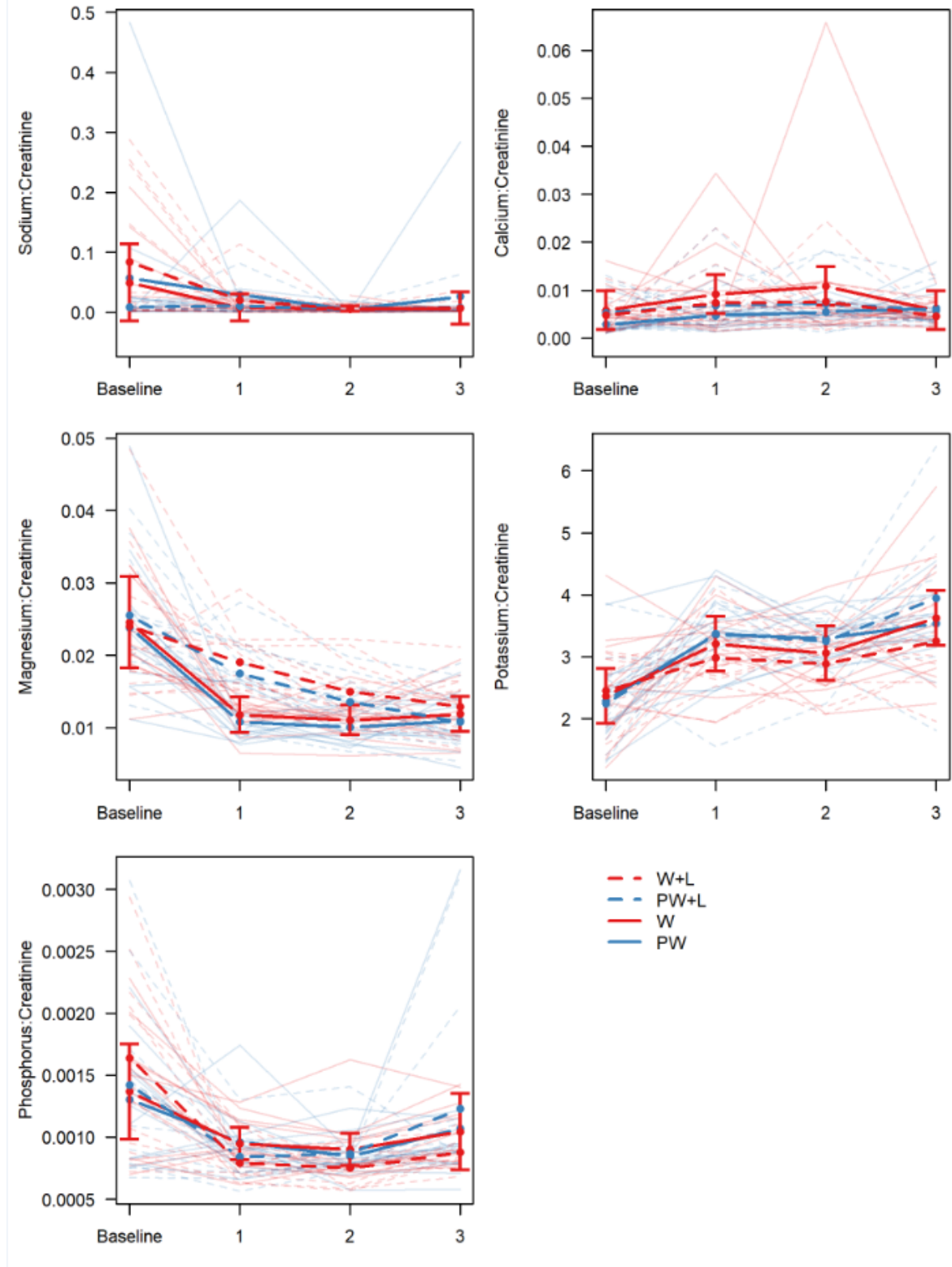


Figure 12. Urine mineral content to Urine creatinine ratio. No thresholds are indicated in the literature.

Horizontal axis label is week (Week 1, Week 2 and Week 3). Lighter coloured lines is the data, solid lines are means.



4.3.3 Protein identifications and quantification between diets

3525 proteins were identified from the membrane fraction (PW n=8, PWL n=12) of these 2181 were quantified (62 %). Using the fold change cut off of $FC > 1.3$, and significance $P < 0.05$. 72 proteins had a higher significance in the PW compared to the PW and L fed lambs rumen epithelium. 78 proteins had a higher significance in the PW + L versus the PW fed lambs rumen epithelium.

4.3.4 Functionally significant proteins and enriched pathways in PW > PWL fed sheep found using WGCNA

Our proteomics experiments with increased identifications and quantitation of protein level between treatments has improved. Weighted gene correlation network analysis (WGCNA) can use quantitative data from labelled MS/MS experiments to find clusters of protein identifications of interest, which are enriched for pathways or cellular processes of functional significance. In our case, we sought to capture the response of rumen epithelium proteins to sheep fed perennial wheat or perennial wheat with Lucerne which represent contrasting diets with a high K^+ and extremely low Na^+ . We used our novel isolation procedure, TMT labelling of proteins to quantitate differences in protein abundance and WGCNA to find significant functional differences in the response to each diet. These findings were then compared to function in the rumen epithelium proteins in sheep fed at 1.5 x maintenance or ad libitum and with different metabolisable energy content or with variation in phenotypic traits related to ‘efficiency’.

Using WGCNA 10 clusters were found with varying numbers of proteins in each (Figure 13); Black n=153, blue n=395, brown= 314, green = 203, magenta n= 94, pink n=111, purple n=77, red n=171, turquoise n=412, yellow n= 251 which were more or less abundant in PW or PW+L fed lamb rumen epithelium proteins. All ensemble protein accession numbers in each cluster list were converted to uniprot KB accession numbers in www.uniprot.org using the retrieve mapping tool. To find function enrichment of uniprot ids for KEGG pathways each cluster list was submitted to Database for Annotation, Visualization and Integrated Discovery (DAVID) v6.8 <https://david.ncifcrf.gov/>, selecting Ovine aries as species and list in the functional annotation tool.

The most interesting cluster in terms of nutrient use appeared to be the purple cluster.

In the WGCNA purple cluster fatty acid degradation had a significant (Benj $P < 0.001$; False Discovery Rate FDR $q < 6.1 \times 10^{-5}$) enrichment score of 4.47 (table 15). Proteins with functional significance related to a biological process (WGCNA) and with fold change greater than 1.3 and ANOVA $P < 0.05$ in PW compared to PWL are represented in Table 16.

Significant clusters examined in PWL > PW fed lambs correlation were black, brown and red Table 15. We found 11 proteins associated with the enrichment of the process and pathway of oxidative phosphorylation in the black, brown and red cluster proteins (Table 16).

Figure 13. Eigen protein expression boxplots represent the protein expression profiles for each module. The number on top indicates the number of proteins in each

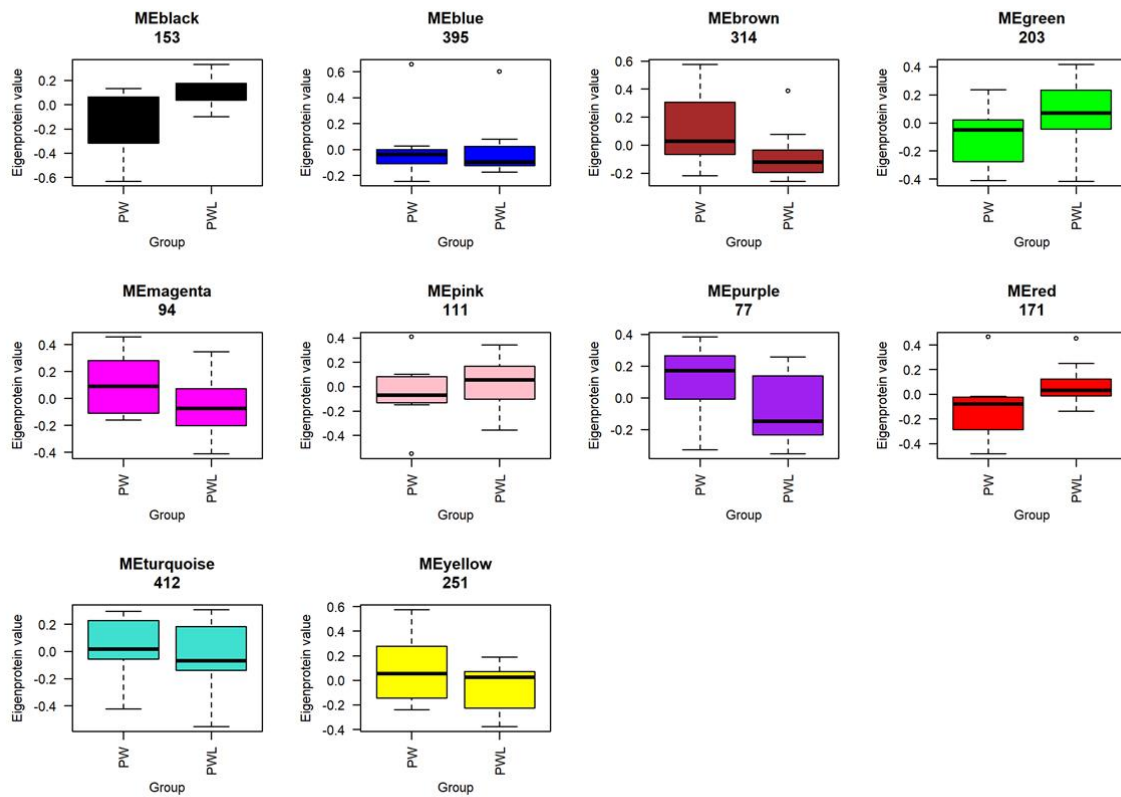


Table 15. DAVID enrichment found KEGG pathway for each diet Enrichment score for KEGG pathway was found using functional annotation clustering table downloaded into excel tab. Uni protein identifiers in each enriched pathway or functional process were listed and checked for significant fold change (1.2) and ANOVA P-value ($P < 0.05$)

KEGG pathway	Enrichment score	Count	P_Value	Fold Change	Benjamini	FDR	cluster
PW > PW + L							
Fatty acid degradation	4.47	6	2.40E-06	2.60E+01	6.60E-05	6.10E-05	purple
PW + L > PW							
Oxidative phosphorylation	6.74	14	1.30E-08	8.00E+00	1.70E-06	1.60E-06	black
Oxidative phosphorylation	2.69	1.00E+01	9.80E-05	5.30E+00	1.90E-02	1.90E-02	brown
Oxidative phosphorylation	6.66	1.40E+01	5.10E-09	8.60E+00	4.90E-07	4.70E-07	red

Table 16. Proteins with functional significance related to a biological process (WGCNA) and with fold change greater than 1.3 and ANOVA P<0.05 in PW compared to PW + L are represented.

Uniprot accession number	Protein name	Gene name	Fold change	P value
PW > PW+L				
W5P610	Chloride intracellular channel protein	CLIC1	1.27	0.003
W5PCE7	Calcium-transporting ATPase	ATP2B3	1.63	0.0001
W5PUC2	Acyl-CoA dehydrogenase short chain	ACADS	1.42	0.005
W5P1M4	Acetyl-CoA acyltransferase 2	ACAA2	1.44	0.014
W5PT19	Phospholipid-transporting ATPase	ATP8B3	1.61	0.003
O18751	Glycogen phosphorylase	PYGM	1.38	0.006
W5PFT7	Fructose-bisphosphatase 2	FBP2	1.37	0.002
W5P5C0	Enolase 2	ENO2	1.51	0.011
W5NZZ4	Protein-serine/threonine kinase	PDK4	1.5	0.05
PW+L > PW				
W5Q4F9	Solute carrier family 40 protein	SLC40A1	1.46 ⁺	0.01
W5PBG4	Calcium uniporter protein	MCU	1.38 ⁺	0.01
W5QAH8	NADH dehydrogenase [ubiquinone] 1 alpha subcomplex subunit 2	NDUFA2	1.31	0.01
W5NYM7	Complex I-B9 (NADH dehydrogenase [ubiquinone] 1	NDUFA3	1.29	0.02

	alpha subcomplex subunit 3)			
W5PE07	NADH dehydrogenase [ubiquinone] iron-sulfur protein 4,	NDUFS4	1.42	0.02
W5PYC8	Complex I-23kD (NADH dehydrogenase [ubiquinone] iron-sulfur protein 8	NDUFS8	1.44	0.01
W5Q5U7	ATP synthase subunit		1.36	0.02
W5PF18	ATP synthase subunit e, mitochondrial	LOC101102454	1.45	0.01
W5PSD1	Uncharacterized protein	LOC101119721	1.29	0.04
W5QFD8	Pyr_redox_2 domain-containing protein		1.40	0.009

Short chain fatty acids are absorbed along a concentration gradient (SLC transporters) with co- or counter ions such as sodium or hydrogen into the rumen via the SLC16A1 or SLC16A4 transporter (also known as MCT1 or MCT4). The two best described SCFA transporters in rumen epithelium and colon are SLC16A1 (also known as MCT1) and SLC16A3 (or MCT4). We detected SLC16A1 which symports H⁺ with SCFAs and SLC16A3 not identified. Other transporters involved with transport of SCFAs are those that exchange Cl⁻, Na, H⁺, K/Cl. We detected chloride anion exchanger (Solute carrier family 26 member 3) SCFA/Cl⁻, Sodium/hydrogen exchanger (NHE) and Na (+)/H (+) exchange regulatory cofactor NHE-RF. CLIC1 was more abundant in PW only marginally within FC cutoff of 1.3.

The significant enrichment for the KEGG pathway short chain fatty acid degradation in PW fed lambs is an important finding. We also observed a higher abundance of 4 proteins involved in the glycolytic pathway. The most relevant being protein-serine/threonine kinase (PDK4). PDK4 enzyme serves to regulate substrate decision making through manipulating the pyruvate dehydrogenase (PDH) complex by encouraging the supply of acetyl CoA to come from beta oxidation of fat rather than combustion of glucose. Acetyl-CoA is then used in the TCA acid cycle and provides the substrates for the electron transport chain to generate ATP (figure 14). In the PW fed epithelium PDK4 was significantly (P<0.05) higher in abundance (1.42 FC) than in the PW+L fed epithelium. Since ACADS had a fold change of 1.42 and ACAA2 a FC of 1.44 we can confirm the fats degraded by these enzymes are specific for short chain fatty acids. Despite this there is a range of longer chain fatty acids which can be utilised, the proteins and metabolic pathways to catabolise these nutrients is present in the peroxisome, a membrane bound sub-cellular compartment.

Our results do not indicate that short chain fatty acid metabolism occurred in the absence of glycolysis (see swath data). Interestingly toll like receptor 3 (TLR3 gene name; TIR domain-containing protein) expressed on the surface of the endosome was identified in PW and PWL fed lambs rumen

epithelium. Downstream intermediate adaptor molecules involved in TLR3 signalling pathways such as TRIF and TRAF (KEGG toll like receptor signalling pathways) were not detected although the nuclear factor kappa B subunit 1 (NF- κ B) was detected. There was no significant fold change in the level of these proteins associated with diet. We also detected IL-36RN and IL1R2 which are known to negatively regulate IL-1 signalling suggesting patterns of cytokines associated with inflammation responses due to a breach of barrier function integrity were not activated (Queen *et al.* 2019). Rather we found significant increase in 4 cytoskeletal structural proteins such as TJP3 (FC 1.31; $P < 0.04$), an uncharacterised protein coding to involucrin of (FC 1.55; $P < 0.031$), keratin 78 (FC 1.42; $P < 0.01$) and Keratin 79 (FC 2.02; $P < 0.02$) associated with the cornification of the basal corneum of PW fed lambs indicating the barrier function was being reinforced in the PW fed lambs and not compromised in the PW+L fed lambs rumen epithelium (Table 17).

Table 17. Proteins with functional significance related to a barrier function biological process (WGCNA) and with fold change greater than 1.3 and ANOVA $P < 0.05$ in PW compared to PW + L are represented.

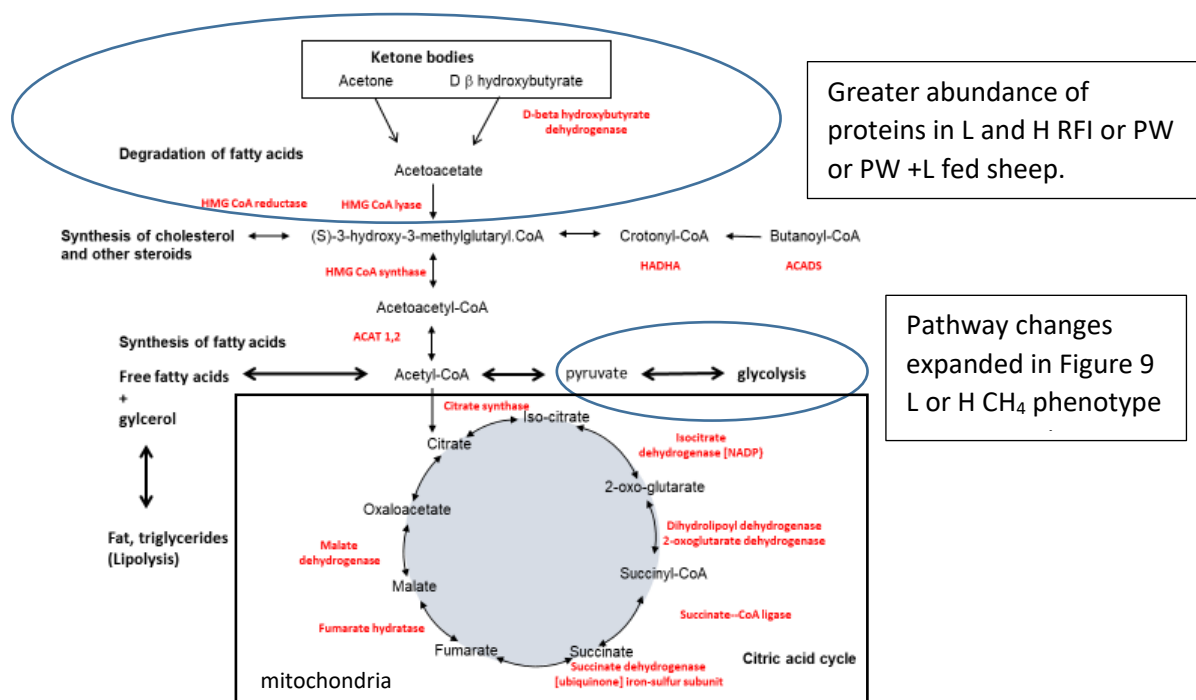
Uniprot accession number	Protein name	Gene name	Fold change	P value
PW > PW+L				
W5PQT0	Tight junction protein 3	TJP3	1.31	0.04
W5QIW9	Cornulin	CRNN	1.44	0.032
W5NQ79	Uncharacterized protein	IVL (involucrin)	1.55	0.031
W5Q5S8	Keratin 79	KRT79	2.02	0.024
W5Q5Q3	Keratin 78	KRT78	1.42	0.011
W5PYU6	Gamma-butyrobetaine hydroxylase 1	BBOX1	1.55	0.016

TLF 2 and 4 are known to impact the metabolic regulation of glycolysis or β oxidation of fats. These TLR's can recognise excess lipids or free fatty acids causing chronic low-level inflammation contributing to the progression of metabolic disorders. New evidence reveals TLR3 regulates glucose metabolism and insulin sensitivity of cells (Strodthoff *et al.* 2015; Woolard and Kevil 2015). TLR activation can cause glycolysis, while interleukin-4 receptor (IL4R) activation can induce β oxidation and enhancement of β -oxidation is associated with tissue repair and hampers pathogenic response. We did not detect IL4R (CD124) in PW and PWL fed lambs rumen epithelium. IL-4 receptor-expressing cells (CD124) include gastrointestinal (human peptide atlas) and T cells which may exist in the epithelium as small populations since they have been reported in stratum corneum by electron microscope studies (Lavker and Maltosky 1970). We identified CD207 (Guilliams *et al.* 2010) which is an identifier specific to dendritic or antigen presenting cells also probably within the epithelium cells isolated using our enzymatic procedure. Associated cytokine signalling proteins downstream of such as IL4R activation include those involved in JAK-STAT signalling pathways. In the PW fed lambs we found Elongator acetyltransferase complex subunit 2, (ELP2; FC 1.48 ; $P = 0.06$), Hepatocyte growth factor-regulated tyrosine kinase substrate (HGS; FC 1.62; $P < 0.02$) and phosphatidylinositol 3-kinase catalytic subunit type 3 (PIK3C3; FC 1.43; ns) had a higher abundance compared to the PW+L fed lambs.

To pass through the mitochondrial membrane with the help of carnitine the fatty acids undergo activation in the cytosol by getting converted to fatty acyl CoA, after which they undergo β -oxidation in the mitochondria. We found gamma-butyrobetaine hydroxylase 1 (1.55; $P < 0.016$) involved in the biosynthesis of carnitine was higher in the PW fed lambs epithelium. Beta oxidation of SCFAs is primarily facilitated by the mitochondria.

Therefore, the key enzymes regulating glycolysis as well as elements of the innate immune system were probably instrumental in determining a preference for energy formation through β oxidation of fatty acids rather than glycolysis in the PW fed lambs epithelium. A different scenario reflected by rumen epithelium proteins PW + L fed sheep existed with a significant enrichment of proteins involved in oxidative phosphorylation pathway of the mitochondria were found and no convincing evidence that energy regulation was preferentially from β -oxidation or glycolysis.

Figure 14. Cross section of metabolic pathways involved in B oxidation of SCFA or glycolysis.



The transport of SCFA in the rumen epithelium seem evident despite the low sodium threshold in the diet. It is difficult to estimate if this limited the availability of sodium to facilitate the co absorption of SCFAs via the SLC16 transporter. However, we identified a component of maxi-anion transporter (SLCOA21 Bond et al. 2021 in draft) hypothesised to exist by Georgi et al. 2014 and Stumpff 2018 and are permeable to SCFAs in the dissociated state (anion). This suggests another mechanism existed which SCFAs could accumulate into the epithelium transcellularly and independent of sodium. Interestingly, as reported by Newell et al. 2020 there were no differences in growth traits of the PW and PW + L fed lambs and only a relatively small difference in feed intake (100g).

In addition, we found higher abundance of 2 transporters in the PW fed lambs. That is chloride intracellular channel protein (CLIC1, FC 1.27; $P < 0.003$) and calcium-transporting ATPase (ATP2B3, FC 1.63; $P < 0.0001$). This coincided with the lower than threshold requirement for Ca in the PW diet. Whereas, in the PW + L diet a calcium uniporter protein (MCU; FC 1.38) of the mitochondrial membrane was significantly higher in abundance. Since the function of calcium is specific for the cell compartment it is used in, these represent two differing responses of calcium transport to calcium

content in the diet. The changes in abundance of the different transporters suggests the epithelium has different strategies to respond to maintain absorption of calcium intracellularly and make it available from the diet. Interestingly, plasma Ca increased during the period the lambs were fed the PW diet. The higher abundance of the Ca ATPase in the rumen epithelium of PW fed lambs may have been in response to reduced Ca in the forage consumed and uptake in the rumen with high levels of K⁺ in the feed. As previously demonstrated by Bhanugopan *et al.* 2015 to high levels of K⁺ in the diet reduce the fractional absorption of calcium in the rumen and increases excretion of K⁺ in the urine. Like Bhanugopan *et al.* 2015, we also observed an increase in the excretion of K⁺ in the urine of the PW fed lambs where the level of K⁺ was above dietary requirements.

Collectively the addition of Lucerne (a legume) to the diet had benefits at the cell level for the efficient use of nutrients from a diet which otherwise has metabolic disturbances associated with it. The positive effects on the diet composition by combining the legume with the perennial wheat are evident.

4.4 Nutrient transport in rumen epithelium

4.4.1 Identification of proteins that transport nutrients and ions in the rumen epithelium

Two main families of transporters were identified, the solute carrier (SLC) family and ATP binding cassette (ABC) transporters. Most members of the SLC group had >3 TMHMM indicating they are integral plasma membrane proteins and a smaller number were located on the membranes of intracellular organelles as described by bioinformatics or literature.

Those that transport carbohydrates were 2 glucose transporters SLC2A1 (GLUT1) and SLC5A1 as well as several SLC35 family transporters which exchange UDP-sugars. We also detected amino acid transporters, including, SLC1A4, SLC1A5, SLC3A2 (neutral amino acids) and SLC18A1 (amine). Lipid transporters found were SLC16A1 (SCFA/lactate), SLC26A3 (SCFA/HCO₃⁻), SLC27A1 (LCFA), SLC27A2 and SLCA4 (fatty acid transport). Those that transport metabolic intermediates were SLC14A1 (urea), SLC44A1, SLC44A2 and SLC44A3 (choline). Eight ABC transporters identified all had multiple transmembrane domains indicating they were core components of multiprotein complexes on the cell surface. ABCA12 and ABCA13 transport fatty acids involved in the formation of the lipid barrier.

Many of the transporters identified regulate cell ion homeostasis through transport of inorganic ions across the plasma membrane. They include (n=43 SLC) SLC9A3 (Na⁺/H⁺), SLC12A4 and SLC12A6 (K⁺/Cl⁻), SLC22A18 (cation), SLC26A2 (anion/sulfate), SLC30A1 and SLC30A7 (Zn²⁺), SLC40A1 (H⁺/metal). Anions transporters identified were the core maxi-Cl channel transporter SLC12A6 which is permeable to Cl⁻ and SCFA anions Sabirov *et al.* 2017. A volume-sensitive outwardly rectifying anion channel (VSOR; LRRC8E) and chloride intracellular channel proteins (CLIC1 and CLIC4), members of the CLC family of chloride gated channels (CLCA2, CLCN1, 2, 3) and the anoctamin family (ANO 6, 9,10) were identified. Three subunits of ATP1 (Na⁺/K⁺), three subunits of ATP2 (Ca²⁺), and ATP8 or ATP9 that transport phospholipids were also found. The ATP1 protein is a major driver of the concentration gradient of solutes in the epithelium at the basal level.

Those that are specific to the transport of metabolites across the membrane of subcellular compartments were the SLC25 Palmieri 2012 and SLC54A2 family. These transport substances across the inner membrane of the mitochondria. ABCD3 family transporter specifically imports acyl-fatty acids across the peroxisome membrane, making FAs available for β fatty acid oxidation Wander and

Waterman 2006. The proteome analysis also identified 9 subunits of the V-ATPase proton pump family that occur in the membrane surrounding the endosome, lysosome and phagosome Okada et al. 2018 and play a role to acidify these compartments during acid hydrolysis of proteins encapsulated by these vesicles. These specialised locations provide the cell with different cellular conditions within organelle membranes that are different to the cytosol broadening the range of cellular functions the cell can perform.

4.4.2 Proteins and the process of nutrient transport

It has now been clearly demonstrated that the permeability of substances between cells through the extracellular space is regulated by pore or leak pathways formed by tight junction proteins such as the claudins. In our case, in ovine tissue and as confirmed by several other studies in caprine and bovine rumen epithelium tissue contains claudin 1 and 4 that play a key role in permeability of substances between cells. These proteins are classified to be predominantly barrier-forming and decrease permeability to cations. Additionally, the tight junction barrier to permeability, established by the claudin proteins and others, also maintains the electrochemical gradients that regulate the flux of nutrients established intracellularly by transcellular ATP driven (ATPase, ABC) transporters, symporter or antiporter transporters (SLC).

Cellular integrity is maintained by proteins that form the structural components of the cells. Our study enabled identification and functional annotation of 81 cell junction proteins classified as tight junction, gap junction and adherens junctions that play a role in cell polarity, cell differentiation and cytoskeletal assembly (L or H CH₄; not shown). Proteins associated with maintenance of the plasma membrane electrochemical potential for nutrient transport by tight junction proteins included, two claudins (CLDN1, CLDN4). Others to note were occludin (OCLN), zona-occludins (TJP1) and junctional adhesion molecule (JAM or F11R). Proteins that connect cells included 2 gap junction proteins (connexin 43, connexin 26) and alpha and beta chains of 4 tubulin proteins. Furthermore, adherens junction proteins were identified that are required for the tight junction between cells in the epithelium structure. These included 3 cadherins (CDH1, CDH3, CDH13), 3 catenins (CTNNA1, CTNNB1, CTNND1), 2 desmocollins (DSC2, DSC3), 2 desmogleins (DSG2, DSG3), desmoplakin (DSP), junction plakoglobin (JUP), plakophilin (PKP3), actinin (ACTN1), vinculin (VCL) and afadin (AFDN).

5. Discussion

5.1 Phenotypes

5.1.1 Phenotypic correlates of more efficient nutrient use in growing sheep: how to pick ‘better doers’.

The present experiment examined the inter-relationships between feed intake, growth, body composition and methane gas emission. At ad libitum feeding levels feed the same diet for 60 days there was significant variation in feed intake between individual sheep. That is the H RFI growing Merino wethers ate more than L RFI wethers for the same liveweight. Traits that explained the most variation in high or low RFI phenotype were LWT60 days, ADG, fat gain EBW, daily CH₄ emission and MY. Phenotypic variation in feed efficiency (residual feed intake, RFI) are reported in numerous studies for beef cattle (Arthur et al. 2001; Basarab et al. 2003; Herd et al., 2000, 2014; Ceacero et al. 2016), dairy cattle (Williams et al. 2011; Derno et al. 2019) and sheep (Zhang et al. 2017; Knott et al. 2008; Rajaei Sharifabadi et al. 2016). The model of feed efficiency used widely in the Australian beef cattle industry (Arthur et al. 2001; Robinson and Oddy 2004) estimates feed intake in relation to LWT and ADG using the model initially described by Koch et al. (1963). Our results and the correlations with feed intake are consistent with this model and the studies above.

In our research we measured feed intake in single pens and had periods of group feeding to allow the sheep to exhibit their normal feeding behaviour, since this has been reported to influence the phenotyping of RFI sheep or cattle (ref). Although not a field study on pasture we did observe significant differences in RFI in the 113 wethers measured according to RFI calculated with LWT60 days and ADG. The feeding regime with ad libitum feeding level of cereal chaff and Lucerne chaff over 60 days allowed us to observe variation in RFI. Of the 113 wethers measured in this experiment roughly half fell into a H and half into a L RFI phenotype. There was a range of liveweights from 25 - 40 kg and the relationship between FI 60days and liveweight stayed linear and positive accounting for the most variation in RFI (63%).

For measurements of RFI in cattle, feed is generally offered ad libitum and is usually based on a concentrate diet although in an experiment by Durunna et al. (2011) cattle fed a grower diet or a finisher diet re rank in their RFI phenotype suggesting the diet composition is also important, whereby the finisher diet has a higher grain or starch content and lower NDF (29%) component. Also Lines et al. (2018) found in heifers feed ad libitum differed in RFI whereas those fed a near maintenance energy level diet did not vary in RFI. Similarly, we found sheep fed ad libitum roughage diet (9.3 ME, 12.6 % CP) although with relatively low estimated digestibility (64% DMD) compared to a concentrate grain rich diet normally feed to cattle in RFI experiments, there was variation in RFI and the H RFI group ate more for the same liveweight gain over 60 days.

Unlike previous research, we used detailed measurements of body composition in live sheep through computer tomography scans and image analysis to link lean, fat and bone deposition during growth to other traits. Body composition has been described as a source of variation in RFI among cattle Herd and Arthur (2009) but its contribution is relatively small (15%). Knott et al. (2008) found inclusion of ultrasound measures of muscle and back subcutaneous fat depth in meat sheep accounted for a greater proportion of the variation in feed energy use. This model improves the calculation of energy use efficiency by accounting for the post absorptive utilisation and ultimate distribution of the feed nutrients. In contrast, in our experiment there was no significant contribution of back subcutaneous fat depth, eye muscle area or eye muscle depth at the C-site

(12th/13th rib) to the model to explain variation in RFI. This may have been related to the accuracy of different methods to relate body composition to the RFI phenotype.

Obviously, computer tomography (CT) scans of the whole sheep's body can be used to assess the distribution of fat into subcutaneous and intramuscular in the empty body weight was more informative in this research than back fat subcutaneous fat alone to explain differences in RFI. In our experiment the addition of subcutaneous and intra-muscular fat EBW increased the explanation of variation in RFI by 3.4 %. Our results suggest H RFI wethers had a greater intramuscular fat level than the L RFI. Although not a dramatic increase it was a significant improvement in the prediction of RFI. It informs us where the fat was deposited which may represent different biological processes (Dodson et al. 2010). Although we did not include visceral fat in and around the digestive system and the information provided is important since it affects the overall quality of the meat in the carcass and would have an impact on the resilience of the animal during periods of seasonal feed gaps. This is particularly relevant to Merino ewes with high wool production and feed intake since the fat score of the carcass is thought to be associated with reproductive performance (Greef et al. 2005; Safari et al. 2005). The exact distribution associated with this association between reproductive performance and fat distribution warrants further investigation using the CT scan method.

Since there is a well described correlation between feed intake and CH₄ emission (Blaxter and Clapperton 1965), it is not surprising that we also found this relationship between the RFI and methane emission trait in sheep. In our experiment we found there was a small but significant contribution of daily CH₄ and MY (+ 5%, total 80.2%) to the regression model also including traits LWT60days, ADG, fat gain EBW. In another study in cattle low RFI produce relatively less methane as compared to cattle with high RFI (Okine et al. 2001; Herd et al. 2002) and it was evident in another comparison of efficient and inefficient cattle (Nkrumah et al. 2005, 2006). A similar result was found in a study of cattle (Hegarty 2007) where they reported RFI explained only a small proportion of the total variance in methane production rate. Although our diet was not directly comparable with their barley grain based diet it had a similar energy content even though the digestibility was lower. Hence this would affect the amount able to be eaten and the mean retention time of the digesta in the digestive system. Although there was a strong positive correlation of feed intake with daily CH₄ emission parameters effecting the fermentation of forage, host digestive characteristics and microbial population (Bond et al. 2018; Ross et al. 2020) are also important factors explaining the variation in CH₄ emission in sheep. In addition, the different pattern of ranking of L or H RFI compared to the linear relationship between daily CH₄ and feed intake suggests these are different traits. We surmise daily CH₄ emission co varies with RFI but is not an important predictor of biological functions underpinning each trait.

Implications of the RFI phenotype in the commercial situation are the Merino wethers that eat less relative to liveweight gain, ADG, may have a slightly lower body condition score than H RFI particularly if feed was restricted. In a situation of these sheep being used as growers for meat that can be turned off in one season when feed is plentiful it makes this trait viable as a selection tool for breeders. However, if keeping these animals for longer for wool production those that ate more and gained more fat may be more resilient to yearly feed availability. As explained in a model for Mediterranean climate in SA (Walkom et al. 2016) recommended a sheep that had higher fat reserves that can take advantage of feed when it is in excess and utilise fat reserves to compensate energy demands when feed is scarce or a lower quality and more expensive through supplementation.

5.2 Quantification of cytosol and membrane proteins by SWATH-MS in rumen epithelium of sheep with low or high CH₄ emission phenotype

We have presented a comprehensive proteomic landscape of the ovine rumen epithelium. This dataset provides a framework which allows better functional annotation of rumen epithelial proteins, thus providing information about the cellular functions driven by those proteins. Since our first attempts to profile proteins of enzymatically isolated rumen epithelium ($n=570$ proteins) Bond et al. 2019, we have been able to substantially increase the depth of proteome coverage by 5 fold ($n=2767$ proteins). Bioinformatics analysis reveals the cellular location and likely function of the proteins not previously annotated.

Enrichment of membrane proteins and the high coverage of proteins identified in the membrane fraction (23 % with TMHMM) allowed us identify many nutrient transporters previously only reported at the transcript level. Compared to our previous attempt to identify these protein transporters we increased the number found 3.5 fold from 25 Bond et al. 2019 to 92 using the current proteomic approach. Two families of transporter proteins were well represented including the solute carrier family (SLC) and ATP binding cassette family (ATP). A transporter that has not been detected in rumen epithelium, SLCO2A1 protein, was found in the present study.

More recently, strong evidence has emerged to support the existence of large conductance anion channels (>300 pSec) in ovine and bovine epithelium [14]. In particular, electrophysiology studies [15, 16] point to the existence of a maxi-Cl channel permeable to Cl⁻ and SCFAs. The identity of molecular candidates for the channel has been debated, but recent evidence clearly defines the core of the maxi-Cl channel as organic anion transporter SLCO2A1 (Sabirov et al. 2018, Georgi et al. 2014). We confirm the presence of SLCO2A1 protein containing 11 transmembrane domains in our rumen epithelium tissue representing an alternative route to transport SCFAs than the well described SLC16A1 (MCT-1) (Graham et al. 2007).

In addition, we identified subunit LRRC8E of the volume-sensitive outwardly rectifying anion channel family (VSOR) (Okada 2018). Recently the transient receptor potential (TRP) channel TRPV3 has been shown to be permeable to Na⁺, Ca²⁺, NH₄⁺ (Schrapers et al. 2018). We identified a related protein TRPM4 which is a Ca²⁺-activated nonselective cation channel mediating cell membrane depolarization Launay et al. 2020.

Supporting information to outline quantitative differences in the metabolites identified in the rumen fluid of fed animals, protein transporters and key metabolic pathways has helped us to track the metabolic fate of key nutrients during their passage through the epithelium. In ruminants, the main products of fermentation of dietary fibre are SCFAs, (acetate, propionate and butyrate) which account for more than 70 % of the animals caloric intake Bergman et al. 1990. In this review it states glucose was rarely detected in rumen fluid or intestinal fluid. However, using modern techniques like NMR we detected concentrations of 7.6 mM in L CH₄ and 5.7 mM glucose in H CH₄ rumen fluid around 3 h after being fed a fibrous diet. In a similar study in dairy cows by Saleem et al. 2013 using NMR they found the concentration of glucose 0.5 mM (prior to feeding a diet with increasing amounts of barley grain). Collectively these findings indicate glucose is available in the rumen fluid in reasonably high concentrations at certain time points during fermentation. Glucose, other mono- or oligosaccharides and SCFA's may be absorbed from the rumen fluid by plasma membrane transporters in the epithelium. Two main glucose transporter families, SLC2A (GLUT) and SLC5A (Na⁺/glucose symporter), have been previously reported in the bovine rumen Ostrowska et al. 2015. Similarly, Aschenbach *et al.* 2000 demonstrated in sheep rumen epithelium gene expression of

SLC5A1 (SGLT1) and its transport of D-glucose from the lumen to the blood *in vitro*. We identified SLC2A1 (GLUT1) and the SLC5a1 protein in the rumen epithelium proteins and associated changes in epithelium enzymes related to glucose metabolism. Coincidentally, we detected higher blood glucose in the L CH₄ serum.

The concentrations of acetate, butyrate and propionate in our research are typical of a rumen fluid in sheep fed a fibrous diet. The time of sampling the rumen fluid coincides with peak methane emission Bond et al. 2016 in the rumen. It is surprising we did not detect a significant difference between any of the metabolites identified in the rumen fluid between L or H CH₄ phenotype. Other evidence suggests we could expect to detect differences in metabolite concentration between L and H CH₄ sheep rumen fluid. These include the L CH₄ sheep phenotype being associated with shorter mean retention time of digesta (MRT) (Bond et al. 2016; Pinares-Patiño et al. 2003), higher proportion of propionate to acetate ratio rumen fluid and the rumen microbiome being enriched by lactic acid forming bacteria such as *Sharpea* (Kamke et al. 2016) of L CH₄ yield sheep. The evidence from these studies supports the idea that different metabolic conditions do occur in L or H CH₄ emitting sheep rumen fluid and these conditions in direct contact with the rumen epithelium result in the differences in protein abundance found.

Collectively our results show glucose, simple saccharides and SCFA's may be utilised to maintain rumen epithelium cell energy homeostasis and to support their high rate of cell division and protein synthesis. The differences in the abundance of enzymes of the glycolytic pathway or methylglyoxal pathway (MGO) in the H or L CH₄ sheep epithelium found reflects different mechanisms of energy use or detoxification occurred between the CH₄ phenotypes probably dependent on the metabolites available for absorption.

To our knowledge the MGO pathway has not been reported in sheep rumen epithelium in previous research, although the genes for the enzymes involved exist in the ovine, caprine and bovine genome. It was once thought D-lactate only occurred from exogenous sources in ruminant epithelium from microbial fermentation of feed or feed stuffs with a relatively high concentration of D-Lactate, such as silage. However, the endogenous production of D-lactate in human cells (and now ovine rumen epithelium) can result from the MGO pathway Ewaschuk et al. 2005. From *in vitro* studies it is clear bovine tissues possess D-lactate dehydrogenase (DLDH) Harmon et al. 1984 and we have evidence DLDH is increased in ovine epithelium tissue in the L CH₄ sheep. Therefore D-lactate can be converted back to pyruvate downstream of the methylglyoxal pathway by DLDH in the L CH₄ epithelium and used in the TCA cycle to produce energy. In addition, the higher level of malic enzyme 1 in the L CH₄ epithelium suggests these cells were also recycling malate from the TCA cycle to provide pyruvate for cellular energy transactions requiring NADH, FADH or ATP. Furthermore, ‘resistin’ which is known to alter the sensitivity of cells to the hormonal control of glucose by insulin pang and le 2006 had a higher abundance in the L CH₄ sheep. Together the results provide evidence that the L CH₄ sheep probably regulate the use of nutrients available for absorption from the rumen fluid more efficiently compared to the H CH₄ sheep.

Differences between the L and H CH₄ epithelium in the abundance of proteins engaged in mechanisms to maintain immunity / cell defence against micro-organisms in the rumen existed. Epithelium utilise phagocytosis to kill microorganisms by production of reactive oxygen species. A variety of extracellular stimuli can activate distinct signalling pathways that converge to initiate expression of NOS₂. Cell wall components of bacteria and fungi can trigger the innate immune signalling cascade, leading to expression of NOS₂. Iron transporter SLC40A1 higher abundance in the H than L CH₄ sheep could be linked to a process called the Fenton reaction. Whereby iron (Fe²⁺) catalyses the conversion of hydrogen peroxide (H₂O₂), a product of mitochondrial oxidative

respiration or processes in the peroxisome, into a highly toxic hydroxyl free radical Winterbourn et al. 2006. Thereby facilitating the action of H_2O_2 to kill bacteria in the epithelium. In the L CH₄ epithelium myeloperoxidase was more abundant. Some phagocytes have the capacity to secrete enzymes called myeloperoxidases that can catalyse a reaction of H_2O_2 and halides such as chloride to produce hypochlorous acid (HOCl; Bakkenist et al. 1980). These hypohalous acids kill bacteria but can also damage normal tissue and thereby contribute to an inflammatory reaction. Also adaptor protein (AP) complex subunit beta had higher abundance in the L CH₄ epithelium. Adaptor protein complexes function is involved in clathrin-dependent endocytosis in which cargo proteins are incorporated into vesicles surrounded by clathrin (clathrin-coated vesicles, CCVs) which are involved in a process by which cells absorb metabolites, hormones, proteins and in some cases viruses by the inward budding of the plasma membrane (invagination). Lastly the L CH₄ epithelium had a greater abundance of an antimicrobial called Azurocidin 1.

5.2.1 Mitochondrial content

This project has reinforced the concept that ruminant feed efficiency (FE) is a difficult to predict (and model) trait with a very complex physiological architecture. Nevertheless, several lines of evidence now exist that the mitochondria plays a role in determining whole animal FE. Based on the Merino wether ‘Better Doer’ experiment we detected a significant association between liver mitochondrial content and whole animal FE ($P = 0.029$). We hypothesize a blood test providing a systemic indication of liver (aerobic) function may hold hope for a candidate diagnostic tool in this space.

Of the 4 tissues that showed a tendency to correlate with sheep FE, all correlations – while modest – were in the same positive direction. Thus, more efficient animals (low intake relative to body mass) tend to have a lower tissue mitochondrial content across liver (correlation of 0.20), rumen (0.18), soleus m. (0.14) and skin (0.05). This is consistent with the reduction in spare physiological capacity argument presented in Hudson (2009). Thinking more broadly about the mitochondrial outcomes of this collaboration, the animal trial run out of Armidale also found whole animal carbon dioxide emissions, a consequence of the activity of the tricarboxylic acid (TCA) cycle in the mitochondrial matrix of the host animals target tissues during cellular respiration, are also associated with FE ($r = 0.303$; $P = 0.003$). Explorations of mitochondrial function within a production efficiency context is an emerging growth area. Our molecular results broadly support those of Kong et al (2017) who found Hereford x Angus steers with low rumen epithelia mitochondrial content were more feed efficient.

Finally, as a consequence of screening ~40 Merino wethers for mitochondrial content across six tissues we have advanced our understanding of how the skeletal musculature, liver, rumen and skin inter-relate metabolically in ruminant production animals. Based on patterns of hierarchical clustering the liver and rumen (representing central control of metabolism and digestion) appear to form a tightly coordinated metabolic axis in sheep that is regulated somewhat independently of the skeletal musculature (a major sink of glucose and other metabolic fuels). Although the experimental design was not explicitly set up to test this, the mitochondrial content in descending order of aerobic capacity for sheep tissues appears to be as follows: liver and muscle > rumen > skin.

6. Conclusion and recommendations

6.1 Rumen epithelial proteins

Rumen epithelial cells play a vital role in barrier, nutrient metabolism and transport, cytokine and hormone signalling, cell adhesion molecules and cell immunity functions. Here we present cytosolic and membrane sub-proteome landscape of ovine rumen epithelium, in-order to examine the cellular processes represented by the proteins. In particular, we sought to identify and functionally annotate proteins involved in the transport and metabolism of nutrients and cell permeability of the epithelium of the rumen wall. A protein transporter (SLCO2A1) previously not identified involved in SCFA and chloride transport was found.

The identifications of nutrient transporters, metabolic pathways and intracellular compartments have defined and expanded our understanding of the processes regulating energy use in the epithelium. Our comprehensive coverage of proteins in the rumen epithelium has been successfully linked to phenotypic differences in growth and feed intake to nutrient use efficiency protein markers in the rumen wall. We anticipate that our resource will facilitate further basic and applied research on sheep as well as other ruminants. Overall the findings highlight the rumen epithelium is well adapted to absorb a range of nutrients depending on those that are available. Therefore, ruminants can use a range of nutrients from different plant feed sources, giving producers flexibility to provide feed to ruminants. How well these are absorbed by the rumen impacts how efficient nutrient use is by the rumen epithelium. This in part contributes to phenotypic variation in traits such as RFI and methane emission.

Although the CH₄ phenotype was correlated to RFI phenotype the results indicate the traits have a different biological process and we recommend they are selected separately.

The main differences in protein abundance found between L or H CH₄ emitting sheep were related to the metabolism of glucose. In addition, we found evidence the immune mechanism epithelium use in response to microbes was different in the L or H CH₄ phenotype. We found a member of the family of antimicrobial proteins ‘cathelicidins’ called Azurocidin 1 had greater abundance in the L CH₄ epithelium. They can kill methanogens, are they secreted by other microbes in the rumen and if secreted by the rumen epithelium in granules could influence the host control of the low CH₄ phenotype. This warrants further investigation for emission abatement in livestock.

Of particular, interest perennial wheat fed had greater abundance of Ca transporter proteins or ion channels in the rumen epithelium. This was associated with mineral imbalance in the fed on offer. Therefore, mineral supplement with salt (Na Cl) and aglime are recommended to overcome this imbalance. In addition, feeding a mixture of a legume such as Lucerne with a cereal crop with High potassium and very low sodium content is recommended to overcome the mineral imbalance and any disturbance to nutrient absorption.

6.2 Mitochondrial content

We discovered liver mitochondrial content is significantly associated with FE. This is an exciting new finding indicating a) sheep liver aerobic capacity is associated with whole animal FE and b) that a circulating test reflecting liver aerobic capacity (or related liver function) might offer future hope for a diagnostic test for FE going forwards. Low mitochondrial content in liver tends to be associated with high efficiency that is low feed intake relative to body mass.

7. References

7.1 Quantification of Low or high methane rumen epithelium proteins

Jiang et al. 2014 The sheep genome illuminates biology of the rumen and lipid metabolism *Science* 2014;344:1173-1168.

Bond JJ, Cameron M, Donaldson AJ, Austin KL, Harden S, Robinson DL and Oddy VH. Aspects of digestive function in sheep related to phenotypic variation in methane emissions. *Anim Prod Sci* 2017;59:55-65.

Pinares-Patiño CS, Hickey SM, Young EA, Dodds KG, MacLean S, Molano G, Sandoval E, Kjestrup H, Harland R, Hunt C, Pickering NK and McEwan JC (2013) Heritability estimates of methane emissions from sheep. *Animal* 7, 316 - 321.

Robinson DL, Goopy JP, Donaldson AJ, Woodgate RT, Oddy VH and Hegarty RS (2014) Sire and liveweight affect feed intake and methane emissions of sheep confined in respiration chambers. *Animal* 8, 1935 – 1944.

Blaxter KL and Clapperton JL (1965) Prediction of the amount of methane produced by ruminants. *British Journal of Nutrition* 19, 511–522.

Bond JJ, Donaldson AJ, Coumans JVF, Austin K, Ebert D, Wheeler D and Oddy VH. Protein profiles of enzymatically isolated rumen epithelium in sheep fed a fibrous diet. *J Anim Sci and Biotech* 2019;10:5.

Kamath KS, Krisp C, Chick J, Pascovici D, Gygi SP and Molloy MP. *Pseudomonas aeruginosa* proteome under hypoxic stress conditions mimicking the cystic fibrosis lung. *J Proteome Res* 2017;16:3917–3928.

Horton P, Park K-J, Obayashi T, Fujita N, Harada H, Adams-Collier CJ and Nakai K. WoLF PSORT: protein localisation predictor. *Nucleic acids research* 2007;35: W585-W587.

Krogh A, Larsson B, von Heijne G, Sonnhammer EL. Predicting transmembrane protein topology with a hidden Markov model: application to complete genomes. *J Mol Biol.* 2001;305:567-80.

Emanuelsson O, Nielsen H, Brunak S and von Heijne G. Predicting subcellular localization of proteins based on their n-terminal amino acid sequence. *J Mol Biol.* 2000;300:1005–1016.

Bendtsen JD, Jensen LJ, Blom N, Von Heijne G and Brunak S. Feature-based prediction of non-classical and leaderless protein secretion. *Protein Eng Des Sel* 2004;17:349–356.

Keerthikumar S, Chisanga D, Ariyaratne D, Al Saffar H, Anand S, Zhao K, Samuel M, Pathan M, Jois M, Chilamkurti N, Gangoda L and Mathivanan S. ExoCarta: A web-based compendium of exosomal cargo. *J Mol Biol.* 2016;428:688-692.

Calvo SE, Clauser KR and Mootha VK. MitoCarta2.0: an updated inventory of mammalian mitochondrial proteins. *Nucleic Acids Res* 2016;44:D1251–D1257.

Wander RJA and Waterman HR. Biochemistry of mammalian peroxisomes revisited. *Annu. Rev. Biochem.* 2006;75:295-332.

Xiang R, McNally J, Rowe S, Jonker A, Pinares-Patino CS, Oddy VH, Vercoe PE, McEwan JC and Dalrymple BP. Gene network analysis identifies rumen epithelial cell proliferation, differentiation

- and metabolic pathways perturbed by diet and correlated with methane production. *Sci Rep.* 2016; 6:39022.
- Sabirov RZ, Merzlyak PG, Okada T, Islam R, Uramoto H, Mori T, Makino Y, Matsuura H, Xie Y and Okada Y. The organic anion transporter SLCO2A1 constitutes the core component of the Maxi-Cl channel. *The EMBO journal* 2017;36:3309-3324.
- Palmieri F. The mitochondrial transport family SLC25: identification, properties and physiology. *Mol aspects med.* 2012;34:465-484
- Kuzinski J, Zitnan R, Warnke-gurgel C and Schweigel M. The vacuolar-type H⁺-ATPase in ovine rumen epithelium is regulated by metabolic signals. *J Biomed Biotechnol.* 2010; 525034:1-12.
- Georgi M-I, Rosendahl J, Ernst F, Günzel D, Aschenbach JR, Martens H and Stumpff F. Epithelia of the ovine and bovine forestomach express basolateral maxi-anion channels permeable to the anions of short chain fatty acids. *Pflugers arch – Eur J Physiol.* 2014;466:1689-1712.
- Stumpff F. A look at the smelly side of physiology: transport of short chain fatty acids. *Pflugers arch – Eur J Physiol.* 2018;470:571-598.
- Gäbel G and Martens H. Transport of Na⁺ and Cl⁻ across forestomach epithelium: mechanism and interaction with short chain fatty acids. In: Suda T, Sasaki Y. and Kawashima R. editors, *Physiological aspects of digestion and metabolism in ruminants.* San diego:Academic press; 1991, p. 129-151.
- Graham C, Gatherer I, Haslam I, Glanville M and Simmons NL. Expression and localisation of monocarboxylate transporters and sodium/proton exchangers in bovine rumen epithelium. *Am. J Physiol Regul Integr Comp Physiol* 2007;292: R997-R1007.
- Müller F, Huber K, Pfannkuche H, Aschenbach JS, Breves G, Gäbel G, Transport of ketone bodies and lactate in the sheep ruminal epithelium by monocarboxylate transporter 1. *Am J Physiol-Gastr L.* 2002;283:G1139-1146.
- Okada Y, Okada T, Islam R and Sabirov RZ. Molecular identities and ATP release activities of two types of volume-regulatory anion channels, VSOR and Maxi-Cl. *Curr Top Membr.*2018;81:125-176.
- Jentsch TJ, Lutter D, Planells-cases R, Ullrich F and Voss FK. VRAC: molecular identification as LRRC8 heteromers with differential functions. *Pflugers arch –Eur J Physiol.* 2016;468:385-393.
- Schrapers KT, Sponder G, Leibe F, Liebe H and Stumpff F. The bovine TRPV3 as a pathway for the uptake of Na⁺, Ca²⁺ and NH₄⁺. *PLoS ONE* 2018;13:e0193519.
- Launay P, Fleig A, Perraud AL, Scharenberg AM, Penner R, Kinet JP. TRPM4 is a Ca²⁺-activated nonselective cation channel mediating cell membrane depolarization. *Cell.* 2002;109:397–407.
- Bergman EN. Energy contributions of volatile fatty acids from the gastrointestinal tract in various species. *Physiol Rev.* 1990;70:567-590.
- Saleem F, Bouatra S, Guo AC, Psychogios N, Mandal R, Dunn SM, Ametaj BN and Wishart DS. The bovine ruminal fluid metabolome. *Metabolomics* 2013;9:360-378.
- Ostrowska M, Jarczak J and Zwierzchowski L. Glucose transporters in cattle - A review. *Animal science papers and reports* 2015;33: 191-212.
- Aschenbach JR, Bhatia SK, Pfannkuche H, Gäbel G. Glucose is absorbed in a sodium-dependent manner from forestomach contents of sheep. *J Nutr.* 2000;130, 2797–2801

Goopy JP, Donaldson A, Hegarty R, Vercoe PE, Haynes F, Barnett M and Oddy VH. Low-methane sheep have smaller rumens and shorter rumen retention time. *British Journal of Nutrition* 2014;111: 578-85.

Pinares-Patiño CS, Ulyatt MJ, Lassey KR, Barry TN and Holmes CW. Rumen function and digestion parameters associated with differences between sheep in methane emissions when fed chaffed Lucerne hay. *The Journal of Agricultural Science* , 2003; 140: 205 – 214.

Jonker A, Hickey S, Boma P, Woju CW, Sandoval E, Maclean S, Calzada MGR, Yu W, Lewis S, Janssen PH, McEwan JC and Rowe S. Individual-level correlations of rumen volatile fatty acids with enteric methane emissions for ranking methane yield in sheep fed fresh pasture. *Animal production Science* 2020; <https://doi.org/10.1071/AN20128>

Kamke J, Kittlemann S, Soni P, Li Y, Tavendale M, Ganesh S, Janssen PH, Shi W, Froula J, Rubin EM and Attwood GT. Rumen metagenome and metatranscriptome analyses of low methane yield sheep reveals a *Sharpea*-enriched microbiome characterised by lactic acid formation and utilisation. *Microbiome*. 2016;4:56.

Ewaschuk JB, Naylor JM and Zello GA. D-Lactate in Human and Ruminant Metabolism *J. Nutr.*2005;135: 1619–1625.

Harmon, D. L., Britton, R. A. & Prior, R. L. (1984) In vitro rates of oxidation and gluconeogenesis from L(+) and D(-)lactate in bovine tissues. *Comp. Biochem. Physiol. B.* 77: 365–368.

Pang S and Le Y. Role of resistin in inflammation and inflammation related diseases. *Cellular and molecular immunology*. 2006; 3: 29-34.

Winterbourn CC, Hampton MB, Livesey JH and Kettle AJ. Modeling the Reactions of Superoxide and Myeloperoxidase in the Neutrophil Phagosome. Implications for microbial killing. *J Biol Chem*. 2006; 281:39860 –39869.

Bakkenist, ARJ, De Boer JEG, Plat H and Wever R. The halide complexes of myeloperoxidase and the mechanism of the halogenation reactions. *Biochimica et Biophysica Acta*. 1980; 613: 337-348.

7.2 Perennial wheat fed sheep; Rumen epithelium proteins

Kamath KS, Krisp C, Chick J, Pascovici D, Gygi SP, Molloy MP. *Pseudomonas aeruginosa* Proteome under Hypoxic Stress Conditions Mimicking the Cystic Fibrosis Lung. *J Proteome Res*. 2017;16:3917-3928.

Jemma X. Wu, Dana Pascovici, Yunqi Wu, Adam K. Walker, and Mehdi Mirzaei. Workflow for Rapidly Extracting Biological Insights from Complex, Multi condition proteomics experiments with WGCNA and PloGO2. *Journal of Proteome Research* 2020;19: 2898-2906.

Bond JJ, Donaldson AJ, Coumans JVF, Austin K, Ebert D, Wheeler D and Oddy VH. Protein profiles of enzymatically isolated rumen epithelium in sheep fed a fibrous diet. *J Anim Sci and Biotech* 2019;10:5.

Bergman EN. Energy contributions of volatile fatty acids from the gastrointestinal tract in various species. *Physiol Rev*. 1990;70:567-590.

Newell MT, Holman BWB, Refshauge G, Shanley AR, Hopkins DL and Hayes RC. The effect of a perennial wheat and lucerne biculture diet on feed intake, growth rate and carcass characteristics of Australian lambs. *Small Ruminant Research* 2020; 192: 106235.

Lavker RM and Maltosky AG. Formation of horny cells. *J Cell Biol* 1970;44:501-512.

Xiang R, McNally J, Rowe S, Jonker A, Pinares- Patiño CS, Oddy VH, et al., Gene network analysis identifies rumen epithelial cell proliferation, differentiation and metabolic pathways perturbed by diet and correlated with methane production. *Sci Rep-UK*. 2016; 6:39022.

Günzel D and Yu ASL. Claudins and the modulation of tight junction permeability. *Physiol Rev*. 2013; 93:525-569.

Trevisi E, Amadori M, Riva F, Bertoni G, Bani P. Evaluation of innate immune responses in bovine forestomachs. *Res Vet Sci*. 2014; 96:69-78

Larsen SB, Cowley CJ, Fuchs E. Epithelial cells: liaisons of immunity. *Curr Opin Immunol*. 2020; 62:45-53.

Kent-Dennis C, Aschenbach JR, Griebel PJ and Penner GB. Effects of lipopolysaccharide exposure in primary bovine ruminal epithelial cells. *J Dairy Sci*. 2020; 103:9587-9603

Guilliams M, Henri S, Tamoutounour S, Ardouin L, Schwartz-Cornil I, Dalod M and Malissen B. From skin dendritic cells to a simplified classification of human and mouse dendritic cell subsets. *Eur. J. Immunol*. 2010; 40: 2089-2094.

Aschenbach JR, Zebeli Q, Patra AK, Greco G, Amasheh S and Penner GB. Symposium review: The importance of the ruminal epithelial barrier for a healthy and productive cow. *J of Dairy Sci*. 2019; 102: 1866-1882.

Bragulla HH and Homberger DG. Structure and functions of keratin proteins in simple, stratified, keratinized and cornified epithelia. *J Anat*. 2009; 214:516-559.

7.3 Mitochondrial DNA content assays

Cantalapiedra-Hijar et al (2018). Review: Biological determinants of between-animal variation in feed efficiency of growing beef cattle. *12:S2* 321-335.

Cassar-Malek I, Bobby C, Picard B, Reverter A, Hudson NJ (2017). Molecular regulation of high muscle mass in developing Blonde D’Aquitaine cattle fetuses. *Biology Open*. 6(10): 1483-1492.

Carmelo V, Kadarmideen H (2020). Genome regulation and gene interaction networks inferred from muscle transcriptome underlying feed efficiency in pigs. *Frontiers in Genetics* 11:650.

Dorji J et al (2020). Mitochondrial protein gene expression and the oxidative phosphorylation pathway associated with feed efficiency and energy balance in dairy cattle. *Journal of Dairy Science* 104: 575-587.

Fu L et al (2017). Proteomic analysis indicates that mitochondrial energy metabolism in skeletal muscle tissue is negatively correlated with feed efficiency in pigs. *Scientific Reports* 7:45291.

Gomez-Perez et al (2012). Long term high fat diet feeding induces skeletal muscle mitochondrial biogenesis in rats in a sex dependent and muscle type specific manner. *Nutrition and Metabolism* 9:15.

Hudson NJ (2009). Symmorphosis and livestock bioenergetics: production animal muscle has low mitochondrial volume fractions. *Journal of Animal Physiology and Animal Nutrition*. 93(1):1-6.

Kong RS, Liang G, Chen Y, Stothard P and Guan L (2016). Transcriptome profiling of the rumen epithelium of beef cattle differing in residual feed intake. *BMC Genomics* 17:592.

Mahmoudi M, Kidd L, Poppi D, Quigley S, Hudson NJ (2019). Development of a molecular assay to estimate mitochondrial content in cattle tissues. 6th EAAP International Symposium on Energy and Protein Metabolism and Nutrition. Mina Gerais, Belo Horizonte. 9-12 September 2019.

Nadal-Casellas et al (2010). Long term high fat diet feeding impairs mitochondrial biogenesis in liver of male and female rats. *Cell Physiol Biochem* 26(3): 291-302.

Reverter A, Okimoto R, Sapp R, Bottje W, Hawken R, Hudson NJ (2017). Chicken muscle mitochondrial content appears coordinately regulated and is associated with performance phenotypes. *Biology Open*. 6(1):50-58.

Short et al (2008). Enhancement of muscle mitochondrial function by growth hormone. *J Clin Endocrinol Metab*. 93(2): 597-604.

8. Appendix

8.1 Feed composition

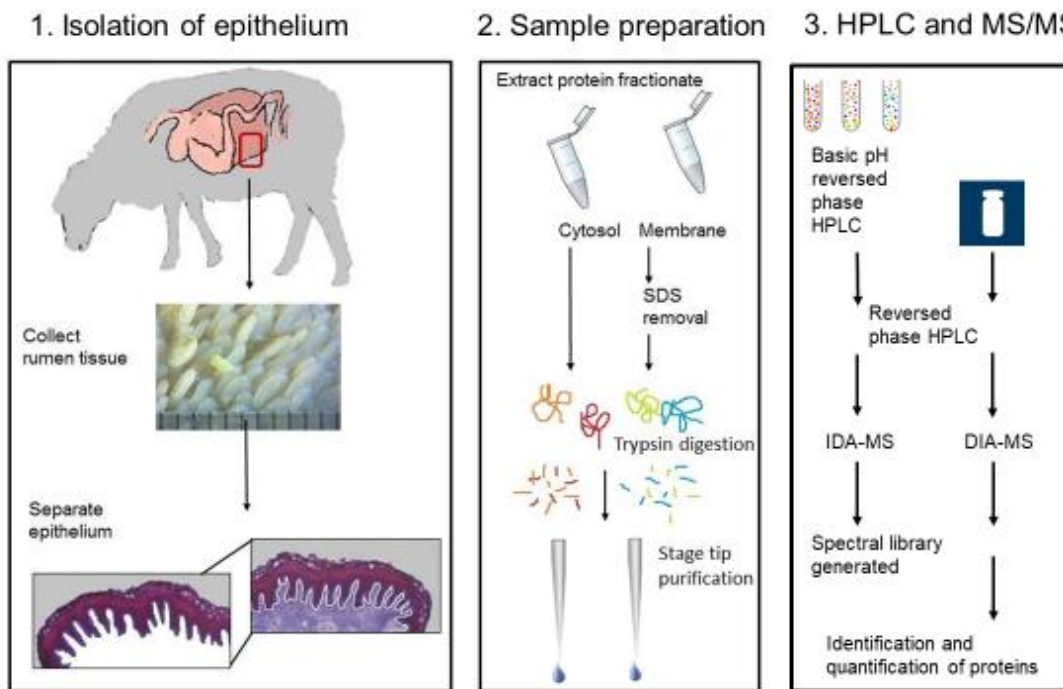
Table 1. Dry matter (DM) content and chemical composition (% DM basis, unless otherwise indicated) of the diets feed for each experiment. A mineral supplement of 0.5 % AgLime (Calcium carbonate) and 0.5 % salt (sodium chloride) was added w/w of the total ration offered in High and low diet. Perennial wheat (PW) diets are taken from Table 2 in Newell *et al.* 2020. NA= information not available.

Feed component	High diet 40:50:10 Barley grain: Lucerne chaff: Cereal chaff	Medium diet 50:50 Lucerne chaff: Cereal chaff	Low diet 30:70 Lucerne chaff: Cereal chaff	PW	PW + Lucerne
Metabolisable energy (MJ /kg DM)	11.6	9.5	9.2	12.0	11.5
Crude protein	14.5	13.9	11.5	24.3	22.1
Dry matter	89.3	90.1	90.1	NA	NA
Neutral detergent fibre	35	49	56	45	40
Acid detergent fibre	20	31	33	NA	NA
Water soluble carbohydrates	5.7	8.1	10.2	NA	NA
DMD*	77	65	63	79	76
Phosphorus	0.20	0.22	0.25	0.25	0.21
Potassium	1.2	1.8	2.1	4.7	3.5
Calcium	0.95	0.83	0.62	0.34	0.82
Magnesium	0.29	0.30	0.23	0.12	0.14
Sodium	0.41	0.37	0.32	0.005	0.012
Chloride	0.12	0.11	0.89	0.74	0.59
Sulphur	0.20	0.22	0.20	0.35	0.31

*Estimated from *in vitro* analysis.

8.2 Workflow diagram for SWATH MS

Figure 1. Workflow of the epithelium proteome analysis 1). Whole depth rumen tissue (n=20) were collected, treated with enzyme and the epithelium isolated by microdissection. 2). Sample preparation; Each epithelial tissue sample was homogenised and fractionated into a cytosol and membrane fraction (n=20/fraction), the protein extracts dialysed and SDS removed prior to trypsin digestion. 3). High pH (HpH) fractionation by HPLC, followed by LC-MS/MS analysis of the peptides in Independent Data Acquisition (IDA-MS) mode. 4) Data-Independent Acquisition-MS (DIA-MS) analysis of individual samples using SWATH-MS procedure for label-free quantification. Protein identifications were made using Ensembl ovine database.



8.3 Tandem mass spectrometry methodology

8.3.1 Quantification of rumen epithelium proteins by SWATH MS

Appendix 2 shows a diagram of the workflow for the SWATH MS procedure.

8.3.2 Offline high pH (HpH) fractionation by HPLC

A portion of cytosolic and membrane samples were separately pooled and fractionated using HpH chromatography. Briefly, the peptide mixture was resuspended in loading buffer (5 mM ammonia (NH₃) solution (pH 10.5), separated into 96 fractions using an Agilent 1260 HPLC system. Peptides were separated on a 55 min linear gradient from 3% to 30% acetonitrile in 5 mM NH₃ solution (pH 10.5) at a flow rate of 0.3 mL/min on an Agilent 300 Extend C18 column (3.5 µm particles, 2.1 mm ID and 150 mm in length). The 96 peptide fractions were consolidated into 17 fractions to adequately sample the peptides separated by HpH in the chromatographic profile. Samples were subsequently vacuum centrifuged and reconstituted in 2 % acetonitrile, 0.1 %, formic acid for LC-MS/MS processing.

8.3.3 LC-MS/MS and data acquisition

Proteins were quantified using SWATH-MS as described in [7] with modifications. Each sample was analysed on a TripleTOF 6600 mass spectrometer (SCIEX) in two stages: Information-Dependent Acquisition-MS (IDA-MS) analysis of BpRP fractionated peptides for spectral library generation, followed by Data-Independent Acquisition-MS (DIA-MS) analysis of individual samples using SWATH-MS procedure for label-free quantification.

Nanoflow LC-MS/MS analysis was carried out in positive ion mode using a Triple TOF 6600 mass spectrometer (SCIEX) equipped with an Eksigent Ultra nanoLC system (Eksigent) and nanoflex cHiPLC module (SCIEX). Peptides (10 µl, approx. 2 µg) were desalted with 2 % acetonitrile, 0.1 % formic acid using a C18 trap (Halo-C18, 160 Å, 2.7 µm, 200 µm x 2 cm) for both information dependant acquisition (IDA) and data independent (DIA, SWATH-MS) experiments.

For IDA, peptides were eluted from a trap column and separated on a cHiPLC C18 column (15 cm x 200 µm, 3 µm, ChromXP C18-CL, 120 Å, 25 °C, SCIEX) using a linear solvent gradient from 2 % acetonitrile (0.1 % formic acid) to 35 % mobile phase B (B: 99.9 % acetonitrile, 0.1 % formic acid) at 600 nL/min over 120 min. For SWATH-MS, data was acquired using a 60 min LC gradient (5-35 % mobile phase B) at 600 nL/min. Liquid chromatography eluent was subjected to positive ion nanoflow electrospray MS analysis (spray voltage 2.5 kV, curtain gas 25) using a nanospray III source (SCIEX) and an uncoated PicoTip Emitter (New Objective, USA). First a TOFMS survey scan (m/z 350-1500, 250 ms) was conducted followed by MS/MS analysis (2+ to 4+; 100 ms each, m/z 100-1800) of the top 20 most intense precursor ions with a dynamic exclusion time of 30 s.

For SWATH experiments, individual samples were analysed in DIA-MS mode using variable m/z windows (100 in total) determined based on precursor m/z densities from IDA data. First, a TOFMS survey scan was acquired (m/z 350-1500) followed by 100 SWATH-MS₂ scans (m/z 350-1500). Each SWATH-MS₂ scan used rolling collision energy and CE spread of 5. SWATH experiments for individual samples were acquired in a randomized order with one blank injection acquired between each sample.

8.3.4 Bioinformatic analysis to predict protein subcellular location and biological function

Protein subcellular localisation into 8 locations was based on the top score given by WoLF PSORT [8] (www.genscript.com/wolf-psort.html). Membrane proteins were predicted using transmembrane helical Markov model (TMHMM) [9] (www.cbs.dtu.dk/services/TMHMM/).

Extracellular proteins were predicted for N-terminal signal peptide cleavage site using TargetP [10] (www.cbs.dtu.dk/services/TargetP/) or secretomeP [11] (www.cbs.dtu.dk/services/SecretomeP/) based on protein sequence motifs. Proteins with a mitochondrial targeting sequence and the cleavage site were predicted using TargetP (mitoTP score >0.5). To determine proteins involved in exocytosis or the mitochondria, databases including exocarta [12] (www.exocarta.org/) and mitocarta [13] (www.broadinstitute.org/files/shared/metabolism/mitocarta/human.mitocarta2.0.html) were used to identify proteins known to occur in these cell compartments. In addition, proteins associated with the cell junctions, endosome, lysosome, phagosome and peroxisome were annotated based on KEGG cellular pathways (www.genome.jp/kegg/pathway.html). Other references used for classification of the peroxisome proteins were [14]. Transporters in the SLC and ABC transporter families were identified according to gene and protein name. We also used website gene names (www.genenames.org/data) to characterise the subcellular location of the transporter and the type of substrate they transport.

8.3.5 Data analysis

For mass spectrometry data a spectra library was generated by performing a combined data search of all the IDA-MS data using the Paragon algorithm (SCIEX) in ProteinPilot (Version 5.0, SCIEX) in thorough ID mode with FDR calculation enabled and allowing biological modification. All the MS/MS spectra from IDA experiments were searched against a reference database for the Ovine proteome (Oar v4, Ensembl, May 2017). Carbamidomethylation of cysteine residues, and an unused cut-off score of 1.3 (95 % confidence) was used for database searches.

For SWATH quantitation, consolidated ProteinPilot IDA search results were imported into PeakView 2.1 with SWATH 2.0 MicroApp (SCIEX) and used as a spectral library. Retention times for all SWATH files were aligned using linear regression model using endogenous peptides across the elution profile. The top 6 most intense fragment ions for each peptide were extracted from the SWATH data using a maximum number of peptides of 100, 75 ppm mass tolerance, peptide confidence threshold of ≥ 0.99 , and a 5 min retention time extraction window. After data processing, peptides with confidence > 99% and FDR < 1% (based on chromatographic feature after fragment extraction) were used for quantitation. The workflow described in the above steps are summarised in figure 1. The search results are available at proteomics identification database PRIDE (<https://www.ebi.ac.uk/pride/archive/>, PRIDE ID:xxxxxx).

Rumen fluid and blood metabolite data was analysed using a general linear model with metabolite as the variable effect and fixed effect of treatment block and phenotype and with a covariable effect of liveweight or DMI fitted to the model if statistically significant.

8.4 Quantification of rumen epithelium proteins by TMT-MS

We used our procedure to isolate rumen epithelium proteins in combination with methods to collect quantitative data on changes in protein level in perennial wheat (PW) or perennial wheat plus lucerne (PW+L) -fed sheep. In addition, rumen epithelium from animals selected as ‘better doers’

and ‘lesser doers’ primarily on divergence in RFI, fed two diets were analysed using TMT-MS. Cell extracts were homogenised and fractionated into a cytosol and membrane fraction and prepared for MS/MS as described in section 3.1.4. Proteins labelled with TMT kit and were quantified using LC MS/MS and relevant software as described previously by Kamath et al. (2017).

8.4.1 Statistical analysis

ANOVA was used to identify were proteins that were significantly more abundant in the PW vs PW+L diet ($P < 0.05$ and fold change > 1.2) in rumen epithelium.

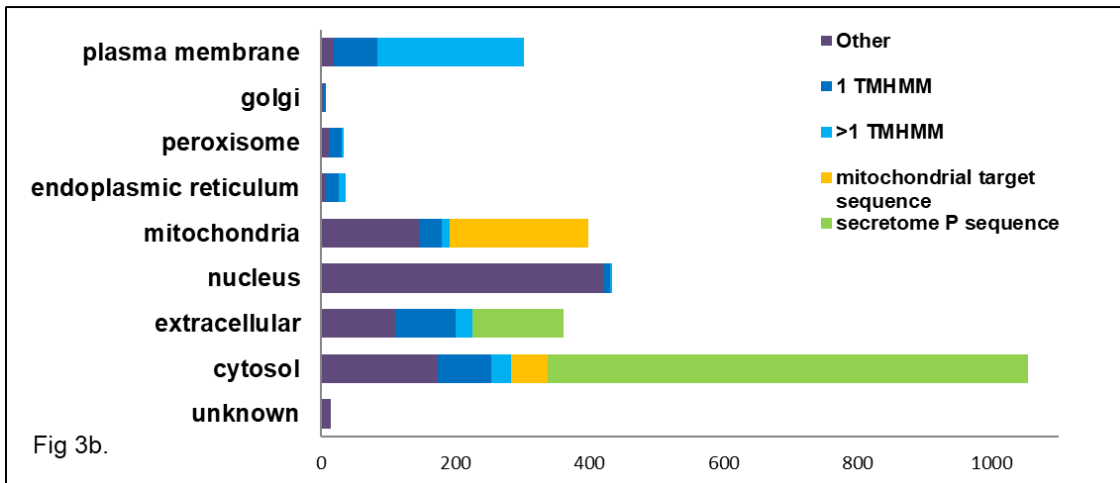
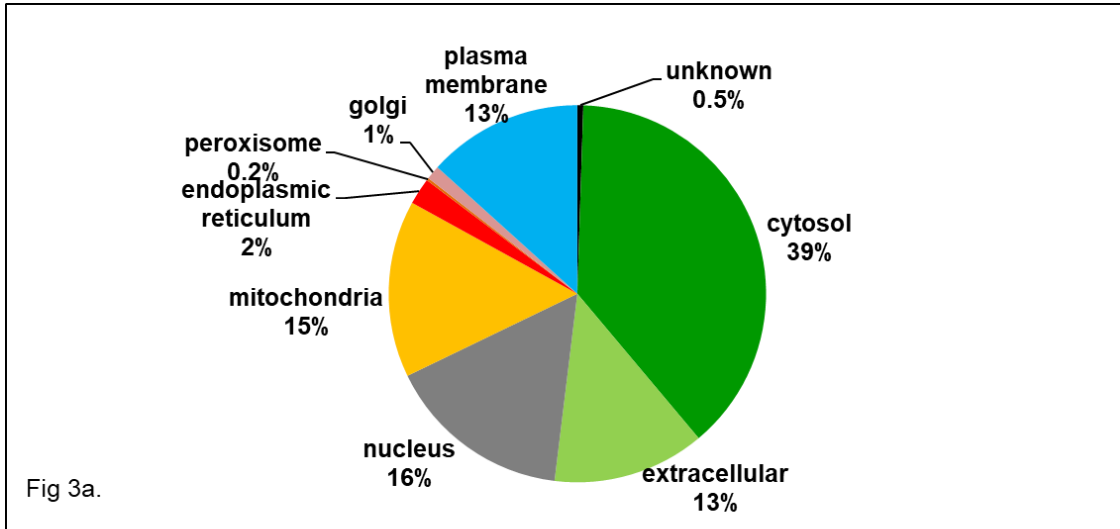
Weighted gene correlation network analysis (WGCNA; Wu et al. 2020) analysis + DAVID functional annotation enrichment analysis was used to interpret functionally significant proteins and metabolic pathways. First WGCNA was applied to the MS/MS quantification of rumen epithelium proteins in PW and PW+L feed sheep. This is a weighted pairwise analysis procedure to find correlations between gene networks or protein functions in all protein identified.

8.5 Assignment of proteins to sub cellular compartment and function

To expand the knowledge of the location and function of the proteins identified we used an array of bioinformatic tools. Subcellular location predictions by WoLF PSORT revealed a large proportion of identified proteins were localised in the cytosol ($n=1062$), nucleus ($n=440$), mitochondria ($n=420$), plasma membrane ($n=368$) or extracellular ($n=361$ Fig 6a). Smaller proportions were assigned to the endoplasmic reticulum ($n=63$) peroxisome($n=33$) or golgi ($n=6$).

Of all the proteins identified 23% were predicted membrane proteins with at least one transmembrane domain (TMHMM) (supplementary file 1). The plasma membrane category had most proteins with multiple transmembrane domains ($n=219 > 1$ TMHMM). Those assigned to the cytoplasm or extracellular compartment were largely single transmembrane domain proteins (1 TMHMM). A proportion of the proteins assigned extracellular contained a predicted secreted protein sorting sequence (Signal P $n=191$ and SecretomeP $n=136$). Of the 420 proteins categorised as mitochondrial up to 207 had a predicted mitochondrial target protein sequence.

Figure 6a) The proportion of protein identifications in subcellular locations predicted by Wolf PSORT. 6b) The distribution of proteins predicted to have a membrane domain (TMHMM), mitochondrial (targetP) or secretory target peptide sequence (SecretomeP) in each subcellular category.



8.6 Publications/communication

8.6.1 Journal articles

Bond JJ, Donaldson AJ, Coumans JVF, Austin K, Ebert D, Wheeler D and Oddy VH, Protein profiles of enzymatically isolated rumen epithelium in sheep fed a fibrous diet. *J Ani. Sci and Biotech* 2019; 10:5

8.6.2 Full journal articles in draft

Bond JJ, Hudson NJ, Khan UH, Dougherty H, Pickford Z, Mackenzie S, Barzegar S, Santos G, Woodgate S, Gyue G, Hein B, Vercoe P and Oddy VH. Phenotypic correlates of more efficient nutrient use in growing sheep: how to pick ‘better doers’ 2021 in draft.

Bond JJ, Hudson NJ, Kamath KS, Wu JX, Khan UH, Mackenzie S, Barzegar S, Santos G, Woodgate S, Woodgate R, Vercoe P and Oddy VH. Low and high residual feed intake (RFI) Merino wethers fed on two different planes of nutrition; Proteomics of the rumen epithelium quantified by TMT MS. 2021 in draft analysis completed.

Pickford Z, Mortimer S, Doyle E, Bond J, Austin K, Mackenzie S, Bond JJ. Wool measures and blood metabolites of sheep. 2022

Khan UH, Dougherty H, Santos G, Vercoe P and Oddy VH. Phenotypic variation in heat expenditure measured using indirect calorimetry in Merino wethers. 2021.

Mitochondrial DNA assay development. Nick H and Jude Bond others

Mitochondrial DNA content in experiment described in paper 1. Nick Hudson, Jude Bond, Umair hassan, Shahram Barzegar,

8.6.3 Conference attendance and proceedings

Bond J, Donaldson A, Wheeler D, Oddy VH, Kamath K and McKay M. (2019) Proteins co-ordinating the processes of cell permeability and nutrient transport in the rumen epithelium of sheep. HUPO Sept, 2019, Adelaide conference centre.

Mahmoudi M., Jeanes A., Kidd L, Poppi D, Quigley S and Hudson NJ (2019). Development of a molecular assay to estimate content in cattle tissues. In: Energy and protein metabolism and nutrition. 6th EAAP International Symposium on Energy and Protein Metabolism and Nutrition, Belo Horizonte, Minas Gerais, Brazil, (401-402). 9-12 September 2019. doi:10.3920/978-90-8686-891-9_122

Northern Beef Research Update Conference Brisbane exhibition centre, 19–22 August 2019. Attendance

National feed intake workshop AAAS Feb 2021 Freemantle WA. Attendance

8.6.4 Meetings

Bond JJ, Kamath KS, McKay M, Khan UH, Austin K, Dalrymple B, Oddy VH, Pascovici D and Mirzaei M. Multi-disciplinary meeting with staff from NSW DPI, APAF and UWA and an industry technical specialist SCIEX mass spectrometry. September 2018, Australian proteome analysis facility, Macquarie university, Ryde, Sydney, NSW.

Bond JJ, Hudson NJ, Gebbels J and Tompkins N. Meeting with MLA R&D Managers to discuss and animal experiment for milestone progression June 2019. North Sydney NSW Australia.

Bond JJ, Kamath KS and McKay M. Novel dual purpose perennial cereals for grazing project (P.PSH.1036). Introduction to rumen epithelium proteome quantification in sheep with different phenotypes and diets. September 2019, NSW DPI Cowra research station, NSW.

Bond JJ, Hudson NJ, Kamath KS, Wu JX. Novel dual purpose perennial cereals for grazing project (P.PSH.1036). A report on preliminary rumen epithelium proteome quantification in lambs feed perennial wheat and perennial wheat and Lucerne. 14th August 2020, NSW DPI Cowra research station, NSW.

8.6.5 Postgraduate students

- PhD student Umair Khan (UWA) has commenced a 6 month placement in Armidale which due to COVID-19 travel restriction turned into a stay till his thesis was finished. Umair has a scholarship with Pakistan government. Supervisors are Dr Brian Dalrymple and Prof Phil Vercoe (UWA), Prof Hutton Oddy and Dr Jude Bond (NSW DPI).
- Honours student Zoe Pickford has completed honours project and thesis on wool phenotype and blood metabolites. Supervisors are Dr Sue Mortimer and Dr Jude Bond (NSW DPI) and Dr Emma Doyle (UNE). Australian wool education trust awarded Zoe a \$7000 scholarship to conduct the undergraduate honours project.
- PhD student Elmer Fernandez enrolled through UQ starts remotely in USA in 2021. Nick and Jude will therefore continue to collaborate in this area beyond the formal end date of the project.
- International atomic energy agency (IAEA) fellows from Myanmar Gyue Gyue and Bo Hein. the (IAEA) completed 1 month fellowship with NSW DPI Armidale and 1 month training with UWA in Phil Vercoe lab. A \$8000 stipend was paid to the project budget for the fellows training.
- A competitive International UQ PhD scholarship awarded to Aamir Khan lapsed due to delays in obtaining a visa. A competitive International UQ PhD scholarship has been awarded to Elmer Fernandez but commencement was delayed due to COVID related travel restrictions. A remote commencement application was submitted and recently approved. Future publications will be aligned with Elmer’s PhD appointment, and collaborator Jude Bond will remain involved with his PhD activities. The design and early implementation of the mitochondrial content assays were presented by Dr Nick Hudson at the International Symposium on Energy and Protein Metabolism conference (2019) in Belo Horizonte, Brazil (Mahmoudi et al 2019). Eventual publication of this and other downstream research activities will be built into the PhD studies of Elmer Fernandez.